Université d'Ottawa · University of Ottawa

TISSUE INJURY AND REMODELING IN RAT HIPPOCAMPAL DENTATE GYRUS FOLLOWING Na^+-K^+-ATPase INHIBITION

BY

AYMAN I. OMAR

This thesis is submitted as a partial fulfillment of the Ph.D. program in Neuroscience

June 2002

Submitted to the Faculty of Graduate and Postdoctoral Studies, University of Ottawa,
Ottawa, Ontario, Canada

Dedication

This thesis is dedicated to my parents

Authorization

14 June 2002

Our ref: PCR/NIC/June02-149

Dr A Omar
Ottawa Health Research Institute
1053 Carling Avenue
Ottawa
Ontario K1Y 4K9
Canada
Fax: (613) 798 4443

Dear Dr Omar

NEUROSCIENCE, Vol 102, Issue 2, 2001, pp 353-359, Omar et al. "Sodium – potassium adenosine...", entire article: Vol 95, Issue 1, 2000, pp 73-80, Omar et al. "Ethidium bromide staining...", entire article

As per your letter dated 7 June 2002, we hereby grant you permission to reprint the aforementioned material at no charge in your thesis subject to the following conditions:

1. If any part of the material to be used (for example, figures) has appeared in our publication with credit or acknowledgement to another source, permission must also be sought from that source. If such permission is not obtained then that material may not be included in your publication/copies.

2. Suitable acknowledgment to the source must be made, either as a footnote or in a reference list at the end of your publication, as follows:

   "Reprinted from Publication title, Vol number, Author(s), Title of article, Pages No., Copyright (Year), with permission from Elsevier Science"

3. Reproduction of this material is confined to the purpose for which permission is hereby given.

4. This permission is granted for non-exclusive world English rights only. For other languages please reapply separately for each one required. Permission excludes use in an electronic form. Should you have a specific electronic project in mind please reapply for permission.

5. This includes permission for the National Library of Canada to supply single copies, on demand, of the complete thesis. Should your thesis be published commercially, please reapply for permission.

Yours sincerely

Helen Wilson
Rights Manager

Your future requests will be handled more quickly if you complete the online form at www.elsevier.com

To whom it may concern:

I, Dr. Bin Hu, hereby authorize the microfilming by the National Library of Canada of the thesis of Ayman I. Omar, titled "Early lesion-induced tissue remodeling in rat dentate gyrus following inhibition of the sodium-potassium pump".

I am a co-author of chapters 2, 3, 4, and 5 of this thesis, titled "Sodium - potassium adenosine triphosphatase inhibition enhances membrane accumulation of DiI in rat hippocampus *in vivo*", "Co-development of necrosis and apoptosis in rat hippocampal dentate gyrus following Na^+,K^+- pump inhibition", "Ethidium bromide staining reveals rapid cell dispersion in the rat dentate gyrus following ouabain-induced injury" and "Enhancement of progenitor cell proliferation and migration in rat hippocampal dentate gyrus following Na^+, K^+- pump inhibition".

Signed: 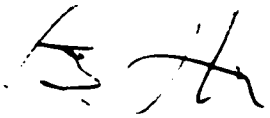

Date: 17 June, 2002

DEPARTMENT OF HEALTH & HUMAN SERVICES

Public Health Service

National Institutes of Health
Bethesda, Maryland 20892
www.nih.gov

Vladimir V. Semyanov, Ph.D
Senior Staff Fellow
Section on Molecular Neurobiology, EPB
NIMH, NIH, Bldg 36, Rm 4C20A, 10 Center Drive MSC 4363
MD Bethesda, 20892-4363
Tel/voice mail: (301) 496-7761; Lab: (301) 496-7782
Fax: (301) 480-9290
E-mail: semyanov@helix.nih.gov

June 10, 2002

To whom it may concern:

I, Dr. Vladimir V. Semyanov, hereby authorize the microfilming by the National Library of Canada of the thesis of Ayman I. Omar, titled "Early tissue remodeling in rat dentate gyrus following inhibition of the sodium-potassium pump".

I am a co-author of chapters 3 and 4 of this thesis, titled "Sodium - potassium adenosine triphosphatase inhibition enhances membrane accumulation of DiI in rat hippocampus in vivo" and "Ethidium bromide staining reveals rapid cell dispersion in the rat dentate gyrus following ouabain-induced injury"

V. Semyanov

Vladimir V. Semyanov

Author's contributions

Chapter 2 *Sodium - potassium adenosine triphosphatase inhibition enhances membrane accumulation of DiI in rat hippocampus in vivo.*

Performed all experiments and analyzed all data. Wrote preliminary drafts and prepared all figures.

Chapter 3 *Co-development of necrosis and apoptosis in rat hippocampal dentate gyrus following Na^+,K^+ - pump inhibition.*

Performed all experiments and analyzed all data. Wrote preliminary drafts and prepared all figures.

Chapter 4 *Ethidium bromide staining reveals rapid cell dispersion in the rat dentate gyrus following ouabain-induced injury.*

Performed all experiments and analyzed all data. Wrote preliminary drafts and prepared all figures.

Chapter 5 *Enhancement of progenitor cell proliferation and migration in rat dentate gyrus following Na^+, K^+ - pump inhibition.*

Performed all experiments and analyzed all data. Wrote preliminary drafts and prepared all figures.

ABSTRACT

Na^+, K^+-ATPase is a ubiquitous membrane enzyme that plays an important role in maintaining neuronal excitability, ionic homeostasis and cell survival. Although failure of the Na^+, K^+-ATPase pump has been implicated in the pathophysiology of a variety of neurological conditions, the timeline and precise sequence of events at the cellular and subcellular levels that follow failure of the pump remain elusive, particularly in the *in vivo* environment.

To this end, we developed an animal model and a set of fluorescence-based cell tagging methods during this thesis research. The methodology involves stereotactically coinfusing the Na^+, K^+-ATPase pump blocker, ouabain with a set of fluorescent tags into the hippocampal dentate gyrus. These fluorescent tags, by undergoing fluorescence enhancement upon binding to specific subcellular targets, therefore allow the probing of subcellular dynamics *in vivo* following inhibition of the Na^+, K^+-pump. Based on this original methodology, we describe several novel types of tissue injury in the rat dentate gyrus following pump failure, which can be summarized as follows:

1. Pump inhibition results in an increase in membrane porosity that occurs as early as the 1-hour time point. Furthermore, pump inhibition enhances uptake of the lipophilic probe, DiI into plasma membranes of dentate granule cells. This increase in DiI incorporation is associated with the appearance of reactive changes characterizing early neuronal injury. Our results suggest that pump inhibition leads to an early increase in membrane permeability followed by a change in membrane phospholipid structure.

2. Pump inhibition triggers a form of cell death with "mixed" apoptotic and necrotic features. The broad-spectrum K^+ channel blocker, charybdotoxin is capable of significantly attenuating the neuronal damage associated with inhibition of the Na^+, K^+ pump, indicating that loss of intracellular K^+ plays an important role in cell death associated with pump inhibition.

3. We describe a novel tissue response whereby pump inhibition triggers the appearance of a radial glia-like cell population that undergoes time-dependent cell dispersion and rearrangement.

4. We found that pump inhibition can simultaneously trigger cell death as well as upregulate progenitor cell proliferation. Migration of such newly born progenitor cells was also enhanced towards areas of cell injury and tissue damage. We suggest that such a host of tissue responses may represent an early endogenous attempt at restoring tissue structural integrity, through the enhancement of proliferation and migration of neural precursor cells as well as re-expression of the radial glial scaffold necessary for progenitor cell migration.

The experimental data reported in this thesis may therefore have important implications in the future development of therapeutic strategies aimed at restoring tissue structural integrity and possibly functional outcome following central nervous system injury.

Table of Contents

List of Figures

Chapter 5

List of Tables

Chapter 3

Chapter 4

List of Abbreviations

$[Ca^{2+}]_i$	intracellular calcium ion concentration
AI	apoptotic index
AMPA	α-amino-3-hydroxy-5-methyl-4-isoxazol-propionic acid
ANOVA	analysis of variance
APAF-1	apoptosis-activating factor
ATP	adenosine triphosphate
AVD	apoptotic volume decrease
BrDU	5'-bromo-2'-deoxyuridine
CA1, 2, 3 or 4	cornu Ammonis subfield 1, 2, 3 or 4, respectively;
Ca^{2+}	calcium ion
CCD	charge-coupled device;
cGMP	cyclic guanosine monophosphate
CuSOD	copper superoxide dismutase
DiI	1,1'-dioctadecyl-3,3,3',3'-tetramethylindocarbocyanine perchlorate
DNA	deoxyribonucleic acid
EAAs	excitatory amino acids
EB	ethidium bromide
ECF	extracellular fluid
EDRF	endothelium-derived relaxing factor
eNOS	endothelial NOS

EthD-1	ethidium homodimer-1
G proteins	guanosine triphosphate binding proteins
GCL	granule cell layer
GTP	guanosine triphosphate
H/E	hematoxylin and eosin
H^2O^2	hydrogen peroxide
iGluRs	ionotropic glutamate receptors
ILC	intensely-labeled cell
iNOS	inducible NOS
K^+	potassium ion
KCl	potassium chloride
L-NAME	L-N(G)-nitro arginine methyl ester
MCAO	middle cerebral artery occlusion
MCL	molecular cell layer
Mg^{2+}	magnesium ion
MGB	medial geniculate body
MnSOD	manganese superoxide dismutase
MPT	mitochondrial permeability transition
MPTP	mitochondrial permeability transition pore
Na^+	sodium ion
Na^+, K^+-ATPase	sodium-potassium adenosine triphosphatase
NaCl	sodium chloride

NI	necrotic index
NMDA	*N*-methyl-D-aspartate
nNOS	neuronal nitric oxide synthase
iNOS	inducible nitric oxide synthase
eNOS	endothelial nitric oxide synthase
NO	nitric oxide
NVI	necrotic volume increase
O^{2-}	superoxide
$ONOO^-$	peroxynitrite
PARP	poly ADP-ribose polymerase
PI	propidium iodide
PKC	protein kinase C
PLC	phospholipase C
PoDH	polymorphic interneurons of dentate hilus
PtdCho	phosphatidylcholine
RVD	regulatory volume decrease
RVI	regulatory volume increase
SEM	standard error of mean
SGZ	subgranular zone
SLM	stratum lacunosum moleculare
SOD	superoxide dismutase
SVZ	subventricular zone

TLE	temporal lobe epilepsy
TRITC	tetrarhodamine isothiocyanate.
TUNEL	terminal deoxynucleotidyl transferase-dUTP nick end labeling
VSCC	voltage-sensitive Ca^{2+} channels
VSOR	volume-sensitive outwardly rectifying

Acknowledgements

First and foremost, I would like to thank my thesis supervisor, Dr. Bin Hu for his outstanding guidance and continuous support without which this thesis would not have seen the light. I am also grateful to Dr. Vladimir Senatorov for his valuable help and fruitful discussions.

I would like to thank members of my thesis advisory committee, Dr. Leo Renaud, Dr. Peter Stys, Dr. Johnny Ngsee and Dr. Mario Tiberi. The guidance that I received during my committee meetings was invaluable in the successful completion of this thesis work. Drs. Renaud, Stys and Hu also thankfully provided me with outstanding letters of recommendation for successful CIHR fellowship as well as successful residency applications.

I would also like to thank my comprehensive examination committee members, Dr. Steffany Bennett, Dr. Kenneth Marshall and Dr. Daniel Small for their valuable comments and discussions.

Finally, I would like to acknowledge financial support provided through a postdoctoral fellowship award from the Canadian Institutes of Health Research (CIHR) under the Canadian Neurotrauma Research Program (CNRP) and graduate admission and excellence scholarships from the Faculty of Graduate and Postdoctoral Studies (FGPS), University of Ottawa.

Chapter 1. General Introduction

Na^+, K^+-ATPase is a ubiquitous membrane enzyme that plays an important role in maintaining neuronal excitability, ionic homeostasis and cell survival. Although failure of the Na^+, K^+-ATPase has been implicated in the pathophysiology of a variety of neurological conditions, the timeline and precise sequence of events at the cellular and subcellular levels that follow failure of the pump remain elusive, particularly in the *in vivo* environment. To this end, we developed an animal model and a set of fluorescence-based cell tagging methods during this thesis research. The first part of this thesis describes two novel types of tissue injury in the rat dentate gyrus following pump failure, namely abnormal membrane accumulation of lipophilic dye in plasma membranes and rapid cell dispersion. In the last two chapters of the thesis, we report a rather unique mode of tissue remodeling triggered by pump inhibition, in which the injured dentate gyrus undergoes a mixture of necrosis and apoptosis as well as activation of stem cell proliferation and migration towards areas of tissue damage. The experimental data reported in this thesis may have important implications in the future development of therapeutic strategies aimed at restoring tissue structural integrity and possibly functional outcome following central nervous system injury.

1.1 Physiology: The Na^+, K^+-ATPase pump

The Na^+, K^+-ATPase pump is an integral membrane protein expressed in all cells of higher eukaryotes. The pump is responsible for translocating sodium and potassium ions across the cell membrane utilizing adenosine triphosphate (ATP) as the driving force. For every two potassium ions translocated into the cell, three sodium ions are pumped out to the extracellular space. Such an asymmetrical ion pumping is not only

essential for the maintenance of Na^+ and K^+ gradients but also increases the level of resting membrane potential (Goldshleger et al., 2001; Jorgensen et al., 1998; Kaplia, 1997; Scheiner-Bobis, 2002; Senatorov et al., 1997; Senatorov et al., 2000). It is estimated that the Na^+, K^+-ATPase pump consumes up to 40% of the energy released by respiration in the brain compared to about 5% in liver and striated muscle (Astrup et al., 1981). The enormous energy utilized by the pump in the brain makes it particularly vulnerable to conditions associated with low energy supplies such as anoxic / ischemic states. In addition, the Na^+, K^+-ATPase pump is unique in that it is specifically inhibited by the cardiac glycosides (e.g. ouabain and digoxin).

1.1.1 Structure / function relationship of the Na^+, K^+- pump

1.1.1.1 Subunit composition and membrane topology

The Na^+, K^+-ATPase pump exists as complexes of α and β subunits. There are 3 isoforms for the α subunit, α_1, α_2 and α_3 and 3 isoforms for the β subunit, β_1, β_2 and β_3. The α_2 and α_3 isoforms are most prevalent in neurons while the α_1 and to a lesser extent the α_2 isoforms are found on glial cells (Brodsky et al., 1990; Guillaume et al., 1990; McGrail et al., 1991). The ouabain affinities for these isoforms vary greatly. For example, the α_1 isoform is relatively resistant to cardiac glycosides, while the α_2 and α_3 isoforms are quite sensitive. Using NIH 3T3 cells transfected with different α isoforms, the dissociation constants (Kd) for ouabain were calculated. It was found that the α_2 and α_3 isoforms had a Kd value of 115 and 1.6 nM, respectively (O'Brien et al., 1994). Furthermore, the α_1 isoform required 48 μM of ouabain for its half-maximal inhibition, a

value ~1000 fold higher than that of the α_2 and α_3, therefore indicating that the order of ouabain affinity for the α isoforms is $\alpha_3 > \alpha_2 >> \alpha_1$. (O'Brien et al., 1994).

The Na^+, K^+-ATPase pump functions as an $\alpha\beta$ dimer and the site of interaction between the two subunits was recently localized to 26 amino acids in the extracellular loop between membrane-spanning domains 7 and 8 (H7-H8) (Lemas et al., 1994). The α subunit plays a major role in the catalytic function of the enzyme since it contains the ATP-binding site, the phosphorylation site and the amino acid sequences essential for the binding of cations as well as cardiac glycosides. On the other hand, the β subunit appears to be involved in maturation of the enzyme, its correct assembly into a stable configuration as well as its targeting to the cell membrane (Ackermann et al., 1990; Geering et al., 1996).

Recent hydropathy analysis predicts that the Na^+, K^+- pump is composed of 10 transmembrane hydrophobic amino acid stretches that traverse the plasma membrane as α helices. Antibody epitope localization studies showed that both the NH_2 and COOH termini were located intracellularly. This is consistent with the even number of domains that traverse the plasma membrane (Felsenfeld et al., 1988; Ovchinnikov Yu et al., 1988). A recent high resolution crystallography study has confirmed the overall shape for the Na^+, K^+- pump and detected cytoplasmic, transmembrane as well extracellular domains (Rice et al., 2001).

1.1.1.2 Reaction cycle of the Na^+, K^+- pump

Biophysical studies on ion transport by the Na^+, K^+- pump led to a widely accepted scheme for the ion transport reactions known as the Post-Albers cycle. This

cycle describes the sequence of reaction steps of coupled ion transport and enzymatic reactions. The transport of both Na^+ and K^+ ions occurs through a "Ping-Pong" mechanism, meaning that they are transported in a sequential fashion (Glynn et al., 1990; Karlish et al., 1976). Initially, three Na^+ ions bind to the enzyme from the cytoplasm and subsequently the enzyme is phosphorylated in a sodium-dependent manner. The enzyme undergoes a conformational change from E_1-P to E_2-P resulting in exposure of the Na^+ binding sites to the extracellular space. Release of the three Na^+ ions to the extracellular space is followed by the sequential binding of two K^+ ions to the cation-binding site of the enzyme (E_2-2K). This is associated with dephosphorylation and a conformational change of the enzyme back to its initial E_1 state. The two K^+ ions are then released into the intracellular space and the cycle is once again repeated. Intermediary states in the reaction sequence include occluded states, E_1-P(3Na) and E_2(2K), where the ions are unable to exchange with either aqueous phase. The net effect of the reaction cycle is generation of a net negative potential on the inside relative to the outside of the cell, a mechanism that underlies the electrogenic nature of the pump (Glynn et al., 1990; Karlish et al., 1976).

1.2 Pathophysiology: Pathological conditions associated with pump inhibition

Ischemia and hypoglycemia are both associated with a reduction in Na^+, K^+-ATPase activity due to reduced ATP levels. The cerebral energy charge however is higher during hypoglycemia (60% reduction) compared to ischemia (90% reduction) (Auer et al., 1988). The drop in pump activity has been shown to occur both during and after hypoxic / ischemic insults (Enseleit et al., 1984; Goldberg et al., 1985).

Furthermore, mechanical trauma is associated with a failure of the Na^+, K^+ pump. For example, a recent study showed that a single pressure wave-transient delivered to the neocortex of rats (mimicking moderate concussive head trauma) resulted in a transient depolarizing shift in the resting membrane potential of dentate interneurons which was shown to be related to inhibition of the Na^+, K^+ pump (Ross et al., 2000). In addition, recent evidence suggests that Na^+, K^+ pump inhibition may play an important role in the pathophysiology of chronic neurodegenerative diseases such as Alzheimer's. A recent study reports a significant reduction of Na^+, K^+ pump activity within 30 min of exposure of cultured rat hippocampal neurons to Aß 25-35 and Aß 1-40 (Mark et al., 1995). The pump activity further declined to less than 40% of basal levels by 3 hr following exposure. The same study reports that both ouabain and Aß exposure led to a significant rise in intracellular Ca^{2+}, which preceded cell death. Inhibition of sodium influx significantly attenuated both Aß as well as ouabain toxicity. Therefore inhibition of the Na^+, K^+ pump plays a key role in the pathophysiology of a variety of acute and chronic neurodegenerative disorders.

1.2.1 Primary consequences of pump inhibition: ion imbalances

Inhibition of the Na^+, K^+-ATPase induces a sequence of excitotoxic events, which has been widely adopted in simulating the ischemic and traumatic cell injury cascade (Garthwaite et al., 1986; Lees, 1991). Indeed, the cytotoxic reactions induced by ouabain, such as those summarized in Fig. 1, and that induced by trauma/ischemia bear striking similarities as both are associated with a rapid loss of K^+ followed by intracellular accumulation of Na^+ and Ca^{2+}, occurrence of spreading depression and necrotic

membrane lysis (i.e. discharge of intracellular content) and delayed neuronal death (Basarsky et al., 1998; Hansen, 1985; Obeidat et al., 1998).

Loss of intracellular potassium is a hallmark event of Na^+, K^+-ATPase blockade. In intact animals, transient anoxia induces, within minutes, a five-fold increase in extracellular K^+ level, which almost instantaneously returns to the baseline upon re-supply of oxygen (Zetterstrom et al., 1995). Such rapid anoxia-induced K^+ efflux may also be facilitated by opening of ATP-sensitive K^+ channels (Halliwell, 1994). The K^+ and Na^+ imbalance can lead to characteristic changes in cell resting membrane potential. In rat medial geniculate body (MGB) maintained in vitro, application of a reversible pump blocker, strophanthidin, produced a small (4 ± 2.6 mV) and transient membrane depolarization followed by a large (48.6 ± 9 mV) and prolonged membrane depolarization. Whole cell patch clamp recordings showed that the small membrane depolarization is mediated by an inward electrogenic current. The large membrane depolarization is on the other hand a result of a transient loss of Na^+ and K^+ gradients (Senatorov et al., 2000). Since ouabain effect has poor reversibility (Senatorov et al., 2000), the resultant ionic imbalance could be sustained for a prolonged time period. There are three main parallel mechanisms that may contribute to intracellular accumulation of Ca^{2+} ions following pump inhibition (Fig.1): 1) Membrane depolarization leading to activation of voltage-sensitive Ca^{2+} channels (VSCC). 2) Opening of calcium-permeable glutamatergic ion channels. 3) Reverse operation of the Na^+,Ca^{2+}-exchanger (Stys, 1998). In addition, other mechanisms that may contribute to Ca^{2+} influx, including inositol triphosphate (IP_3), activation of ryanodine receptors on the endoplasmic reticulum as well as Ca^{2+} influx through non-specific cation channels.

Interestingly, it has recently been shown that in white matter, ouabain can induce glutamate release via reverse operation of sodium-dependent glutamate transport in rat spinal dorsal columns. This leads to AMPA receptor activation and calcium-mediated white matter injury (Li et al., 2001).

The converging effects between excitotoxic activation of glutamate receptors and the sustained rise in intracellular Na^+ and Ca^{2+} could lead to both acute cell injury and delayed neuronal death (Balestrino, 1995; Tanaka et al., 1999). Furthermore, severe depletion of intracellular K^+ may activate signaling pathways leading to neuronal apoptosis. Indeed, ouabain treatment can result in cytochrome *c* release from mitochondria, caspase-3 activation and DNA fragmentation in cultured cortical neurons (Xiao et al., 2002). Therefore, it becomes apparent that the molecular events underlying pump inhibition and ischemic cell death are not simply arranged in a hierarchical fashion but rather a much more complex chain reaction of events with both inhibitory as well as stimulatory loops within the cascade. The individual cell death mechanisms following pump inhibition are further discussed below.

Figure 1. Consequences of Na^+, K^+- pump inhibition. Inhibition of the Na^+, K^+- pump leads to membrane depolarization, Na^+ influx and K^+ efflux which in turn results in a rise in intracellular Ca^{2+} concentration, glutamate release and activation of cell death pathways (see text for details).

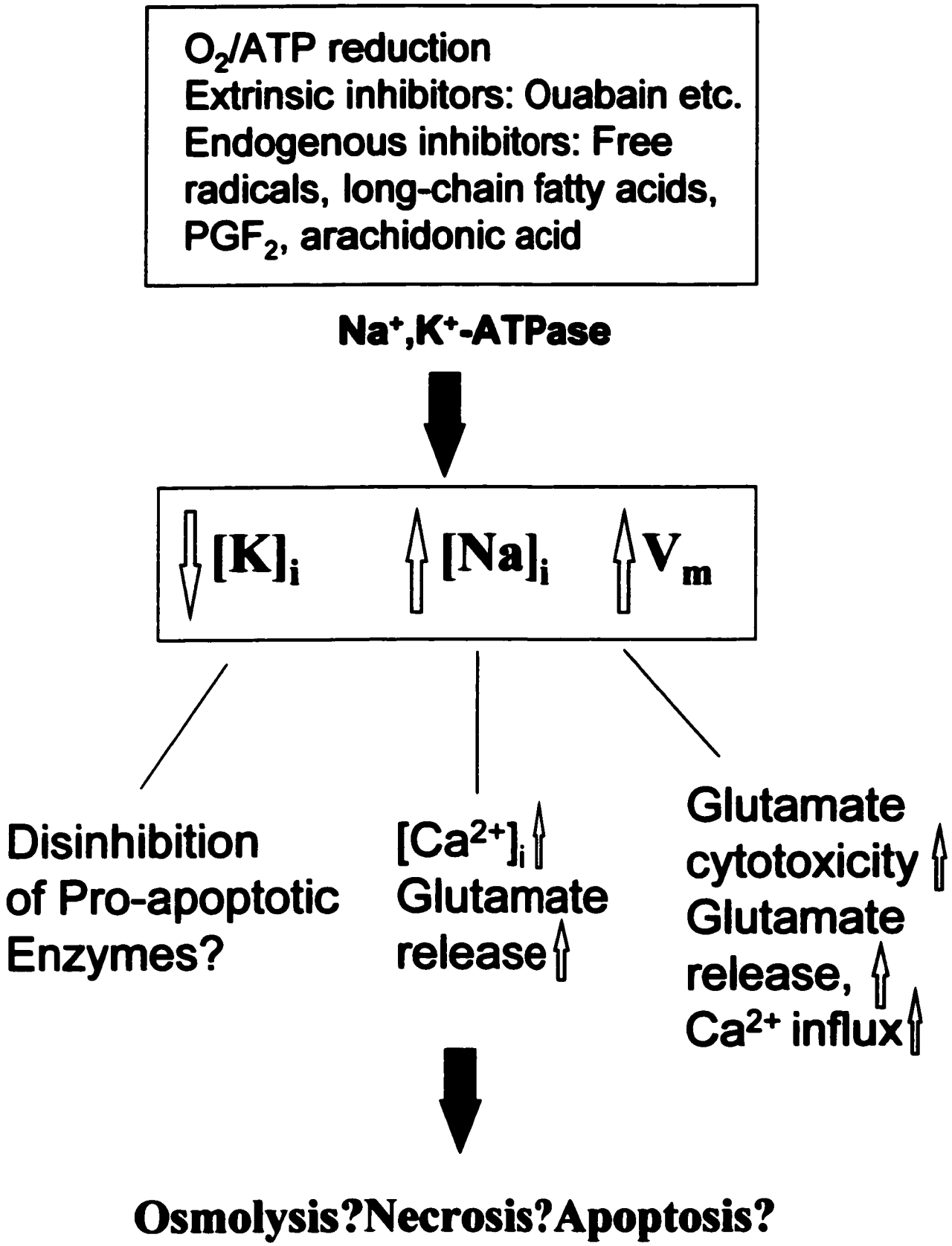
O_2/ATP reduction
Extrinsic inhibitors: Ouabain etc.
Endogenous inhibitors: Free radicals, long-chain fatty acids, PGF_2, arachidonic acid
Na^+,K^+-ATPase
$\downarrow[K]_i$ $\uparrow[Na]_i$ $\uparrow V_m$
Disinhibition of Pro-apoptotic Enzymes?
$[Ca^{2+}]_i\uparrow$ Glutamate release$\uparrow$
Glutamate cytotoxicity$\uparrow$ Glutamate release,$\uparrow$ Ca^{2+} influx$\uparrow$
Osmolysis?Necrosis?Apoptosis?

1.3.1 Glutamate-mediated excitotoxic cell death

One of the most widely accepted theories regarding the mechanism of neuronal cell death following traumatic / ischemic insults is that of excitotoxicity-mediated cell death (Choi, 1992; Choi, 1994; Dugan et al., 1994; Sattler et al., 2001; Skaper et al., 2001). The theory of excitotoxicity initially was put forward based on the observations of Lucas and Newhouse in 1957 (Lucas et al., 1957). They were able to show that retinal neuron cell death was induced upon exposure to glutamate. Olney and coworkers later discovered that glutamate was not the only amino acid capable of inducing neuronal cell death. They found that other "excitatory amino acids, EAAs" were capable of inducing a similar effect (Olney, 1969; Olney et al., 1969). Subsequently, it was determined that glutamate-induced excitotoxic cell death plays a major role in various neurological conditions including but not limited to trauma, stroke and even chronic neurodegenerative states such as Alzheimer's disease (Doble, 1999; Dodd, 2002; Faden et al., 1988; Faden et al., 1989; Grilli et al., 2000; Guo et al., 1999; Ludolph et al., 2000; Rossi et al., 2000; Stys, 1998; Szatkowski et al., 1994).

Cerebral ischemia and traumatic brain injury are associated with an early primary cell death resulting from the physical impact in the case of mechanical trauma or due to edema and hemorrhage in both cerebral ischemia and traumatic brain injury (Ayata et al., 2002; Bernardini et al., 2001; Bernstein et al., 2001; del Zoppo et al., 2000). The initial insult is usually followed by a secondary cascade of downstream molecular and biochemical events leading to cell injury and death (Brott et al., 2000; Lee et al., 1999a). Traumatic / ischemic insults result in widespread energy failure as a result of depletion of the energy stores and a drop in ATP (Lee et al., 1999b; Yoshino et al., 1991), leading to

pump failure (Ross et al., 2000; Stys, 1998). The rise in extracellular glutamate concentration is a result of depolarization-induced release as well as reverse operation of glutamate transporters due to energy failure in addition to collapse of the Na^+ gradient normally used for glutamate re-uptake (Li et al., 2001; Li et al., 2000; Li et al., 1999; Rossi et al., 2000). Intracerebral microdialysis studies have demonstrated a six-fold increase in extracellular glutamate concentration following fluid-percussion injury (a traumatic brain injury model) in the rat, (Demediuk et al., 1989; Hayes et al., 1992; Katayama et al., 1990). Monitoring glutamate levels in extracellular fluid (ECF) of humans suggests that elevation of glutamate is directly proportional to the magnitude of the initial insult particularly in the setting of an elevated intracranial tension (Bullock et al., 1995a; Bullock et al., 1995b; Zauner et al., 1995a; Zauner et al., 1995b). In addition, loss of the Na^+ gradient normally established across cell membranes results in the reverse operation of the Na^+/Ca^{2+} exchanger, which leads to elevation of the cytosolic Ca^{2+} concentration (Stys, 1998).

Glutamate released from pre-synaptic terminals acts on a number of glutamatergic receptors on post-synaptic neurons. Glutamatergic receptors are divided into ionotropic glutamate receptors (iGluRs) linked to ion channels and metabotrobic glutamate receptors linked to guanosine triphosphate (GTP) binding proteins (G proteins) that are associated with activation or inhibition of downstream signal transduction cascades. Ionotropic glutamate receptors are further subdivided into 3 major subtypes, namely *N*-methyl-D-aspartate (NMDA), α-amino-3-hydroxy-5-methyl-4-isoxazol-propionic acid (AMPA) and kainate. Activation of NMDA receptors by glutamate results in calcium ion influx leading to elevation of $[Ca^{2+}]_i$ levels (Madden, 2002; Pin et al., 1995; Schoepp, 1994).

Selective NMDA receptor antagonists have been shown to reduce calcium influx and attenuate cell death in neuronal cell cultures following a brief intense exposure to glutamate (Choi et al., 1988). Calcium influx can also be mediated through activation of AMPA and kainate receptors. However, activation of NMDA receptors results in a rapid rate of calcium influx whereas AMPA and kainate receptor activation result in a slower rate of calcium influx. This difference correlates with the time course of cell death upon exposure to NMDA, AMPA or kainate. Exposure of cultured cortical neurons briefly (3-5 min) to NMDA triggers a rapid and widespread neuronal cell death, "rapidly-triggered excitotoxicity" (Munir et al., 1995). On the other hand, exposure of the same cultured neurons to even high levels of kainate requires hours to induce the same effect, "slowly-triggered excitotoxicity" (Gwag et al., 1997).

1.3.2 Ca^{2+} cytotoxicity

Pathological intracellular Ca^{2+} concentrations have been shown to directly inhibit Na^+, K^+- pump activity (Tobin et al., 1973). In addition, elevated cytosolic Ca^{2+} concentrations result in pathological over-activation of various enzymes leading to cell degradation. For example, calcium-mediated phospholipase A_2 overactivation results in membrane phospholipid breakdown and generation of arachidonic acid. Arachidonic acid is further metabolized into prostaglandins through the cycloxygenase pathway. Both prostaglandins and arachidonic acid are known potent inhibitors of the Na^+, K^+- pump and their levels have been shown to markedly increase following cerebral ischemia (Bonventre et al., 1993; Sapirstein et al., 2000). Intracellular calcium accumulation also results in nitric oxide synthase (NOS) activation leading to generation of nitric oxide

(NO), calpains leading to cytoskeletal breakdown, endonucleases leading to internucleosomal cleavage as well as caspase activation ultimately resulting in neuronal cell death (Chan, 1994; Chan, 1996; White et al., 2000) (Figure 1).

1.3.3 Free radical-mediated toxicity

Free radicals are a normal metabolic product mainly produced as a result of oxidative metabolism in the mitochondria. These are highly reactive molecules with one or more unpaired electrons and are therefore capable of inducing varying degrees of oxidative damage to DNA, lipids and proteins (Cross et al., 1987; Halliwell, 1987). It has been estimated that 2 – 3% of oxygen consumption is utilized in the generation of free radicals (Floyd et al., 1997). The two major types of free radicals that are involved in neuronal ischemic injury are oxygen free radicals and nitric oxide. Since free radicals are a physiological by-product of oxidative metabolism, there are a multitude of enzymes capable of neutralizing their deleterious effects under physiological conditions. Some of these enzymes include superoxide dismutase (SOD), catalase and glutathione peroxidase. Furthermore, free radical scavengers such as glutathione, α-tocopherol and β-carotene have similar free radical neutralizing effects (Cross et al., 1987; Halliwell, 1987).

During ischemia / reperfusion, the endogenous defense mechanisms are overwhelmed by the excessive free radical generation, which ultimately results in DNA and protein damage as well as lipid peroxidation (Murin et al., 2001). The main free radical species produced during ischemia / reperfusion are superoxide (O^{2-}) and NO. Superoxide is mainly produced in the mitochondria as a result of oxygen metabolism through the electron transport chain. This molecule is relatively innocuous and is

normally metabolized to hydrogen peroxide (H_2O_2) in the mitochondria by manganese superoxide dismutase (MnSOD) (Macmillan-Crow et al., 2001). Copper superoxide dismutase (CuSOD) on the other hand metabolizes the cytosolic superoxide. Hydrogen peroxide in turn is converted to H_2O by glutathione peroxidase and catalase (Hosler et al., 1996).

1.3.3.1 Nitric Oxide

Nitric oxide, known also as endothelium-derived relaxing factor (EDRF), mediates vasodilation and relaxation of vascular smooth muscle (Ignarro et al., 1987). Garthwaite and coworkers discovered that EDRF mediates elevation of neuronal cyclic guanosine monophosphate (cGMP) as a result of NMDA receptor activation. EDRF levels were found to be elevated as a result of Ca^{2+} influx through NMDA receptor channels and therefore this molecule was proposed to play an important role in signal transduction cascades as well as cell-cell signaling. Eventually, NO was hypothesized to play an important role in glutamate-mediated excitotoxicity (Garthwaite et al., 1988; Garthwaite et al., 1989).

EDRF or nitric oxide is normally generated from L-arginine through the enzyme nitric oxide synthase (NOS). There are three different isoforms of NOS that have been characterized so far (Bredt et al., 1994; Marletta, 1994). Neuronal NOS (nNOS) and endothelial NOS (eNOS) are both constitutively expressed and are activated in a calcium-dependent manner. Inducible NOS (iNOS) is activated in a calcium-independent manner and is induced mainly through inflammatory and immunological stimuli. All isoforms of NO are upregulated in response to ischemic injury either through elevation of cytosolic

calcium (mediated by nNOS and eNOS) or as a result of the associated inflammatory response (mediated by iNOS activation) (Wiesinger, 2001). In fact, cerebral cortical NO levels increase from a baseline level of 10^{-8} M to approximately 10^{-6} M following transient middle cerebral artery (MCA) occlusion in rats (Malinski et al., 1993). Furthermore, inhibition of nNOS both pharmacologically or through genetic manipulation (gene deletion) infers specific resistance of cultured neurons to NMDA-induced cell death and can also result in a reduction of infarct volume in rats following transient focal ischemia (Dawson et al., 1996; Yoshida et al., 1994).

1.3.3.2 Peroxynitrite

Superoxide reacts with NO to produce peroxynitrite ($ONOO^-$), another highly reactive free radical capable of producing tissue damage (Kooy et al., 1994). These highly reactive oxygen species ultimately result in lipid peroxidation leading to the disruption of neuronal plasma membranes. As previously mentioned, SOD converts superoxide to H_2O_2 and therefore reduces $ONOO^-$ production. Administration of SOD in a form capable of crossing the blood brain barrier is capable of reducing ischemic damage and the associated edema in rat stroke models (Liu et al., 1989). Transgenic mice over-expressing Cu/Mn SOD showed decreased mitochondrial release of cytochrome *c*, attenuated caspase activation and apoptotic cell death following global ischemia in rats (Sugawara et al., 2002).

Inhibition of NO production has been shown to be both neuroprotective as well as neurotoxic. This apparent paradox is borne out of the fact that some NO isoforms reduce neuronal damage while others may exacerbate the process. For example, pre-treatment

with L-N(G)-nitro arginine methyl ester (L-NAME) an NO synthase inhibitor, was found to protect against lipid peroxidation in gerbil brain following cerebral ischemia (Caldwell et al., 1995). However, other studies have demonstrated an enlargement of infarct volume in eNOS knockout mice. This is because nNOS and iNOS isoforms are associated with neurotoxicity while eNOS activation results in cerebral vasodilation, improved cerebral perfusion and therefore neuroprotection (Huang et al., 1994).

The role of oxygen free radicals in post-ischemic neuronal injury can be summarized as follows: Glutamate receptor over-activation results in elevation of $[Ca^{2+}]_i$ leading to stimulation of nNOS and mitochondrial production of superoxide. NO and superoxide react to produce $ONOO^-$, which in turn causes damage to DNA, lipids and proteins.

1.3.4 Role of the mitochondria

There has been a growing body of evidence to support the role of mitochondria as effectors of both apoptotic and necrotic cell death following cerebral ischemia (Puka-Sundvall et al., 2001; Reichert et al., 2001; Sims et al., 2002; Solenski et al., 2002). The various molecular cascades triggered by an ischemic insult may ultimately converge into a common molecular event at the mitochondrial level, namely the mitochondrial permeability transition (MPT). MPT results from opening of a multiprotein pore (mitochondrial permeability transition pore, MPTP) that bridges the inner and outer mitochondrial membranes. Opening of the MPTP results in release of intermembrane proteins such as cytochrome *c* and apoptosis-activating factor (APAF-1), both of which are involved in activation of downstream effectors of apoptosis (Cai et al., 1998). Various

events can trigger MPTP opening including ATP depletion, intracellular Ca^{2+} overload, receptor-mediated death signals and free radicals. The resultant effect may be either apoptosis or necrosis depending on the number of mitochondria involved and ATP availability (Leist et al., 1997). During ischemic injury, generation of free radicals and Ca^{2+} overload both result in the mitochondrial permeability transition which in turn results in further mitochondrial superoxide production, release of mitochondrial Ca^{2+} and energy failure, all known triggers for necrotic cell death. On the other, MPT-induced release of cytochrome *c* and APAF-1 results in the activation of downstream caspases (a family of serine proteases involved in apoptosis) such as caspase-9. As a result, caspase-3 an executor of apoptosis, is finally activated by caspase-9 leading to apoptotic cell death (Bernardi et al., 2001; Shi, 2001; Zamzami et al., 2001).

MPT is also under tight inhibitory control. The Bcl family proteins can either promote or inhibit MPT. For example, Bcl-2 and Bcl-X_L are known inhibitors of MPT and are therefore anti-apoptotic proteins, often deregulated in several neoplastic conditions. On the other hand, Bax and Bcl-X_S are known to promote MPT and are therefore pro-apoptotic proteins. Up-regulation of Bax has been demonstrated in CA1 neurons following transient forebrain ischemia (Ferrer et al., 1998; Krajewski et al., 1995). On the other hand, Bcl-2 infusion using a herpes simplex viral (HSV) vector into the CA1 region resulted in attenuation of CA1 neuronal damage following bilateral common carotid artery occlusion (Lawrence et al., 1997). It should be noted however that Bcl-2 family proteins may exert neuroprotective effects independent of their actions on the MPTP (Green et al., 1998).

1.3.5 Caspases

Caspases or *c*ysteinyl *asp*artate-specific protein*ases* are a family of substrate-specific cysteine proteinases that play a central role in the initiation and execution of apoptosis. Caspases cleave proteins at specific sites adjacent to aspartate residues. They are constitutively expressed as inactive proenzymes that are activated by autoproteolysis or by cleavage through other caspases (Nicholson et al., 1997). So far, 14 members of the caspase family have been identified. Our knowledge of this family of proteases came about through the work of Horvitz and colleagues on *caenorhabditis elegans*. A significant number of cells generated in this worm die during development and the genes inhibiting or promoting this cell death were subsequently identified (*ced* genes) (Ellis et al., 1991). The three main genes identified are *ced-3*, *ced-4* (pro-apoptotic) and *ced-9* (anti-apoptotic). *Ced-9* bears high sequence homology to the mammalian bcl-2 proto-oncogene that is involved in the inhibition of apoptosis. On the other hand, *ced-4* bears high sequence homology to the mammalian *Apaf-1*, while caspase 3 or Yama (the Hindu god of death) bears the highest sequence homology to *ced-3* (Hengartner, 1999; Kaufmann et al., 2001; Spector et al., 1997; Zou et al., 1997).

The involvement of caspases in cell death has been largely delineated through the use of caspase knockout models. Caspase 3 knockouts display a markedly affected cerebral development, with failure of neuronal apoptosis resulting in multiple hyperplastic lesions and disorganized cell deployment particularly in the hippocampus, cortex, striatum, retina and cerebellum (Kuida et al., 1996). These results present strong evidence supporting the crucial role played by caspases in neuronal apoptosis. The mechanisms by which caspases mediate cell death are however not completely

elucidated. However, caspases are believed to mediate cell death by cleaving DNA repair proteins such as poly ADP-ribose polymerase (PARP) and DNA-dependent protein kinase (DNA-PK) as well as proteins involved in mRNA splicing (U1-70 K) and cytoskeletal reorganization (Kumar, 1997).

Caspase-3 appears to play a crucial role during the "execution phase" of apoptosis. The activation of caspase-3 is achieved through a mitochondrial-dependent and a mitochondrial-independent pathway. On the other hand, inhibition of caspase-3 is mediated by caspase-3 inhibitory proteins such as inhibitor of apoptosis proteins 1 and 2 (IAP-1, IAP-2) and neuronal apoptosis inhibitory protein (NAIP) (Holcik et al., 2001; Perrelet et al., 2002).

The mitochondrial-dependent pathway (as previously mentioned) involves release of cytochrome *c* and Apaf-1 into the cytosol. This in turn activates caspase-9, which results in caspase-3 cleavage and activation. On the other hand, caspase-3 may be activated by caspase-8 through a mitochondrion-independent pathway, involving activation of death domain receptors such as Fas and tumor necrosis factor receptor (TNF-R). Increased expression of Fas ligand has been observed after transient MCA occlusion in rats (Herdegen et al., 1998). In addition, recombinant Fas ligand induced apoptosis in primary neurons *in vitro*, while transgenic mice expressing dysfunctional Fas ligand showed infarct volumes significantly smaller than those found in wild-type animals (Martin-Villalba et al., 1999).

Caspase-3 activation has been detected in the setting of cerebral ischemia in several animal models. Two hours following MCA occlusion in mice, Namura et al observed caspase-3 activation, 30 to 60 minutes following reperfusion (Namura et al.,

1998). In a rat 4-vessel occlusion (4VO) model, Chen et al detected caspase-3 activation initially at 4 hours following the transient ischemic insult and the caspase-3 activity thereafter peaked at the 24 to 72 hour time points. In this model, caspase-3 activation was detected in areas where cell death subsequently ensued, namely the hippocampus and caudate / putamen (Chen et al., 1998). Administration of caspase inhibitors attenuated cell death and reduced the infarct volume. In a rat cardiac arrest model, caspase inhibitors reduced the infarct volume and had a therapeutic window of up to 9 hours after reperfusion (Hara et al., 1997).

1.3.6 Calpains

Calpains are a family of Ca^{2+}-dependent cysteine proteases. There are two ubiquitously expressed calpain isoforms in neurons, namely calpain I (μ-calpain) and calpain II (m-calpain). Both calpain isoforms are absolutely dependent on Ca^{2+} for their activation. Calpain I requires 3 to 50 μM of Ca^{2+} for its half maximal proteolytic activity *in vitro*, while calpain II requires a Ca^{2+} concentration of 0.2 to 1 mM (Cong et al., 1989). The physiological role of calpains is not fully understood but they are believed to play a role in neurite outgrowth (Song et al., 1994), long term potentiation (Denny et al., 1990) dendritic remodelling (Faddis et al., 1997) as well as cell motility and migration (Glading et al., 2002).

Under physiological conditions, calpains are activated by increased cytosolic Ca^{2+} concentrations and are inhibited in the presence of the specific endogenous inhibitor, calpastatin. The known substrates for the calpains include microtubule-associated protein 2 (MAP-2), α-spectrin, protein kinase C (PKC) and Ca^{2+}/calmodulin kinase II, all of

which have been shown to be degraded following cerebral ischemia (Johnson et al., 1997; Melloni et al., 1989; Murachi, 1990). Under cerebral ischemic conditions, the pathological elevation of the cytosolic Ca^{2+} concentration results in uncontrolled activation of calpains and consequently cleavage and degradation of plasma membranes (Shi et al., 2000) and cytoskeletal proteins (Kampfl et al., 1996). Plasma membrane and cytoskeletal breakdown results in disruption of cellular integrity, increased membrane permeability and ultimately neuronal cell death.

1.4 Early Tissue Reactive Changes

Early tissue reactive changes are a host of morphological changes that have been observed in ischemia and following ouabain treatment. These include tissue-swelling, vacuolization, cell shape and volume changes and finally cell elimination. To date, no study has provided an in depth analysis of the time line and possible mechanisms for such changes particularly *in vivo*. Furthermore, whether such changes represent the development of a necrotic or apoptotic form of cell death remains the subject of intense debate.

1.4.1 Apoptosis versus Necrosis

Necrosis and apoptosis are two morphologically and biochemically distinct forms of cell death. The decision of whether a cell will die via a necrotic or apoptotic pathway depends in large part on the nature and severity of the insult (Bonfoco et al., 1995). Excitotoxicity with the resultant glutamate release, Na^+ influx and cellular swelling is usually associated with necrosis. The prevailing thought was that ischemic insults in the

central nervous system resulted in excitotoxicity-induced necrotic cell death. Recently however, there has been a growing body of evidence indicating that apoptosis or programmed cell death plays an important role in ischemic brain injury (Chalmers-Redman et al., 1997; Davis et al., 1997; Macaya, 2000).

Necrotic cell death is typically characterized by cellular and organelle swelling, disruption of the plasma membrane and ultimately disintegration of the nucleus and cytoplasmic organelles. Extrusion of the intracellular contents into the extracellular space provokes microglial activation, leucocytic infiltration and activation of an inflammatory response. On the other hand, apoptosis is characterized by an orderly and well-orchestrated series of programmed events ultimately resulting in cell elimination. Morphologically, apoptosis is characterized by cell volume decrease and shrinkage, maintenance of plasma membrane integrity and preservation of cytoplasmic organelles. At the nuclear level, there is compaction and condensation of the chromatin and eventually DNA cleavage into nucleosomes of ~200 base pairs (Martin, 2001; Nijhawan et al., 2000; Olney, 1990; Roy et al., 1999; Rubin, 1997).

Following cerebral ischemia, the mode of neuronal cell death rarely fits into one or the other rigid definitions of necrosis or apoptosis. This created a great deal of confusion and was the subject of intense debate in recent years (Roy et al., 1999). A new concept emerged suggesting that the mode of cell death in the central nervous system following ischemic insults falls along a "continuum" spanning the spectrum of morphological and biochemical signatures of either forms of cell death (MacManus et al., 2000). As will be noted, ischemic insults can trigger a multitude of molecular cascades that are capable of committing a cell to both an apoptotic and/or a necrotic fate.

1.4.2 Role of loss of intracellular K^+ in triggering cell death

Apoptotic cell shrinkage or apoptotic volume decrease (AVD) is commonly mediated through K^+ efflux, which has been shown to occur following Na^+, K^+- pump inhibition (Trimarchi et al., 2002; Xiao et al., 2001). In fact, intracellular K^+ ion concentration was shown to play a key role in the activation of death enzymes. It was shown that K^+ at normal intracellular levels exerts a "tonic suppressive force" on two key apoptotic enzymes, caspase-3-like protease and the internucleosomal DNA cleavage nuclease. Efflux of K^+ with the consequent decrease in intracellular K^+ concentration was shown to disinhibit these two key pro-apoptotic enzymes leading to apoptotic cell death (Hughes et al., 1997). It therefore appears that K^+ not only plays a key role in cell shrinkage, but is also directly involved in the induction of apoptosis. In addition, a recent study demonstrated that cell shrinkage due to disordered volume regulation is an early prerequisite to apoptosis. Blocking K^+ channels was shown to prevent both cell shrinkage as well as apoptotic cell death probably due to K^+ retention (Maeno et al., 2000). The role of intracellular K^+ concentration in triggering cell death *in vivo* has never been examined however, since an *in vivo* technique for such an experiment is lacking. We have attempted to address this issue in our current project by simultaneously infusing ouabain with the broad-spectrum K^+ channel blocker, charybdotoxin into the rat dentate gyrus. Indeed, we show that blocking K^+ channels significantly attenuated the neuronal damage associated with pump inhibition, possibly due to K^+ retention and the consequent inhibition of pro-apoptotic enzymes (see chapter 3).

1.4.3 Tissue swelling, volume regulation and the Na^+, K^+- pump

Volume regulation is a fundamental cell property of paramount importance since cells are continuously responding to intra- and extracellular osmotic perturbations. One of the functions of the Na^+, K^+- pump is the maintenance of cell volume. The Na^+, K^+- pump can achieve steady-state volume regulation by offsetting passive "leaks" of diffusible solutes lost to the extracellular space and thereby restoring the intracellular osmotic pressure. This is known as the "pump-leak balance mechanism" (Macknight, 1988).

1.4.3.1 Regulatory volume decrease (RVD)

When cells are exposed to a hypotonic insult, the cells swell as a result of the osmotic gradient created between the intra- and extracellular compartments. Swelling in turn, triggers a series of volume regulatory mechanisms termed "regulatory volume decrease, RVD" (Hoffmann, 1986; Hoffmann et al., 1989; Lo et al., 1995). RVD is achieved through KCl efflux as a result of activation of K^+ and Cl^- channels. In addition, the electroneutral operation of cotransporters such as the K^+-Cl^- symporter and the K^+-H^+ and Cl^--HCO_3^- antiporters further contribute to the volume decrease (Hazama et al., 2000; Okada et al., 2001). During a swelling emergency, cells rapidly extrude K^+ through the operation of the available K^+ channels. In order to maintain electroneutrality, the simultaneous efflux of anions accompanies K+ efflux. Anion efflux is achieved through the activation of a variety of swelling-activated anion channels, the most ubiquitous and specific of which is the volume-sensitive outwardly rectifying (VSOR) anion channel (Bond et al., 1998; Hazama et al., 2000). The molecular identity of the VSOR channel is

not firmly established, however VSOR activity has been shown to be sensitive to cytosolic free Mg^{2+} and is also largely dependent on the non-hydrolytic binding of ATP (Patel et al., 1998). Recently, this channel was proposed to belong to the ClC family of chloride channels, specifically the ClC-3 channel subtype (Duan et al., 1997).

1.4.3.2 Regulatory volume increase (RVI)

A hypertonic insult, on the other hand, induces cell shrinkage as a result of an osmotic pulling force of the extra- on the intracellular compartment. Osmotic cell shrinkage triggers volume correction mechanisms known as "regulatory volume increase, RVI". Depending on the cell type, RVI is achieved by three different cotransporter-dependent mechanisms all of which result in NaCl and water influx. NaCl influx is mediated either by the parallel operation of the Na^+-H^+ and Cl^--HCO_3^- antiporters or the operation of Na^+-$2K^+$-Cl^- and Na^+-Cl^- symporters (Hara et al., 1999; Su et al., 2002a; Su et al., 2002b).

It should be noted however that the occurrence of cell volume regulation in the face of physiological osmotic changes has been recently challenged. It was shown that the CA1 cells maintained in a brain slice preparation did not undergo volume regulation except in the face of extreme osmotic challenges (Andrew et al., 1997). Furthermore, it was shown that volume regulation occurs in the dendritic region and not in the cell body. It is argued that the data obtained from brain cell cultures exposed to extreme osmotic stress do not accurately reflect physiological shifts in osmolality under *in vivo* conditions (Andrew et al., 1997).

1.4.3.3 Apoptotic volume decrease (AVD)

In contrast to osmosis-induced cell shrinkage and swelling, volume changes associated with necrosis and apoptosis usually occur under normotonic conditions. Cell shrinkage is a major hallmark of apoptotic cell death whereas cell swelling is usually associated with necrosis (Kerr et al., 1972; Wyllie, 1980). Apoptotic cell shrinkage proceeds in two distinct stages. The first stage occurs prior to DNA fragmentation and the formation of apoptotic bodies and is termed apoptotic volume decrease (AVD) (Benson et al., 1996). The second stage is associated with DNA condensation, fragmentation and the formation of the membrane-bound apoptotic bodies that characterize late stages of apoptosis (Benson et al., 1996). AVD presumably occurs through a similar mechanism as RVD that is through the activation of K^+ and Cl^- channels leading to KCl efflux (Maeno et al., 2000). The cell shrinkage associated with AVD proceeds without triggering RVI (or may override it) since cell death is usually associated with impaired volume regulatory mechanisms. Maeno and coworkers showed that AVD results in cell shrinkage due to apoptosis-associated impaired volume regulation. Furthermore, they showed that cell shrinkage is a prerequisite to apoptosis and that blocking cell shrinkage by blocking volume-sensitive K^+ channels can rescue cells from apoptotic cell death (Maeno et al., 2000). Bortner and Cidlowski showed that cells exposed to continuous hypertonic stress can result in the induction of apoptosis in cells lacking the RVI mechanism (Bortner et al., 1996).

1.4.3.4 Necrotic volume increase (NVI)

Necrotic cell death is associated with cell swelling, termed necrotic volume increase (Kroemer et al., 1998). Necrotic insults and dissipation of ATP may lead to impairment of the pump-leak mechanism, as a result of membrane leakage, Na^+ and Cl^- influxes and entry of water into the cell (Lipton, 1999). However, cell shrinkage can also occur due to induction of apoptotic cell death and apoptotic volume decrease (Banasiak et al., 2000). During cerebral ischemia, a lactic acid build up (due to anaerobic metabolism) results in further aggravation of cell swelling. This acidification (lactacidosis) stimulates NaCl influx through activation of the Na^+-H^+ and Cl^--HCO_3^- antiporters (Lomneth et al., 1990; Staub et al., 1990; Staub et al., 1996). Furthermore, swelling is exacerbated under ATP-deficient conditions since the VSOR anion channels are inhibited by decreased intracellular ATP (Oiki et al., 1994).

1.5 Neurogenesis in the dentate gyrus

Two potential areas show considerable promise for the development of novel therapeutic approaches for cerebral traumatic / ischemic damage. The first area involves designing pharmacological interventions that target various points along the ischemic injury cascade (*neuroprotection*). On the other hand, the recent discovery of multipotent stem cells in the central nervous system has led the way to intense investigation into their potential for neural cell replacement. Studying stem cell proliferation and migration following injury can ultimately result in the development of novel strategies directed at reconstruction of damaged neural networks (*neuroregeneration*).

Functional recovery following traumatic or ischemic brain damage is usually limited in adulthood due to the inability of the brain to regenerate itself. On the other hand, injury to other body tissues such as the skin is usually followed by a rapid healing process mainly due to the proliferation of the self-renewing stem cell population located in the deep layers of the epidermis immediately adjacent to the basal lamina. These stem cells are capable of rapid proliferation giving rise to a committed progenitor cell population, which ultimately differentiates into epidermal cells resulting in rapid cell replacement. This same scenario takes place in other body tissues that possess a cellular regenerative capacity (e.g. the bone marrow). Therefore, understanding stem cell biology carries an enormous potential for discovering novel therapeutic strategies for a wide variety of diseases involving cell loss and tissue damage.

1.5.1 Stem cell proliferation in adult dentate gyrus

Neural tissue has widely been viewed as lacking structural plasticity and self-regenerative capacity. Limited functional recovery had been attributed to axonal regeneration mechanisms but generation of new neurons in the adult brain was deemed impossible. This view has been maintained by the clinical observation of brain-injured patients who fail to show any significant functional recovery particularly following diffuse brain damage. However, this dogma has been challenged as a result of the discovery of a multipotent stem cell population in the brains of a variety of adult species such as rats, mice, tree shrews, marmoset monkeys and more recently in adult humans (Arsenijevic et al., 2001b; Eriksson et al., 1998; Gould et al., 2002; Gould et al., 1999; Gross, 2000; Kempermann, 2002; Kempermann et al., 1998; Kempermann et al., 2000;

Kornack et al., 1999). To date, these stem cells have been identified in a number of central nervous system locations, namely the subgranular zone (SGZ) of the dentate gyrus, the subventricular zone (SVZ) adjacent to the lateral ventricles and along the ventricular neuroaxis in the brain and spinal cord (Alonso, 1999; Luskin, 1998; Nait-Oumesmar et al., 1999; Weiss et al., 1996). Recently, generation of new neurons was also documented in the neocortex of adult mice (Magavi et al., 2000).

The stem cells of the SGZ continue to proliferate well into adulthood giving rise to progenitor cells committed to a neuronal or glial cell lineage (Gage et al., 1998; Palmer et al., 1997). Some newly born cells migrate into the superficial regions of the adjacent granule cell layer (GCL) and differentiate into mature granule neurons where they extend projections to their post-synaptic targets, form functional synapses and ultimately integrate into the hippocampal circuitry (Song et al., 2002; Stanfield et al., 1988; van Praag et al., 2002). Scott and co-workers have shown that kindling in rats enhanced neurogenesis by 75-140%, leading to the appearance of numerous newly born granule neurons (Scott et al., 1998). In a global ischemia model, Liu et al found a 12-fold increase in cell birth in the dentate subgranular zone, 1-2 weeks after 10 min bilateral common carotid artery occlusion (Liu et al., 1998). On the other hand, newly born cells in the adult subventricular zone undergo long range cell migration along a tangential migratory pathway known as the rostral migratory stream and end in the olfactory bulb where they differentiate into mature olfactory bulb interneurons (Alvarez-Buylla et al., 1988). The regulation of neural stem cell proliferation, migration and differentiation is mediated through growth factors similar to what occurs during hematopoiesis in the bone marrow (Arsenijevic et al., 1998; Arsenijevic et al., 2001a; Palmer et al., 1999; Qian et al., 1997).

The ability of the adult brain to support stem cell proliferation and the subsequent long range cell migration has pointed to the possibility of utilizing *in vitro* expanded stem cells for transplantation into the adult brain. It remains to be shown that transplanted stem cells will be capable of migrating into areas of brain damage, differentiating into neurons and ultimately reconstructing damaged circuitry (Brustle et al., 1996; Brustle et al., 1999; Jones et al., 1998).

1.5.2 Radial glia in adulthood and during brain development

During the developmental process of corticogenesis, migrating neuroblasts utilize a complex system of radial glial processes as a scaffold that directs them towards their final destination. In the embryonic dentate gyrus, radial glia are situated in the subgranular zone and extend their processes in a radial direction passing through radially oriented columns of granule cells and spanning the molecular cell layer towards the pial surface (Edwards et al., 1990; Rickmann et al., 1987). This radial glial population has been shown to increase in number coincident with waves of progenitor cell proliferation presumably to support the ensuing wave of migration. However, following completion of corticogenesis, these radial glia rapidly disappear, approximately 2 to 3 weeks postnatal, by differentiating into mature stellate astrocytes (Voigt, 1989). Recently, it has been shown that the adult rat dentate gyrus retains a population of radial glial cells in the SGZ, however their processes are retracted in adulthood and only traverse the GCL (Gould et al., 1997b).

Studies have shown that ischemic and epileptic injury and intrahippocampal kainic acid injections increase proliferation of the progenitor cells in the dentate gyrus

(Gould et al., 1997a; Gray et al., 1998; Parent et al., 1997). It is unknown whether this increase in progenitor cell proliferation is associated with a concomitant increase in radial glial cell number, similar to what occurs during corticogenesis. Seki and Arai have reported that the processes of the radial glia-like cells are closely associated with the dendritic growth of the newly generated granule cells in the adult dentate gyrus (Seki et al., 1999). However, to our knowledge at this time, the issue of injury-induced radial glial network remodeling has not yet been directly addressed. Embryonic mouse neocortical neurons, when transplanted into adult mouse primary somatosensory cortex undergoing targeted photolytic cell death, may induce de-differentiation of mature stellate astrocytes into the developmentally transient radial glia and result in the re-expression of the radial glial network (Leavitt et al., 1999). It is possible that the re-expression of the radial glial network is part of an overall intrinsic tissue reparative attempt to support the migration of the newly born cells.

A large body of evidence currently indicate that radial glia are the neural stem cells in the central nervous system. It was shown that radial glia, both during development and in adulthood, are capable of undergoing asymmetric divisions giving rise to a radial glial cell as well as a neural progenitor. The newly generated radial glial cell serves as a stem cell while the neural progenitor migrates along the radial glial process that guides it to its final destination. It is therefore clear that radial glia serve a dual role, generation of new neurons and glia as well as guidance of progenitor cell migration (Alvarez-Buylla et al., 2001; Malatesta et al., 2000; Miyata et al., 2001; Noctor et al., 2002; Tamamaki et al., 2001).

1.6 Objective

To better understand the effects of Na^+, K^+- pump inhibition *in vivo*, we utilized a technique whereby ouabain is directly administered into the dentate gyrus through stereotactic microinfusion. We have developed original methodology for cellular and subcellular tagging *in vivo*, based on fluorescent probe technology. This methodology was subsequently employed in studying cellular and subcellular responses that occur early in the time course following pump inhibition. Fluorescent molecular probes are molecules that are usually non-fluorescent in the aqueous phase but undergo significant fluorescence enhancement upon binding to specific subcellular targets. These subcellular targets include DNA (probed by ethidium bromide, propidium iodide and Hoechst 33342) and membrane phospholipids (probed by the carbocyanine, DiI). The stereotactic intrahippocampal infusion of these fluorescent probes together with ouabain, therefore allows delineation of the cellular and subcellular dynamics *in vivo* following inhibition of the Na^+, K^+- pump.

The aim of the present thesis work therefore is to characterize the early (first 12 hours) cellular and subcellular responses of dentate gyrus neurons and dentate progenitor cells to inhibition of the Na^+, K^+- pump *in vivo*, which to the best of our knowledge has never been done before.

Chapter 2.

A.I. Omar, V.V. Senatorov, and B. Hu. 2001. Sodium - potassium adenosine triphosphatase inhibition enhances membrane accumulation of DiI in rat hippocampus *in vivo*. Neuroscience. 102 (2): 353 – 359.

Title: **Sodium - Potassium Adenosine Triphosphatase Inhibition Enhances Membrane Accumulation of DiI in Rat Hippocampus *In Vivo***

Author: A.I. Omar, V.V. Senatorov, and B. Hu

Origin of Work: Laboratory of Dr. Bin Hu

Loeb Health Research Institute

Ottawa Hospital - Civic Campus

University of Ottawa

Ottawa, Ontario

Canada, K1Y 4E9

Source: *Neuroscience*, Volume 102, Number 2, pages 353-359, January, 2001

Running Title: Rapid DiI Uptake in the Hippocampus

Correspondence: Bin Hu, MD, Ph.D.

Loeb Health Research Institute

1053 Carling Ave

Ottawa Hospital - Civic Campus

Ottawa, Ontario

Canada K1Y 4E9

Tel: 613-761-5355

Fax: 613-761-5330

binh@civich.ottawa.on.ca

Statistics: Text, 25 pages; figures, 3

Abbreviations: CA1, 2, 3 or 4, Cornu Ammonis subfield 1, 2, 3 or 4, respectively; CCD, Charge-coupled device; DiI, 1,1'–dioctadecyl-3,3,3',3'–tetramethylindocarbocyanine perchlorate; GCL, Granule cell layer; H, Hilus; H&E, Hematoxylin and Eosin; MCL, Molecular cell layer; Na^+, K^+, ATPase, Sodium-potassium adenosine triphosphatase; PoDH, Polymorphic interneurons of dentate hilus; TRITC, Tetrarhodamine isothiocyanate.

ABSTRACT

Transient brain ischemia induces significant alterations in lipid structures of neuronal membrane, which is believed to result from lipid peroxidation and free radical attack. Such a membrane structural change may serve as an important histological marker of cell injury. In the present study, we examined how the dynamics of DiI / membrane incorporation may reflect early membrane metabolism and dynamic changes following sodium - potassium pump inhibition. Ouabain (1mM) was stereotactically co-administered with either 1,1'-dioctadecyl-3,3,3',3'-tetramethyl-indocarbocyanine perchlorate "DiI" (50μg/ml) or ethidium homodimer (4μM) into the granule cell layer of the adult rat hippocampus. Tissue was cryosectioned and examined with epifluorescence microscopy at 1, 2, 3, 4, 6, 8, and 72 hours post-injection. Alternate sections were stained with thionine or haematoxylin and eosin to evaluate morphological changes. Ouabain-induced pump inhibition resulted in a dramatic increase in DiI fluorescence in granule cell layer neurons as early as 4 hours post-injection. This increase in DiI incorporation coincided both spatially and temporally with the appearance of reactive changes characterizing early neuronal injury. However, the fluorescence increase was not a result of membrane breakdown because ethidium homodimer, a membrane impermeable nucleic acid probe used for labeling cells with compromised membranes, when applied in a similar fashion, failed to show any fluorescence changes. The results of this study suggest that pump inhibition results in a specific increase in membrane lipophilicity possibly due to altered lipid structure.

Key Words: Fluorescence, Neuron, Dentate Gyrus, Ouabain

INTRODUCTION

One of the earliest events following focal neuronal ischemia is a rapid decline in activity of the energy dependent Na^+, K^+, ATPase pump.[17] Failure of the pump during anoxic/ischemic conditions results in loss of the Na^+ gradient normally established across cell membranes and a reverse operation of the Na^+/Ca^{++} exchanger leading to $[Ca^{++}]_i$ over-accumulation.[14,31,32] Pathological $[Ca^{++}]_i$ levels results in phospholipase enzyme over-activation that produces membrane phospholipid breakdown, changes in membrane phospholipid composition and fluidity and finally, loss of membrane integrity.[2,7,19] This phospholipase over-activation may be mediated via a direct Ca^{++} dependent or a G-protein dependent mechanism resulting from excessive glutamate release.[8,21,35] It is generally believed that such injury-induced alterations in the membrane lipid environment may in turn affect the conformation and functional activities of membrane proteins.[15] Early therapeutic intervention, before such terminal events, is therefore crucial in the determination of the long term neurological sequelae. Following brain ischemia, therapies initiated during the "therapeutic window" (first 4-6 hours) usually carry the most favourable outcome.[26] In this respect, a better understanding of such early processes may aid in the development of new and improved treatment strategies.

Currently, there are few experimental options available by which neuronal membrane dynamic changes following injury can be detected *in situ* in the adult central nervous system. However, carbocyanine dyes have been widely utilized to determine the degree of membrane fluidity through measurements of the DiI lateral mobility along the plane of lipid bilayers.[3] Furthermore, studies using egg yolk phosphatidyl choline liposomes show that the thidiocarbocyanines undergo large fluorescence enhancement in

response to alterations in liposomal phospholipid content.[5] We therefore investigated how the dynamics of DiI / membrane incorporation may reflect early membrane metabolism and dynamic changes induced by Na^+, K^+ pump inhibition. This issue was examined through direct intrahippocampal administration of DiI together with the Na^+, K^+ pump blocker, ouabain. Preliminary results of this study have been reported in an abstract form.[24]

EXPERIMENTAL PROCEDURES

Preparation

Male Long Evans rats (300 - 350 g) were anesthetised with intramuscular injections of 0.2 ml/300 g body weight of a Ketamine (Ketalar®) and Xylazine (Rompun®) mixture according to the following regimen: 4 ml of Ketamine (50 mg/ml) + 1ml of Xylazine (20 mg/ml). After attaining a surgical anaesthetic plane, Halothane (2-3% in 100% oxygen) was used for maintenance throughout the surgery. The anaesthesia, surgical and experimental protocol was approved by the Animal Care Council of the Ottawa Hospital, which ensures conformity with the guidelines of the National Institutes of Health and the Canadian Council on Animal Care. After mounting onto a stereotactic frame, a midsagittal scalp incision was performed, the skull exposed and periosteum removed. A burr hole was drilled into the skull at stereotactic coordinates corresponding to the dentate gyrus granule cell layer (Bregma: - 3.8; Lateral: 2.2; and Ventral to the dura: 3.3).[25]

A borosilicate micropipette was filled from its rear with 1μl (50μg/ml) solution of 1,1'-dioctadecyl-3,3,3',3'-tetramethylindocarbocyanine perchlorate ('DiI'; Molecular Probes Inc, Eugene, OR) and 1μl (1mM) of ouabain (Sigma Aldrich Corp., St. Louis, MO) and then lowered towards the target site. The solution was pressure injected using a 1 ml syringe attached through plastic tubing to the back of the micropipette at a rate of 0.3 - 0.5 μl/ min as monitored through the level of the meniscus through a stereomicroscope. The micropipette was then left in place for 10 - 15 min to minimize backdiffusion of the solution. The contralateral hippocampus was used as a control, where 1μl (50μg/ml) of DiI together with 1μl of physiological saline were injected at

identical stereotactic coordinates (Fig.1). In some experiments, DiI was substituted with ethidium homodimer (EthD-1, 4μM; Molecular Probes Inc., Eugene, OR) to test for the specificity of the dye. At the end of the procedure, the burr hole was filled with bone wax and the scalp sutured.

(Fig 1. near here)

Tissue processing

A series of 14 rats were used during this experiment. At varying time points following the injections (1, 2, 3, 4, 6, 8, and 72 h, n=2 at each time point), rats were deeply anaesthetized with sodium pentobarbital (Somnotol®, 0.22 ml/100 g body weight, i.p.) and were then transcardially perfused with 200 ml of 4% paraformaldehyde in 0.1 M phosphate buffer at pH 7.4, following a brief flushing of the vasculature with 60 ml of saline. Brains were immediately cryosectioned at 30μm spacing. Sections were then mounted on gelatin-coated slides, and examined uncoverslipped. Alternate sections were randomly selected for staining with thionine (0.25 %) or haematoxylin & eosin (H&E) in order to examine cell morphology.

Data analysis

Thionine and H&E stained sections were examined with a light microscope, while DiI and ethidium homodimer were visualized using an Olympus epifluorescence (IX50) microscope. Images were captured through a tetrarhodamine isothiocyanate (TRITC) filter (Chroma Technology Corporation, Vermont, Brattleboro, U.S.A.) using a Sony

CCD colour video camera connected to a PC equipped with a framegrabber and image acquisition software (Northern Exposure, Empix Imaging Inc., Mississauga, Canada).

Quantitative analysis of images was performed on a Macintosh [Power PC] computer with NIH Image 1.62 software (U.S. National Institutes of Health; available from the Internet by anonymous ftp from zippy.nimh.nih.gov). Fluorescence yield measurements were obtained from 10 sections, 60μm apart. Data analysis was performed by an examiner blinded to the interventions. Data is expressed as mean ± SEM. ANOVA and Student's *t*-test were used for statistical analysis and results were considered statistically significant at $p < 0.05$.

RESULTS

Temporal profile of DiI fluorescence changes

Time series measurements at 1, 2, and 3 hours following ouabain injection revealed minimal labeling and DiI fluorescence in both ouabain treated and non-treated hippocampi in all six rats (data not shown). A sharp rise in DiI fluorescence was however clearly seen in pump-inhibited GCL, 4 hours post-injection (Fig. 2a). The fluorescence yield from the ouabain injected side was 30.87 ± 3.81 versus 2.41 ± 1.49 from the saline injected side, which in turn gave rise to ~15 fold difference, ($p < 0.0001$). This surge in DiI fluorescence continued at the 6 and 8 hour time points. Fluorescence yield from the ouabain treated side at the 6 hr time point was 36.80 ± 10.60 versus 15.20 ± 3.80 from the control side, ($p < 0.05$), while 8 hr post-injection, fluorescence yield from the ouabain treated side was 52.22 ± 8.30 versus 13.37 ± 3.76 from the saline treated control, giving rise to a 2 - 4 fold difference ($p < 0.001$). At 72 hours, however, the DiI fluorescence yield from the ouabain treated side (33.80 ± 3.00) was significantly lower than the saline treated control (53.20 ± 5.10; $p < 0.01$) representing an approximately 35% drop from the previous 8 hour value. Furthermore, in contrast to DiI, the membrane impermeable nucleic acid probe, ethidium homodimer, when applied in a similar fashion failed to show detectable labeling in GCL neurons (data not shown).

(Fig.2 near here)

DiI fluorescence enhancement coincides spatiotemporally with reactive cell change

To examine a possible relationship between DiI fluorescence and reactive neuronal changes that usually precede acute excitotoxic cell death, we analysed the nissl counter-stained sections. Four hours following pump inhibition, we found typical reactive neuronal changes, which included cell volume and shape alterations, chromophilia and vacuolation (Fig. 2c,d). The GCL neurons exhibited a dramatic volumetric decrease while polymorphic neurons of the dentate hilus (CA4) changed their shape from rounded to triangular or fusiform. This reactive change appeared no earlier than 4 hours following Na^+, K^+-ATPase inhibition. Interestingly, the GCL related surge in DiI fluorescence was also initially observed at the 4 hour time point, suggesting a close temporal relationship between the two phenomena.

Decrease in DiI fluorescence yield coincides spatiotemporally with excitotoxic cell loss

The significant decrease in fluorescence yield in the GCL at 72 hours (Fig. 3a,b) could well be attributed to the excitotoxic cell death, which usually follows Na^+, K^+-ATPase inhibition. Indeed, a dramatic cell loss of ouabain-treated GCL neurons was found at 72 hours when H&E stained sections were analysed (Fig. 3c,d). The cell loss was more pronounced in the polymorphic interneurons of the dentate hilus, which showed a total cell loss and replacement of this layer with large vacuoles (Fig. 3c).

(Fig. 3 near here)

DISCUSSION

Inhibition of Na^+,K^+-ATPase by ouabain has been used as an experimental model to study ischemic cell death, which typically takes place in about 48 hours following an ischemic insult in the rat hippocampus.[16,28] Our results showed that ouabain-induced Na^+, K^+-ATPase inhibition resulted in a drastic increase in DiI fluorescence 4 hours following administration of ouabain. It also shows a close temporal relationship with the onset of early reactive cell changes similar to that observed in ischemic tissue.

Dynamics of DiI / membrane uptake may reflect structural changes in phospholipid bilayer

Previous biophysical studies showed that the fluorescence intensity of cyanine dyes within a lipid bilayer can be affected by large changes in transmembrane voltage.[29] However, two lines of evidence suggest that this mechanism may not play a dominant role in ouabain-induced DiI fluorescence surge. Firstly, the cationic carbocyanine dyes have been previously shown to accumulate on hyperpolarized membrane and, upon membrane repolarization, to translocate (flip-flop) within the lipid bilayer giving rise to a voltage-dependent fluorescence enhancement.[20] Alternatively, fluorescence may change due to dye quenching.[9] Since ouabain is known to induce a large membrane depolarization (rather than hyperpolarization) in neurons,[27] the above voltage mechanism cannot explain our results. Secondly, ouabain-induced membrane depolarization occurs within minutes after drug application;[33] yet, DiI surge reported here was only evident after a 4 h delay. Finally, our data suggest that the DiI fluorescence enhancement reflects a specific structural change in the phospholipid bilayer rather than a nonselective loss of

membrane integrity since the membrane impermeable fluorescent probe, ethidium homodimer which has been widely utilized in assessing membrane integrity,[4] failed to permeate through GCL neuronal membranes at time points where the DiI fluorescence enhancement took place. This negative labeling by ethidium homodimer however, does not rule out the possibility of a minor degree of membrane permeability change. Indeed, we have shown in a previous study, that the co-infusion of ouabain with the membrane impermeable nucleic acid intercalating dye, ethidium bromide into the dentate GCL results in a faint fluorescence signal from the treated granule cells.[23] This signal was evident as early as one hour post-infusion and thereafter increased in a time dependent manner. The faint labeling with ethidium bromide likely reflects a mild increase in membrane permeability. However, since the ethidium homodimer molecule is bulkier and less membrane permeable than ethidium bromide, negative labeling with ethidium homodimer likely indicates that overt membrane disintegration did not take place at these early time points.

Other factors that should be taken into consideration when interpreting these data, include the possibility of dye diffusion from the injection site prior to the onset of membrane disintegration. If ethidium homodimer rapidly diffused away from the injury site, later membrane disintegration may not be detected. On the other hand, prolonged fixation periods may interfere with the stability of the dye within the tissues. To overcome this possible source of error, we eliminated the post-fixation step, and brains were immediately sectioned following transcardial perfusion.

Morphological changes accompanying DiI fluorescence surge

Four hours following pump inhibition, GCL neurons exhibited typical reactive changes similar to the previously reported early ischemic neuronal changes,[34] characterized by cell volume and shape alterations, chromophilia and vacuolation. Remarkably, the ouabain-induced DiI fluorescence surge has also been detected at the 4 hour time point suggesting a probable mechanistic linkage. However, whether such a temporal co-incidence between the enhanced DiI membrane incorporation and early reactive neuronal shape changes reflects alterations of membrane volume and/or surface area remains to be determined. Nissl stained sections at the 4 hour time point revealed two types of cell shape alterations. Granule cells have apparently undergone shrinkage while neighbouring neurons in the dentate hilus have undergone, in most instances, a change from a rounded to a triangular or fusiform shape. Nevertheless, DiI fluorescence yields from both regions were comparable, suggesting membrane surface area may not be a critical factor. Cell shrinkage following inhibition of the Na^+,K^+-ATPase rather than swelling has been documented before, which has been attributed to a reversed operation of a Na^+/Ca^{2+} exchanger and the resultant efflux of taurine, glycine and other amino acids.[30]

Our data show that at the 72 hour time point, DiI fluorescence yield dropped from the ouabain treated granule cells when compared to the saline treated control, which morphologically coincided with complete granule cell loss as revealed through H&E staining. The continued rise in DiI florescence yield from the saline treated granule cells at 72 hours post-injection, can be explained by a slow diffusion of the dye in the

extracellular space and its continued incorporation as well as lateral diffusion into neuronal membranes under physiological conditions.[13]

Possible mechanisms underlying DiI enhancement following neuronal Na^+,K^+ pump inhibition

A possible mechanism that may account for membrane accumulation of DiI may be related to membrane lipid fluidity. Three lines of argument support this possibility. First, increase in membrane fluidity or lipophilicity is invariably associated with large enhancement of DiI lateral mobility.[3] Second, enhancement of membrane fluidity has been reported in ischemic tissue within 2-4 hours following reperfusion,[11] a time window similar to one reported here. Third, increase in membrane fluidity can be ascribed to lipid peroxidation and the production of free radicals,[7] both factors found in the ouabain model of ischemia.[17]

The DiI molecule is composed of a fluorophore component and a side chain similar to the fatty acyl chain of phospholipid molecules. Using fluorescence polarization microscopy, Axelrod[1] showed that during cell uptake, the DiI molecule inserts its side chain into the outer leaflet of the phospholipid bilayer with an orientation perpendicular to the plane of the membrane while its fluorophore component becomes oriented in a parallel direction on the surface of the plasma membrane. Since under normal physiological conditions there is a continuous turnover of membrane lipids, their rate of breakdown being normally counterbalanced by their rate of synthesis,[18] a higher rate of membrane disposition from intracellular stores may be expected during phospholipase (activated at pathological levels during anoxic/ischemic conditions) mediated membrane

breakdown. In addition, other brain defence mechanisms may come into play, such as activation of superoxide dismutase, catalase and glutathione peroxidase - antioxidant enzymes that are involved in free radical elimination.[7] Such membrane repair mechanisms may account for the failure to detect any differences in DiI fluorescence prior to the 4 hour time point. In this regard, it may be worth mentioning that during this same time window, neuroprotective agents are found to be most effective.[26] In this context, the increase in DiI fluorescence yield following ouabain infusion may be explained by a preferential redistribution of the DiI molecules from the aqueous phase into the damaged membranes. The tight parallel packing of the membrane phospholipid molecules may be lost as a result of membrane damage leading to accommodation of a higher number of DiI molecules per membrane unit area which may therefore account for the enhanced time dependent DiI / lipid incorporation. In strong agreement with this hypothesis, a recent study employing a lipid-specific spin probe coupled with electron paramagnetic resonance imaging, demonstrated a decrease in lipid order and loosening of the tight packing of the phospholipid acyl chains within the interior of gerbil synaptosomal membrane, 3-12 hours following transient carotid occlusion.[11] This was attributed to the formation of peroxides within the membrane as a result of oxygen free radical attack as well as the phospholipase induced cleavage of damaged alkyl side chains resulting in an increase in the space available between phospholipid molecules. Alternatively, an alteration in the membrane phospholipid composition together with the associated changes in membrane fluidity, may well explain the increase in the fluorescence yield of DiI already present in the membrane. This possibility is supported by a previous study that indeed showed a strong correlation between fluorescence

changes of cyanine dyes incorporated into biological membranes and changes in membrane phospholipid content.[5] In fact, membrane content of phosphatidylcholine, phosphatidylethanolamine and phosphatidylserine has been shown to significantly change in response to ischemia / reperfusion injury.[6]

The translocation or "flip-flop" of phosphatidylserine from the cytosol to the outer leaflet of lipid bilayers is also seen during the early stages of apoptosis. A recent study employing an Annexin V (a phospholipid binding protein with high affinity to phosphatidylserine) labeling assay showed that following a hypoxic-ischemic insult, Annexin V binding increases in the CA1 region of the rat hippocampus, 48 -168 hours post-insult.[36] In addition, a study of a B-cell lymphoma line indicated that phosphatidylserine expression on the outer leaflet of plasma membranes and the loss of membrane asymmetry may be an early and reversible apoptotic event.[12] In agreement with these studies, our data demonstrate morphological features suggestive of apoptosis together with a delayed onset of membrane changes, albeit at a more rapid rate which may possibly reflect the more severe nature of the insult as well as the particular hippocampal field involved.

Degradation of membrane phospholipids may in addition play an important role in the pathogenesis of neurodegenerative disorders such as Alzheimer's disease. Studies of the plasma membrane of Alzheimer's disease temporal cortex have shown a defect of lipid composition in the form of a decrease in the ratio of plasmalogen to nonplasmalogen ethanolamine glycerophospholipids.[10,22,37] This altered ratio has been shown to result in a change in the critical temperature at which the lipid bilayers remain stable, which may differ significantly from the ambient physiological temperature resulting in

destabilization of the neuronal membranes involved in the neurodegenerative process.[10,22,37] It follows therefore that studying the early neuronal membrane changes may provide significant insight into the mechanisms underlying various pathophysiological states, including but not limited to ischemic and neurodegenerative conditions.

CONCLUSION

In summary, we show that by co-application of ouabain, DiI fluorescence signals are intensified by 3-15 fold within a short period of time. This data suggests that DiI can serve as a useful marker for revealing early membrane damage *in vivo*. However, validity of DiI as a marker for membrane ischemic damage may be further addressed through eliciting similar responses in models employing interruption of blood flow such as middle cerebral artery occlusion.

ACKNOWLEDGEMENTS

This work was supported by the Medical Research Council (MRC) of Canada and partially by the Heart and Stroke Foundation of Canada. We wish to acknowledge Mr. D.M. Mooney for his assistance with analysing the data.

REFERENCES

1. Axelrod, D. (1979). Carbocyanine dye orientation in red cell membrane studied by microscopic fluorescence polarization. *Biophys. J.* **26**, 57-574.

2. Bonventre, J. V. (1997). Roles of phospholipases A2 in brain cell and tissue injury associated with ischemia and excitotoxicity. *J. Lipid Mediat. Cell Signal.* **17**, 71-79.

3. Boullier, J. A., Brown, B. A., Bush, J. C. Jr. and Barisas, B. G. (1986). Lateral mobility of a lipid analog in the membrane of irreversible sickle erythrocytes. *Biochim. Biophys. Acta*. **856**, 301-309.

4. Decherchi P., Cochard P. and Gauthier P. (1997) Dual staining assessment of Schwann cell viability within whole peripheral nerves using calcein-AM and ethidium homodimer. *J. Neurosci. Methods* **71**, 205-213.

5. Deleers, M., Servais, J. P., de Laveleye, F. and Wulfert, E. (1984). Effect of lipid composition changes on carbocyanine dye fluorescent response. *Biochem. Biophys. Res. Commun*. **123**, 178-185.

6. Enseleit, W.H., Domer, F.R., Jarrott, D.M., and Baricos, W.H. (1984) Cerebral phospholipid content and Na+,K+-ATPase activity during ischemia and postischemic reperfusion in the mongolian gerbil. *J. Neurochem.* **43**, 320-327.

7. Farooqui, A. A. and Horrocks, L. A. (1998). Lipid peroxides in the free radical pathophysiology of brain diseases. *Cell. Mol. Neurobiol.* **18**, 599-608.

8. Ferguson, J. E. and Hanley, M. R. (1991). The role of phospholipases and phospholipid-derived signals in cell activation. *Curr. Opin. Cell Biol.* **3**, 206-212.

9. Freedman, J. C. and Hoffman, J. F. (1979). The relation between dicarbocyanine dye fluorescence and the membrane potential of human red blood cells set at varying Donnan equilibria. *J. Gen. Physiol.* **74**, 187-212.

10. Ginsberg, L., Xuereb, J.H. and Gershfeld, N.L. (1998) Membrane instability, plasmalogen content, and Alzheimer's disease. *J. Neurochem.* **70**, 2533-2538.

11. Hall, N. C., Carney, J. M., Cheng, M. S. and Butterfield DA. (1995). Ischemia/ reperfusion-induced changes in membrane proteins and lipids of gerbil cortical synaptosomes. *Neuroscience.* **64**, 81-89.

12. Hammill, A.K., Uhr, J.W., Scheuermann, R.H. (1999) Annexin V staining due to loss of membrane asymmetry can be reversible and precede commitment to apoptotic death. *Exp. Cell Res.* **251**, 16-21.

13. Honig, M. G. and Hume, R. I. (1989). DiI and diO: versatile fluorescent dyes for neuronal labelling and pathway tracing. *Trends Neurosci.* **12**, 333-341.

14. Kiedrowski, L. (1999) N-methyl-D-aspartate excitotoxicity: relationships among plasma membrane potential, Na(+)/Ca(2+) exchange, mitochondrial Ca(2+) overload, and cytoplasmic concentrations of Ca(2+), H(+), and K(+). *Mol. Pharmacol.* **56**, 619-632.

15. Lee, A. G. (1998). How lipids interact with an intrinsic membrane protein: the case of the calcium pump. *Biochim. Biophys. Acta.* **1376**, 381-390.

16. Lees GJ, Lehmann A, Sandberg M, Hamberger A. The neurotoxicity of ouabain, a sodium-potassium ATPase inhibitor, in the rat hippocampus. *Neurosci. Lett.* **120**, 159-162.

17. Lees, G. J. (1991). Inhibition of sodium-potassium-ATPase: a potentially ubiquitous mechanism contributing to central nervous system neuropathology. *Brain Res. Brain Res. Rev.* **16**, 283-300.

18. Lehninger, A. L., Nelson, D. L. and Cox, M. M. (1993). *Principles of Biochemistry*, 2nd edn, p. 254, Worth Publishers, New York.

19. Martin, L. J., Al-Abdulla, N. A., Brambrink, A. M., Kirsch, J. R., Sieber, F. E. and Portera-Cailliau, C. (1998). Neurodegeneration in excitotoxicity, global

cerebral ischemia, and target deprivation: A perspective on the contributions of apoptosis and necrosis. *Brain Res. Bull.* **46**, 281-309.

20. Melikyan, G. B., Deriy, B. N., Ok, D. C. and Cohen, F. S. (1996). Voltage-dependent translocation of R18 and DiI across lipid bilayers leads to fluorescence changes. *Biophys. J.* **71**, 2680-2691.

21. Nemoto, E. M. and Chavko, M. (1993). Membrane lipid degradation during ischemia and impact on the monolayer surface pressure area diagram (SPAD). *Mol. Chem. Neuropathol.* **19**, 25-35.

22. Nitsch, R.M., Blusztajn, J.K., Pittas, A.G., Slack, B.E., Growdon, J.H. and Wurtman, R.J. (1992) Evidence for a membrane defect in Alzheimer disease brain. *Proc. Natl. Acad. Sci. U. S. A.* 89, 1671-1975.

23. Omar, A.I., Senatorov, V.V., Hu, B. (2000) Ethidium bromide staining reveals rapid cell dispersion in the rat dentate gyrus following ouabain-induced injury. *Neuroscience.* **95**, 73-80.

24. Omar, A. I., Senatorov, V. V. and Hu, B. (1999). Enhanced membrane uptake of a lipophilic fluorescent probe following intrahippocampal ouabain administration: a possible *in vivo* marker of membrane damage. *Soc. Neurosci. Abstr.* **25**, 995.

25. Paxinos, G. and Watson, C. (1998). *The Rat Brain in Stereotaxic Coordinates.* 4th edn., Academic Press, Sydney.

26. Pulsinelli, W. A., Jacewicz, M., Levy, D. E., Petito, C. K. and Plum, F. (1997). Ischemic brain injury and the therapeutic window. *Ann. N. Y. Acad. Sci.* **835**, 187-193.

27. Senatorov, V. V. and Hu, B. (1997). Differential Na^+,K^+-ATPase activity in rat lemniscal and non-lemniscal auditory thalami. *J. Physiol.* **502**, 387-395.

28. Scheufler, E., Urenjak, J., Osikowska-Evers, B., Beile, A., Guttmann, I., Wilffert, B., Tegtmeier F. and Peters, T. (1992). Ouabain-induced changes of calcium and potassium in slices of hippocampus of the rat: comparison to hypoxia and effect of R 56865. *Neuropharmacology.* **31**, 481-486.

29. Sims, P. J., Waggoner, A. S., Wang, C. H. and Hoffman, J. F.(1974). Studies on the mechanism by which cyanine dyes measure membrane potential in red blood cells and phosphatidylcholine vesicles. *Biochemistry.* **13**, 3315-3350.

30. Smith, T. W., Rasmusson, R. L., Lobaugh, L. A. and Lieberman M. (1993). Na^+/K^+ pump inhibition induces cell shrinkage in cultured chick cardiac myocytes. *Basic Res. Cardiol.* **88**, 411-420.

31. Stys, P.K., Sontheimer, H., Ransom, B.R., Waxman, S.G. (1993) Noninactivating, tetrodotoxin-sensitive Na+ conductance in rat optic nerve axons. *Proc. Natl. Acad. Sci. U. S. A.* **90**, 6976-6980.

32. Stys, P.K., Waxman, S.G., Ransom, B.R. (1992) Ionic mechanisms of anoxic injury in mammalian CNS white matter: role of Na+ channels and Na(+)-Ca2+ exchanger. *J. Neurosci.* **12**, 430-439.

33. Tanaka, E., Yamamoto, S., Kudo, Y., Mihara, S. and Higashi, H. (1997). Mechanisms underlying the rapid depolarization produced by deprivation of oxygen and glucose in rat hippocampal CA1 neurons in vitro. *J. Neurophysiol.* **78**, 891-902.

34. Towfighi, J., Zec, N., Yager, J., Housman, C. and Vannucci, R. C. (1995). Temporal evolution of neuropathologic changes in an immature rat model of cerebral hypoxia: a light microscopic study. *Acta Neuropathol. (Berl.)* **90**, 375-386.

35. Wieloch, T. and Siesjo, B. K. (1982). Ischemic brain injury: the importance of calcium, lipolytic activities, and free fatty acids. *Pathol. Biol. (Paris).* **30**, 269-277.

36. Walton, M., Sirimanne, E., Reutelingsperger, C., Williams, C., Gluckman, P. and Dragunow, M. (1997) Annexin V labels apoptotic neurons following hypoxia-ischemia. *Neuroreport.* 22, 3871-3875.

37. Wells, K., Farooqui, A.A., Liss, L. and Horrocks, L.A. (1995) Neural membrane phospholipids in Alzheimer disease. *Neurochem. Res.* **20**, 1329-1333.

Fig. 1. Experimental configuration for Ouabain and DiI or ouabain and ethidium homodimer co-injection into the dentate gyrus granule cell layer (GCL). The image is of a Nissl stained section of the dentate gyrus captured at a level corresponding to the plane of the stereotactic injection site. Arrowheads represent micropipette tracks. GCL: granule cell layer; MCL: molecular cell layer; H: hilus; CA1, 2 and 3: cornu ammonis 1, 2 and 3 respectively.


MCL
H

Fig. 2. Ouabain-induced DiI fluorescence surge and morphological changes 4 hours post-injection. (a) Shows the fluorescence signal obtained from the GCL neurons. Note the dramatic ouabain-induced increase in DiI incorporation and fluorescence yield (30.87 ± 3.81; n=2) compared to the saline treated GCL (2.41 ± 1.49; b, arrows). (c) Nissl-stained section from the ouabain treated hippocampus shows reactionary response characterized by shrinkage of granule cells. (d) Nissl-stained section of the contralateral saline treated hippocampus where cells retain normal morphological appearance. GCL: granule cell layer; MCL: molecular cell layer; H: hilus. Scale bars: 100μm.

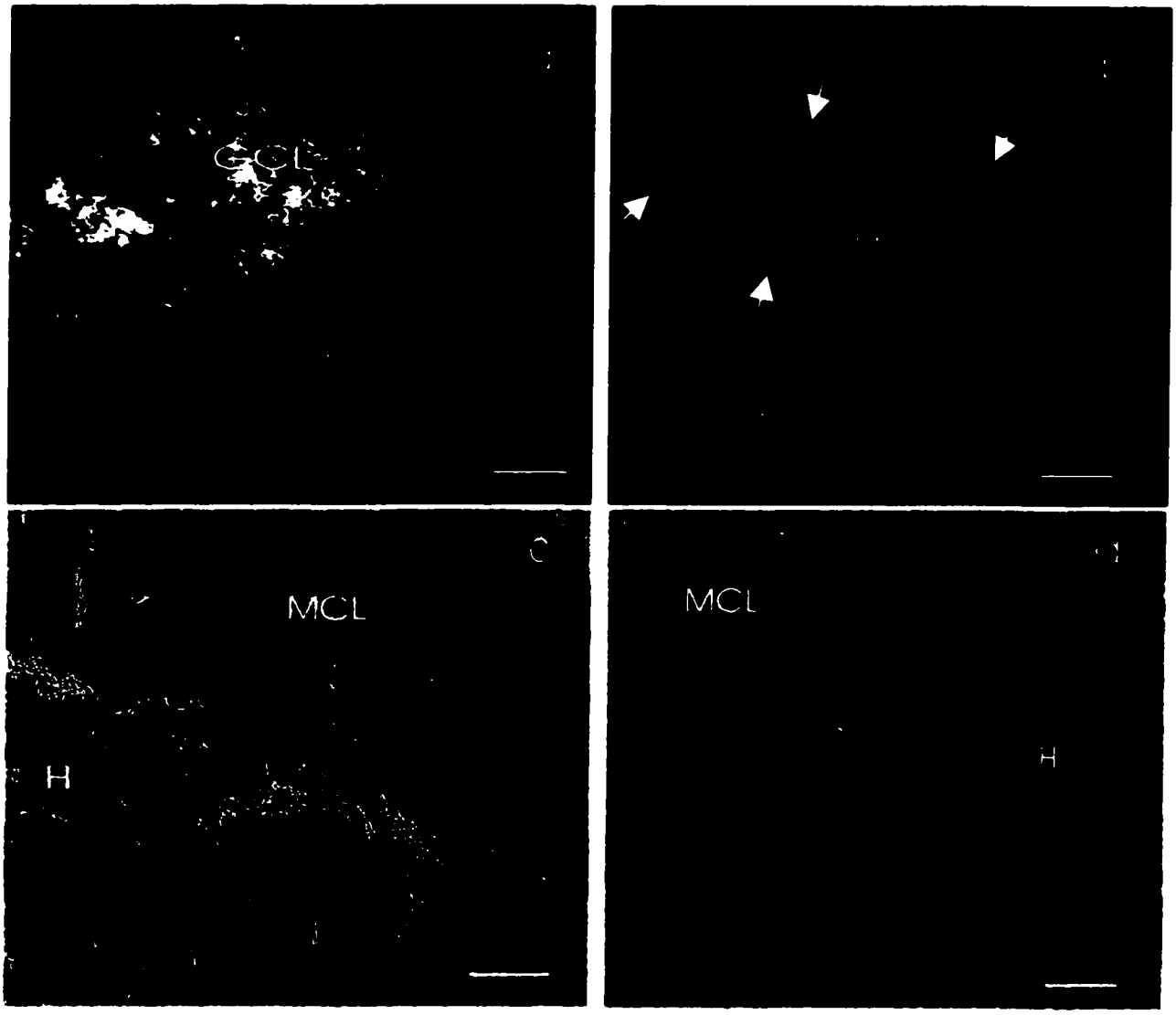
GCL
MCL
H
MCL
H

Fig. 3. Reduction in ouabain-induced DiI fluorescence and cell death in the granule cell layer. (a) Fluorescence from ouabain-treated GCL neurons exhibited reduced level of signals (arrows), 72 hours following Na^+, K^+- ATPase inhibition (33.80 ± 3.00; n=2). (b) Shows a corresponding area from the DiI/saline treated GCL neurons 72 hours post-injection (53.20 ± 5.10). (c) Image of an H&E stained section showing GCL neuronal loss 72 hours following Na^+, K^+- ATPase inhibition. Note the complete loss of the polymorphic neurons of the dentate hilus and their replacement with large vacuoles (arrows) and the glial infiltration of the hilar and molecular cell layers. (d) Image of an H&E stained section showing saline treated (control) hippocampus 72 hours following surgery. Note the preservation of hippocampal neurons and their healthy morphological appearance. GCL: granule cell layer; MCL: molecular cell layer; PoDH: polymorphic dentate hilus. Scale bars: 250μm.

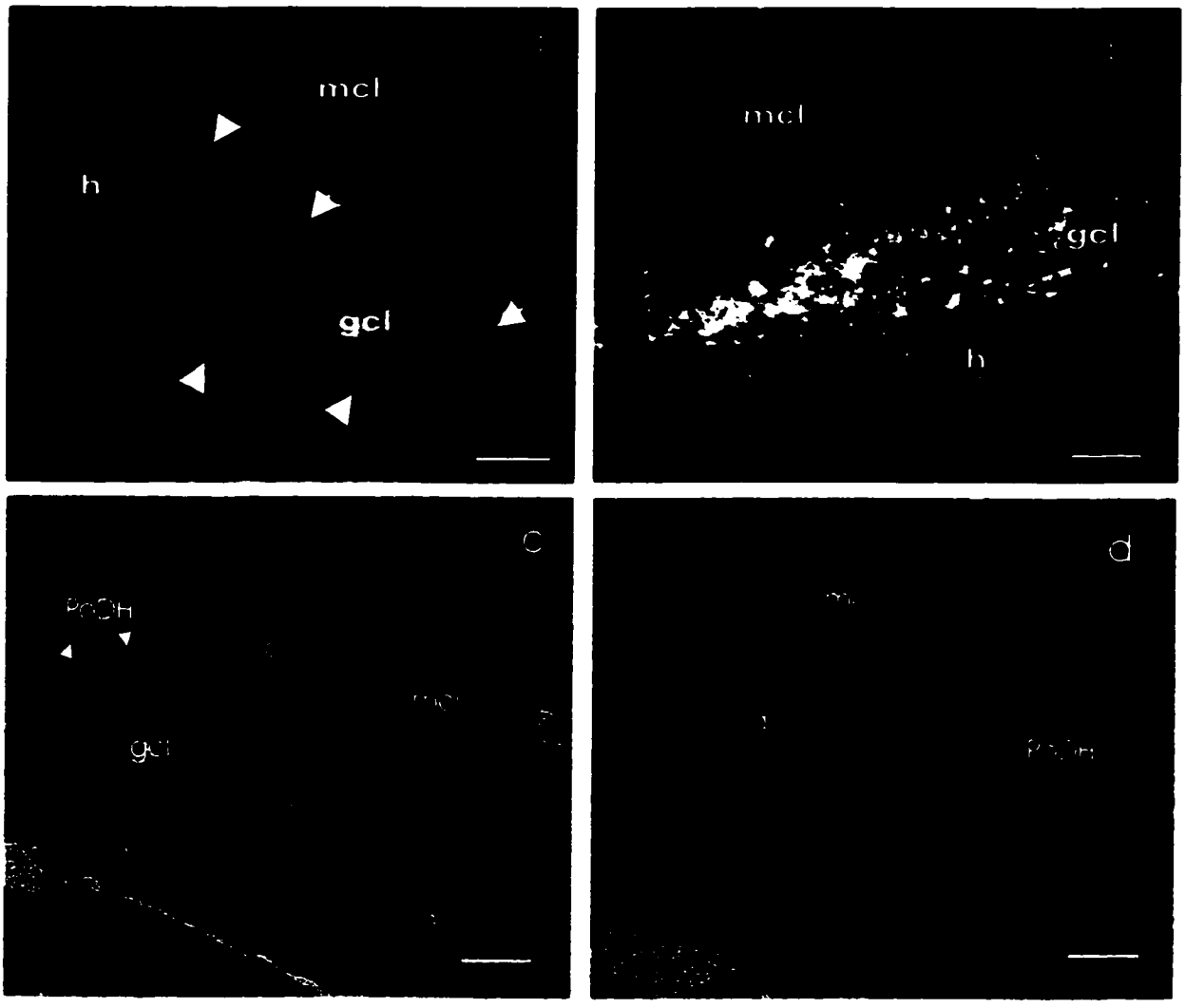
mcl
h
gcl
mcl
gcl
h
c
PrCH
gcl
d

Chapter 3.

A.I. Omar and B. Hu. Co-development of necrosis and apoptosis in rat hippocampal dentate gyrus following Na^+,K^+- pump inhibition. To be submitted to Experimental Neurology.

Title: **Co-Development of Necrosis and Apoptosis in Rat Hippocampal Dentate Gyrus Following Na^+, K^+- Pump Inhibition.**

Author: A.I. Omar and B. Hu

Origin of Work: Laboratory of Dr. Bin Hu

Loeb Health Research Institute

Ottawa Hospital - Civic Campus

University of Ottawa

Ottawa, Ontario

Canada, K1Y 4E9

Running Title: Co-development of necrosis and apoptosis

Correspondence: Bin Hu, MD, Ph.D.

Loeb Health Research Institute

1053 Carling Ave

Ottawa Hospital - Civic Campus

Ottawa, Ontario

Canada K1Y 4E9

Tel: 613-761-5355

Fax: 613-761-5330

binh@civich.ottawa.on.ca

Statistics: Text, 31 pages; figures, 4

ABSTRACT

The mode of cell death following an acute ischemic or traumatic insult to the brain remains a controversial issue. Studies have shown that both necrotic and apoptotic cell death may occur in the brain following such insults (Fukuda et al., 1999; Sheldon et al., 2001; Zeng et al., 2000; Kazahari et al., 1996; Guglielmo et al., 1998; Portera-Cailliau et al., 1997; Martin et al., 1998). A recurring question is whether ischemia and/or trauma to the brain may elicit the "classical" features of apoptosis. Recently, MacManus and colleagues proposed that insults to the brain result in a mode of cell death that does not fit the classical definitions of necrosis or apoptosis, but rather falls along a "continuum" sharing features common to both forms of cell death (MacManus and Buchan, 2000). In this study, we sought to examine this issue in an *in vivo* model of acute neuronal death triggered by Na^+, K^+- pump inhibition. Pump inhibition is associated with influx of Na+ and Ca^{2+}, both known triggers for necrosis as well as efflux of K^+, a known trigger for apoptosis. In order to investigate the mode of cell death triggered by pump inhibition, we utilized fluorescent molecular probes (ethidium bromide and Hoechst 33342) as well as conventional morphological techniques to detect signs of necrosis and apoptosis. Our results indicate that dentate granule cells undergo a rapid and early form of cell injury, characterized by marked cell shrinkage, nuclear condensation and pyknosis, morphological features suggestive of apoptotic cell death. However, these same cells had early loss of membrane integrity, while DNA fragmentation as well as formation of apoptotic bodies were rarely encountered at all time points examined. Furthermore, co-infusion of ouabain with charybdotoxin, a broad-spectrum K^+ channel blocker, provides robust tissue protection, leading to significant reduction in tissue infarction and cell

shrinkage. These results suggest that neuronal injury and death induced by Na^+, K^+, ATPase inhibition shares features common to both apoptotic and necrotic cell death. Such hybrid tissue damage can largely be prevented by reducing pathological efflux of intracellular K^+.

KEYWORDS: Necrosis, Apoptosis, Dentate Gyrus, Trauma, Ischemia, Ouabain, Na^+, K^+ - pump

INTRODUCTION

Ischemic and traumatic insults to the central nervous system trigger a host of acute and chronic tissue responses (Kampfl et al., 1996; Buki et al., 2000; Smith et al., 1997; Bramlett et al., 1997; Yang et al., 2001; Doble et al., 2001). The characterisation of the pathophysiological phenomena as well as the key molecular players involved in such a response is of critical importance in devising therapeutic strategies for neuronal salvage. A widely accepted theory is that of excitotoxic cell death following trauma and ischemia (Lee et al., 1999; Tirosh et al., 2000). Excitotoxicity usually results in necrotic cell death characterized by loss of membrane integrity, cell swelling and the disruption of cellular organelles (Cheung et al., 1998; Gwag et al. 1997; Regan et al., 1995). Necrotic cell death usually occurs as a result of Na^+ and Ca^{2+} influx and the associated massive glutamate release (Cheung et al., 1998). Recently however, there has been a flurry of evidence suggesting that necrosis may not be the only form of cell death in the central nervous system following acute insults. Several studies have presented evidence for the occurrence of neuronal apoptosis following transient focal ischemia (Murita-Fujimura et al., 2001; Cao et al., 2001; Guegan and Sola, 2000). Apoptosis on the other hand, has been shown to occur following loss of intracellular K^+ (Bortner et al, 1997). Failure of the Na^+, K^+ pump commonly occurs during and after traumatic/ischemic insults and is known to result in Na^+ and Ca^{2+} influx as well as K^+ efflux. We therefore hypothesised that pump inhibition could trigger a mixed apoptotic/necrotic cell death similar to that detected following cerebral ischemic insults.

There is no single criterion however that a dying cell has to satisfy to be labeled apoptotic. Rather, a combination of morphological and biochemical methods are

frequently employed in concert to define apoptosis (Mark and Willingham, 1999; Allen et al., 1997). Of particular interest is the hypothesis raised by MacManus and co-workers. These authors suggest that ischemic cell death does not fit the classical definitions of necrosis or apoptosis, but rather falls along a "continuum", sharing features common to both forms of cell death (MacManus and Buchan, 2000).

Morphologically, apoptosis is characterized by intact plasma membranes and cellular organelles, nuclear condensation, DNA fragmentation and the formation of apoptotic bodies (Kerr et al., 1972). Several techniques can be employed in the study of neuronal apoptosis. For example, DNA fragmentation can be detected by TUNEL labeling of breaks at 3-OH ends in DNA strands. (Mangili et al., 1999). This technique however lacks specificity for apoptosis since DNA strand breaks have also been seen in necrotic cell death (Labat-Moleur et al., 1998; Ishimaru et al., 1999). Hoechst 33342 has also been widely used to study DNA conformational changes associated with apoptosis. This membrane permeable fluorescent probe binds to all DNA within cells and may therefore provide a sensitive means for detecting DNA condensation, fragmentation as well as the formation of apoptotic bodies (Matsuo et al., 2001; Foglieni et al., 2001; Maciorowski et al., 1998; Whiteside et al., 1998; Belloc et al., 1994). Apoptotic cells undergoing DNA condensation usually exhibit higher fluorescence peaks when labeled by Hoechst 33342 (Ormerod et al., 1993a). In addition, previous studies have demonstrated apoptotic bodies after the *in vitro* labeling of tissue sections by ethidium bromide using high power magnification fluorescence microscopy (Ellerby et al., 1997; Pulera et al., 1998). We utilized this method to further identify apoptotic bodies in tissue sections.

Na^+, K^+, ATPase pump inhibition in the adult rat hippocampus triggers a host of cellular injury events that closely mimic that induced by ischemic/traumatic insults (Lees, 1991; Lees and Leong, 1996; Lees et al., 1990). We have previously reported the occurrence of "reactive cell change" in the early hours following pump inhibition in the rat dentate gyrus (Omar et al., 2000). We observed the rapid appearance of markedly shrunken cells with condensed and pyknotic nuclei primarily in the granule cell layer and the hilus of the dentate hippocampus as early as 4 h following pump inhibition. A similar tissue reaction has been described following ischemic insults (Towfighi and Mauger, 1998; Brown and Brierly, 1972). Nevertheless, conventional morphometric approaches provide little insight into the underlying pathological mechanisms. In this study we sought to address this issue by probing the membrane and DNA changes of the dentate gyrus cells following ouabain-induced insult. This is achieved by the application of different fluorescent markers that have been shown *in vitro* to be specifically indicative of cell necrosis or apoptosis (Ormerod et al., 1993a,b; Matsuo et al., 2001; Foglieni et al., 2001). Part of the results of this study has been published in an abstract form (Omar and Hu, 2001b).

METHODS

Animal Preparation

The detailed methodology has been described elsewhere. [39] Briefly, Male Long-Evans rats (300-350 g; Charles River, Canada) were initially anesthetized with pentobarbital (Somnotol®, 0.12 ml/kg body weight, ip). After attaining a surgical plane of anesthesia, rats (n = 24) were fitted with a nose cuff connected to a wall vaporizer unit delivering a combination of Halothane™ (2-3%) and oxygen (100%) throughout the surgery. The anesthesia, surgical and experimental protocol was approved by the Hospital Animal Care Council, which ensures conformity with the guidelines of the National Institutes of Health and the Canadian Council on Animal Care.

After mounting onto a stereotactic frame, a midsagittal scalp incision was performed, the skull exposed and periosteum removed. Two burr holes were drilled into the skull at stereotactic coordinates corresponding to the dentate gyrus granule cell layer (Bregma: -3.8; Lateral: 2.2; and Ventral to dura: 3.3) (Paxinos and Watson, 1982). A Hamilton microsyringe was filled with the following solutions: For the control side, it was filled with 1 µl of saline with 1 µl of Hoechst 33342 (Molecular Probes Inc., Eugene, OR) or 1 µl of a 40µM solution of ethidium bromide (EB; Molecular Probes Inc., Eugene, OR); For the experimental side, it was filled with 1 µl of ouabain (1 mM; Sigma Aldrich Corp., St. Louis, MO) and 1 µl of Hoechst 33342 or ouabain plus EB. In a separate group of experiments, in which we tested the effect of blocking K^+ efflux on ouabain-induced cytotoxicity, ouabain was coinfused with the broad-spectrum K^+ channel blocker, charybdotoxin (200nM; Alomone labs, Canada). As control, ouabain was coinfused with saline on the contralateral hippocampus. The syringe was then slowly lowered into the

granule cell layer (3.3 mm ventral to the dura). The solutions were gently infused at a rate of 0.2 - 0.5 µl / min as monitored through the level of the meniscus observed under a stereomicroscope and the microsyringe was then left in place for 10 - 15 min to minimize back-diffusion of the solution. The same procedure was repeated in the contralateral hippocampus. The scalp was then closed with 4-0 prolene sutures.

Tissue Processing

The rats were postoperatively hosted in an incubator (30°C) for 30 min until fully recovered from anesthesia. For postoperative analgesia, Buprenorphine was given every 6 h for the first 24 h following surgery. At 2, 4, 6, 8 and 12 hour time points following surgery, rats were deeply anesthetised with sodium pentobarbital (Somnotol, 0.22 ml/100 g body weight, i.p.) and were then transcardially perfused with 200 ml of 4% paraformaldehyde in 0.1 M phosphate buffer at pH 7.4. The rats were decapitated and their brains sectioned in the coronal plane on a cryostat, at 40µm spacing. Some sections were Nissl or Hematoxylin and Eosin-stained (H/E) using standard techniques. Nissl and H/E-stained sections were examined with a light microscope while Hoechst 33342 was visualized using a conventional epifluorescence microscope (Olympus IX50 / IX70) equipped with an UV filter set (excitation maxima of 355 nm and an emission maxima of 465 nm).

To detect apoptotic bodies, we performed ethidium bromide staining of tissue sections as previously described (Ellerby et al., 1997; Pulera et al., 1998). Briefly, sections were incubated with a solution of ethidium bromide (2.5µg/ml) in H_2O for 5 minutes and examined under rhodamine fluorescence microscopy. The criteria used for

defining apoptotic bodies were evidence of nuclear fragmentation into 2 or more distinct bodies as previously described by Pulera et al., (1998).

Data Analysis

Images are digitally captured online using a Sony charge-coupled device (CCD) color video camera connected to a PC equipped with a framegrabber, controlled by Northern Eclipse software (Empix Imaging Inc., Mississauga, Canada). All images were first collected using a (X10) objective lens in order to include the entire dentate gyrus. Total fluorescence yield was analysed using the Northern Eclipse software which line-scans an area of fluorescence and plots the results as a grey scale value from 0 - 255 (where 0 is darkest and 255 is brightest).

Analysis of H/E and nissl-stained sections was performed using Northern Eclipse software after digitally acquiring images under transmission illumination. Nissl and H/E stained sections were analysed for degree of cell shrinkage as well as areas of vacuolization and tissue swelling. Excel was used for statistical analysis (Student's t-test and ANOVA) and all data are expressed as mean ± SEM.

RESULTS

Na^+, K^+ Pump Inhibition Results in an Early Increase in Membrane Permeability

We first examined membrane permeability changes following co-infusion of EB and ouabain. At the 2 h survival period, mild EB fluorescence emission was detected from the dentate granule cells as well as the hilar neurons (Fig. 1). The mean fluorescence yield was 8.04 ± 1.37 from the pump inhibited cells compared to 3.84 ± 0.28 from the vehicle-treated control ($P < 0.05$). Examination of tissue specimens at increasing survival periods revealed a time dependent increase in membrane permeability following Na+, K+ pump inhibition. Four hours following pump inhibition, granule and hilar neurons both exhibited a rise in the mean EB fluorescence yield compared to the control (Fig. 1). Mean fluorescence yield 4 h following pump inhibition was 34.44 ± 4.92 compared to 11.88 ± 0.86 from the saline-treated control ($P < 0.05$).

A further rise in mean EB fluorescence yield was observed at the 6 h survival period. Pump-inhibited granule and hilar cells had a mean fluorescence emission of 108.5 ± 12.04 compared to a control value of 32.54 ± 2.74 ($P < 0.01$). At the 12h survival period following pump inhibition, mean EB fluorescence yield was 145.02 ± 8.13 from the pump-inhibited cells versus 55.34 ± 6.12 from the vehicle-treated control. Overall, the steepest rise in EB fluorescence yield following pump inhibition occurred between the 4 and 6 h time points. At the 4h time point EB fluorescence yield was 4.28 times that of the 2h time point ($P < 0.01$/One-way ANOVA). At 6h, EB fluorescence yield was 3.15 times that of the 4h survival period following pump blockade. However, a difference in EB fluorescence yield of 74.06 was found between pump-inhibited cells at 6h compared to 4h versus a difference of 26.04 between the 4 and 2h time points, indicating that more EB

was admitted into the cells between the 4 and 6h time points than between the 2 and 4h periods (Fig 2).

(Figure 1 near here)

Na^+, K^+ Pump Inhibition Results in DNA Condensation

Examination of tissue specimens 2 h following pump inhibition revealed early labeling of nucleic acid by Hoechst 33342. Labeling was faint on both ouabain treated and control sides. Mean H33342 fluorescence yield at the 2 h time point was 30.36 ± 0.6 from pump inhibited side versus 29.28 ± 1.18 from the saline treated control ($P = 0.45$). At the 4 h time point, however labeling of the granule cell layer of the dentate gyrus with Hoechst 33342 was more intense than the earlier 2 h time point both from the pump-inhibited and the control sides. In addition, a subpopulation of cells within the granule cell layer appeared with intense H33342 labeling. These cells were not seen on the saline treated side. The overall mean H33342 fluorescence yield at 4 h was 131.86 ± 6.74 from the pump-inhibited side versus 92.5 ± 2.26 from the saline-treated control ($P < 0.05$). No further increase in Hoechst 33342 uptake and fluorescence emission was observed at longer survival periods. Mean H33342 fluorescence yield at 6 h was 123.8 ± 10.1 from the pump-inhibited side versus 86.3 ± 9.8 from the saline-treated control ($P < 0.05$ for ouabain-treated versus control). There was no statistically significant increase however in the mean H33342 fluorescence yield when the 6 h was compared to the 4 h time point. At the 12 h time point the mean H33342 fluorescence yield was once again 128.58 ± 1.12

from the pump-inhibited side versus 133.1 ± 7.8 from the saline-treated control ($P < 0.05$) (Figure 4).

On the other hand, examination of ethidium bromide-stained revealed that DNA condensation was rarely associated with DNA fragmentation or the formation of apoptotic bodies at all time points examined (data not shown).

(Figure 2 near here)

Correlation of Cell Morphology to Hoechst 33342 and Ethidium Bromide Fluorescence Changes

To determine the morphological changes that may be accompanying the EB and H33342 fluorescence responses, we performed hematoxylin and eosin staining (H/E) of sections chosen at random. Sections were then subjected to digital image analysis and the mean object count (average number of cells / image) as well as the mean percentage object area was computed. This latter parameter measures the total area occupied by cells divided by the total area of image, therefore reflecting the degree of cell shrinkage. To measure granule cell shrinkage, the area occupied by the granule cells was selected by the selection tool and used to calculate the mean object count.

At the 2 h time point, the mean object count was 227.7 ± 3.03 from the pump-inhibited side versus 232.3 ± 3.6 from the saline-treated control ($P = 0.34$). On the other hand, the mean percentage object area was 18.96 ± 0.67 from the pump-inhibited side versus 19.49 ± 0.76 ($P = 0.61$). At the 4 h time point however, there was a significant drop in the mean percentage object area from the pump-inhibited side reflecting a

dramatic cell shrinkage following pump inhibition (Fig. 4). The mean percentage object area at 4 h was 8.66 ± 0.23 from the pump-inhibited side versus 19.27 ± 0.72 from the saline-treated control ($P < 0.0001$). On the other hand, there was no statistically significant change in the number of cells from both sides, a mean of 226.2 ± 3.21 from the pump-inhibited side versus 230.4 ± 2.82 from the saline-treated control ($P = 0.34$).

Values obtained at the 6 h time point were as follows: The average number of cells was 227 ± 3.21 from the pump-inhibited side versus 230.4 ± 2.82 from the saline-treated control ($P = 0.39$). Furthermore, there was no statistically significant change in the average number of cells at the 6 h time point compared to 4 h. On the other hand, there was an ~ 22% drop in the mean cell area at the 6 h time point (6.74 ± 0.23) when compared to the earlier 4h (8.66 ± 0.23 time point ($P < 0.0001$). The mean cell area from the saline-treated control at 6 h was 18.67 ± 0.82 ($P < 0.0001$ compared to the pump-inhibited side at the same time point).

At the 12 h time point the average number of cells was 196 ± 1.8 from the pump-inhibited side versus 231.8 ± 5.97 from the saline-treated control ($P < 0.001$). This drop in the average number of cells per image represents ~ 16% drop compared to the control side and is only observed beginning at the 12 h time point. Earlier time points do not show any cell loss, only cell shrinkage. The mean percentage object area or mean cell area per image was 6.09 ± 0.22 from the pump-inhibited side versus 18.93 ± 0.84 from the saline treated control representing an ~ 68% drop in the mean cell area in the pump inhibited side versus control values at 12 h. There was however, no statistically significant change in the average cell area when 12 h values were compared to the 6 h time point.

(Figure 3 near here)

(Figure 4 near here)

The K^+ Channel Blocker Charybdotoxin Significantly Attenuates Cell Injury Associated with Pump Inhibition

In order to examine the role of loss of intracellular K^+ in ouabain cytotoxicity, we co-infused ouabain with charybdotoxin into the dentate region. Charybdotoxin (ChTX) is a 37 amino acid peptide found in the venom of the Israeli scorpion, *Leiurus quinquestriatus*. It is a potent inhibitor of the large Ca^{2+}-activated K^+ channels (Miller et al., 1985). The degree of necrotic and apoptotic tissue damage associated with pump inhibition and charybdotoxin-mediated neuroprotection were assessed using two separate indices. The necrotic index (N.I.), which is derived from the ratio between the area of tissue vacouolization and area of healthy cells and the apoptotic index (A.I.), which measures the area occupied by shrunken cells vs. area occupied by healthy cells. At the 8 hr time point following ouabain infusion, a significant number of shrunken cells were found in the dentate areas that also showed varying degrees of cell loss, tissue vacuolisation and tearing (split), reminiscent of necrosis and infarction (Fig. 5 and Table 1). In sharp contrast, in the dentate gyrus where ouabain was co-infused with charybdotoxin, the tissue damage was dramatically reduced as shown by a significant drop in both necrotic as well as apoptotic indices (Figure. 5 and Table 1). Interestingly, charybdotoxin also partially prevented cell shrinkage in the CA1 region and the resultant effect was the appearance of shrunken cells alternating with healthy-looking neurons (Figure 5, E and F and Table 1). On the other hand, the control side (ouabain alone)

exhibited uniform cell shrinkage throughout the CA1 layer. These observations are consistent with earlier *in vitro* studies demonstrating K^+ channel blockers as protective against apoptotic cell death (Maeno et al., 2000).

(Figure 5 near here)

(Table 1 near here)

DISCUSSION

The exact mechanisms underlying cell injury and death following traumatic / ischemic insults in the central nervous system has long been a controversial issue. Whether cell death is effected through an apoptotic or necrotic pathway following such insults continues to be a subject of intense debate. Understanding the host of changes that occur following these insults particularly in the acute stages (<3h) or the "therapeutic time window" is of paramount importance in designing strategies directed at neuronal salvage (Marler et al., 2000; NINDS Stroke Trial, 1995; Clark et al., 1999). This study was designed with this issue in mind.

Our results indicate that the mode of cell injury and death in the granule cell layer of the rat hippocampus following Na^+, K^+ -ATPase pump inhibition shares features of both apoptotic as well as necrotic cell death, which can be differentiated *in vivo* using specific fluorescent probes. To our knowledge, this is an original methodology that has not been adopted in previous studies.

We have shown that granule cells undergo an acute increase in membrane permeability at 2 h detected by an increase in the fluorescence yield of the membrane impermeable DNA intercalating dye, Ethidium Bromide. This increase in membrane permeability is a hallmark of necrotic cell injury and death. Interestingly, this early membrane injury was not accompanied by any change in cell morphology as detected by H/E staining. In fact, cells have retained their normal morphological appearance, suggesting that early neuronal necrosis *in vivo* lacks severe swelling as often encountered in vitro (Senatorov et al., 2000; Gwag et al., 1997; Regan et al., 1995). We observed areas of extensive vacuolisation, however it is unclear at this point whether this

accumulation of fluid is intra or exctracellular. Since pump inhibition is associated with K^+ efflux, it may be that loss of intracellular K^+ may result in cell shrinkage while the extracellular accumulation of K^+ may result in tissue swelling and vacuolisation. In fact, loss of intracellular K^+ is involved in cell shrinkage as well as the induction of apoptosis (Bortner et al., 1997). Regulatory volume decrease is mediated through K^+ and Cl^- efflux accompanied by water efflux. Pump inhibition results in K^+ and water efflux and may therefore explain the accumulation of water in the extracellular compartment and the appearance of vacuoles. In addition, a recent study demonstrated that cell shrinkage due to disordered volume regulation is an early prerequisite to apoptosis. Blocking K^+ channels in HeLa and U937 cells was shown to prevent both cell shrinkage as well as apoptotic cell death probably due to K^+ retention (Maeno et al., 2000). Our study shows for the first time that blocking K^+ channels *in vivo* is capable of significantly attenuating the neuronal damage associated with inhibition of the Na^+, K^+ pump, indicating that loss of intracellular K^+ plays an important role in cell death associated with pump inhibition. We have shown that blocking K^+ efflux not only markedly reduced the number of shrunken cells, but also resulted in a dramatic reduction in tissue vacuolisation and swelling. The reduction in tissue vacuolisation (commonly associated with necrosis) is probably due to intracellular K^+ retention, which may reduce the electrical gradient for sodium influx and thereby reduce the downstream activation of necrosis. The involvement of both apoptosis and necrosis in ischemic neuronal injury raises the interesting possibility of intervention using a combination of apoptotic and necrotic pathways as targets for neuronal salvage (Lee et al., 1999; Choi, 1996). This combination approach may prove more useful in the future treatment of ischemic strokes.

At the 4, 6 and 12 h time points, there was a steady increase in the mean EB fluorescence yield, both from the pump-inhibited granule cells as well as the saline-treated cells albeit at a significantly lower degree. The increase in membrane permeability in the saline-treated granule cells probably reflects varying degrees of mechanical cell damage. Once again, the increase in cell permeability was not accompanied by cell swelling as might be expected in cells dying through a purely necrotic pathway. In fact, cells underwent cell shrinkage starting at the 4 h time point and the shrinkage further intensified at 6 h.

Cell shrinkage is one of the hallmarks of cells dying through apoptosis (Allen et al., 1997; Kerr et al., 1972). Indeed, we found that beginning at 4 h following pump inhibition, granule cells undergo enhanced Hoechst 33342 emission and a subpopulation of these granule cells exhibit a particularly intense Hoechst 33342 fluorescence yield compared to saline-treated cells. Hoechst 33342 binds preferentially to DNA rich in thymidine and adenine base pairs and is widely used as a marker for DNA condensation that accompanies apoptotic cell death in various cell types (Foglieni et al., 2001; Maciorowski et al., 1998; Whiteside et al., 1998; Belloc et al., 1994). Cells undergoing DNA condensation exhibit higher fluorescence peaks compared to cells with relaxed DNA conformations (Ormerod et al., 1993 a,b). The difference in H33342 fluorescence emission between normal and apoptotic cells is attributed to a more rapid membrane uptake of H33342 by cells undergoing apoptosis (Ormerod et al., 1993b). To further characterize the cells with intense H33342 emission, we examined the same slides after H/E staining. We found cells exhibiting intense H33342 emission co-localized spatiotemporally with shrunken cells with characteristic pyknotic nuclei, indicating that

the enhancement in H33342 fluorescence may reflect DNA condensation. While the rise in EB fluorescence continued, reflecting a continuous increase in membrane compromise, the mean H33342 fluorescence yield plateaued after reaching a peak at the 4 h time point. The mean H33342 fluorescence yield at 2 h did not show a statistically significant difference when pump-inhibited granule cells were compared to control. This indicates that the DNA conformational changes detected by H33342 in our preparation begins after a 4 h delay following pump inhibition.

Previous reports have shown that following transient cerebral ischemia, granule cells died by a mode of cell death that does not fit established criteria for apoptotic and necrotic cell death (Fukuda et al., 1999). Furthermore, it is suggested that neuronal cell death following experimental stroke occurs along a "continuum" extending from pure apoptosis to pure necrosis (MacManus and Buchan, 2000; Roy and Sapolsky, 1999). In fact, a recent study demonstrated a direct link between early excitotoxic, calcium-mediated m-calpain activation and activation of the pro-apoptotic caspase-3 following neonatal brain hypoxia-ischemia. It was shown that cell death was initially mediated by the necrosis-associated m-calpain activation, which in turn triggered caspase-3, a key player in the execution of the apoptotic program (Blomgren et al., 2001). These results are consistent with our data that show early membrane compromise characterizing necrotic cell death followed by cell shrinkage and nuclear condensation, features characteristic of apoptosis.

In summary, we show here that pump inhibition-induced injury in granule cells may follow a temporal sequence of events: An early incremental rise in membrane permeability starting as early as 2 h with no accompanying cell swelling or

morphological changes characteristic of necrosis. At 4 h following pump inhibition, DNA condensation begins to occur accompanied by a further increase in membrane compromise together with dramatic cell shrinkage. This cell shrinkage continues to increase together with a further increase in membrane disintegration. However no further increase in DNA condensation takes place following the 4 h time point. DNA condensation, however, is rarely accompanied by the formation of apoptotic bodies at all time points as might otherwise be expected from cells undergoing purely apoptotic cell injury and death. Cell loss on the other hand begins at 12 h and the process is completed at the 72h time point. At this time cells are replaced by a glial and macrophage infiltrate responsible for phagocytosis of dying cells as well as post-injury tissue remodeling (Omar et al., 2001a).

ACNOWLEDGEMENTS

This work was supported by the Heart and Stroke Foundation of Canada (HSF) and the Canadian Institutes of Health Research (CIHR). A.O. is a recipient of a Post-Doctoral Fellowship Award from the Canadian Institutes of Health Research (CIHR) under the Canadian Neurotrauma Research Program (CNRP).

REFERENCES

1. ALLEN R.T., HUNTER W.J. 3RD., and AGRAWAL D.K. (1997). Morphological and biochemical characterization and analysis of apoptosis. J. Pharmacol. Toxicol. Methods **37**, 215-228.

2. BELLOC F., DUMAIN P., BOISSEAU M.R., et al. (1994). A flow cytometric method using Hoechst 33342 and propidium iodide for simultaneous cell cycle analysis and apoptosis determination in unfixed cells. Cytometry **17**, 59-65.

3. BLOMGREN K., ZHU C., WANG X., et al. (2001). Synergistic activation of caspase-3 by m-calpain after neonatal hypoxia-ischemia: a mechanism of "pathological apoptosis"? J. Biol. Chem. **276**, 10191-10198.

4. BORTNER C.D., HUGHES F.M. JR., CIDLOWSKI J.A. (1997). A primary role for K^+ and Na^+ efflux in the activation of apoptosis. J. Biol. Chem. **272**, 32436-32442.

5. BRAMLETT H.M., DIETRICH W.D., GREEN E.J., and BUSTO R. (1997). Chronic histopathological consequences of fluid-percussion brain injury in rats: effects of post-traumatic hypothermia. Acta Neuropathol. (Berl.) **93**, 190-199.

6. BROWN A.W., and BRIERLEY J.B. (1972). Anoxic-ischaemic cell change in rat brain light microscopic and fine-structural observations. J. Neurol. Sci. **16**, 59-84.

7. BUKI A., OKONKWO D.O., WANG K.K., and POVLISHOCK J.T. (2000). Cytochrome c release and caspase activation in traumatic axonal injury. J. Neurosci. **20**, 2825-2834.

8. CAO G., MINAMI M., PEI W., et al. (2001). Intracellular Bax translocation after transient cerebral ischemia: implications for a role of the mitochondrial apoptotic signaling pathway in ischemic neuronal death. J. Cereb. Blood Flow Metab. **21**, 321-333.

9. CHEUNG N.S., PASCOE C.J., GIARDINA S.F., JOHN C.A., and BEART P.M. (1998). Micromolar L-glutamate induces extensive apoptosis in an apoptotic-necrotic continuum of insult-dependent, excitotoxic injury in cultured cortical neurones. Neuropharmacology **37**, 1419-1429.

10. CHOI D.W. (1996). Ischemia-induced neuronal apoptosis. Curr. Opin. Neurobiol. 6, 667-672.

11. CLARK W.M., WISSMAN S., ALBERS G.W., JHAMANDAS J.H., MADDEN K.P., and HAMILTON S. (1999). Recombinant tissue-type plasminogen activator (Alteplase) for ischemic stroke 3 to 5 hours after symptom onset. The ATLANTIS Study: a randomized controlled trial. Alteplase Thrombolysis for Acute Noninterventional Therapy in Ischemic Stroke. J.A.M.A. **282**, 2019-2026.

12. DOBLE A. (1999). The role of excitotoxicity in neurodegenerative disease: implications for therapy. Pharmacol. Ther. **81**, 163-221.

13. ELLERBY H.M., MARTIN S.J., ELLERBY L.M., et al. (1997). Establishment of a cell-free system of neuronal apoptosis: comparison of premitochondrial, mitochondrial, and postmitochondrial phases. J. Neurosci. **17**, 6165-6178.

14. FOGLIENI C., MEONI C., and DAVALLI A.M. (2001). Fluorescent dyes for cell viability: an application on prefixed conditions. Histochem. Cell. Biol. **115**, 223-229.

15. FUKUDA T., WANG H., NAKANISHI H., YAMAMOTO K., and KOSAKA T. (1999). Novel non-apoptotic morphological changes in neurons of the mouse hippocampus following transient hypoxic-ischemia. Neurosci. Res. **33**, 49-55.

16. GUEGAN C., and SOLA B. (2000). Early and sequential recruitment of apoptotic effectors after focal permanent ischemia in mice. Brain Res. **856**, 93-100.

17. GUGLIELMO M.A., CHAN P.T., CORTEZ S., et al. (1998). The temporal profile and morphologic features of neuronal death in human stroke resemble those observed in experimental forebrain ischemia: the potential role of apoptosis. Neurol. Res. **20**, 283-296.

18. GWAG B.J., KOH J.Y., DEMARO J.A., YING H.S., JACQUIN M., and CHOI D.W. (1997). Slowly triggered excitotoxicity occurs by necrosis in cortical cultures. Neuroscience **77**, 393-401.

19. ISHIMARU M.J., IKONOMIDOU C., TENKOVA T.I., et al. (1999). Distinguishing excitotoxic from apoptotic neurodegeneration in the developing rat brain. J. Comp. Neurol. **408**, 461-476.

20. KAMPFL A., POSMANTUR R., NIXON R., et al. (1996). mu-calpain activation and calpain-mediated cytoskeletal proteolysis following traumatic brain injury. J. Neurochem. **67**,1575–1583.

21. KAZAHARI S., TAKIZAWA S., OGAWA S., HABU S., and SHINOHARA Y. (1996). Identification of neuronal death and DNA fragmentation in early stage after rat transient forebrain ischemia. Rinsho Shinkeigaku **36**, 451-455.

22. KERR J.F., WYLLIE A.H., and CURRIE A.R. (1972). Apoptosis: a basic biological phenomenon with wide-ranging implications in tissue kinetics. Br. J. Cancer **26**, 239-257.

23. LABAT-MOLEUR F., GUILLERMET C., LORIMIER P., et al. (1998). TUNEL Apoptotic Cell Detection in Tissue Sections: Critical Evaluation and Improvement. Journal of Histochemistry and Cytochemistry **46**, 327-334.

24. LEE J.M., ZIPFEL G.J., and CHOI D.W. (1999). The changing landscape of ischaemic brain injury mechanisms. Nature **399** (6738 Suppl.), A7-14.

25. LEES G.J., and LEONG W. (1996). Interactions between excitotoxins and the Na+/K+-ATPase inhibitor ouabain in causing neuronal lesions in the rat hippocampus. Brain Res. **714**, 145-155.

26. LEES GJ. (1991). Inhibition of sodium-potassium-ATPase: a potentially ubiquitous mechanism contributing to central nervous system neuropathology. Brain Res. Brain Res. Rev. **16**, 283-300.

27. LEES G.J., LEHMANN A., SANDBERG M., and HAMBERGER A. (1990). The neurotoxicity of ouabain, a sodium-potassium ATPase inhibitor, in the rat hippocampus. Neurosci. Lett. **120**, 159-162.

28. MACIOROWSKI Z., DELIC J., PADOY E., et al. (1998). Comparative analysis of apoptosis measured by Hoechst and flow cytometry in non-Hodgkin's lymphomas. Cytometry **32**, 44-50.

29. MACMANUS J.P., and BUCHAN A.M. (2000). Apoptosis after experimental stroke: fact or fashion? J. Neurotrauma **17**, 899-914.

30. MAENO, E., ISHIZAKI, Y., KANASEKI, T., et al. (2000). Normotonic cell shrinkage because of disordered volume regulation is an early prerequisite to apoptosis. Proc. Natl. Acad. Sci. U.S.A. **97**, 9487-9492.

31. MANGILI F., CIGALA C., and SANTAMBROGIO G. (1999). Staining apoptosis in paraffin sections. Advantages and limits. Anal. Quant. Cytol. Histol. **21**, 273-276.

32. MARK C. and WILLINGHAM. (1999). Cytochemical methods for the detection of apoptosis. J. Histochem. Cytochem. **47**, 1101-1110.

33. MARLER J.R., TILLEY B.C., LU M., et al. (2000). Early stroke treatment associated with better outcome: the NINDS rt-PA stroke study. Neurology 55, 1649-1655.

34. MARTIN L.J., AL-ABDULLA N.A., BRAMBRINK A.M., KIRSCH J.R., SIEBER F.E., and PORTERA-CAILLIAU C. (1998). Neurodegeneration in excitotoxicity, global cerebral ischemia, and target deprivation: A perspective on the contributions of apoptosis and necrosis. Brain Res. Bull. **46**, 281-309.

35. MATSUO A., WATANABE A., TAKAHASHI T., et al. (2001). A simple method for classification of cell death by use of thin layer collagen gel for the

detection of apoptosis and/or necrosis after cancer chemotherapy. Jpn. J. Cancer Res. **92**, 813-819.

36. MORITA-FUJIMURA Y., FUJIMURA M., YOSHIMOTO T., and CHAN P.H. (2001). Superoxide during reperfusion contributes to caspase-8 expression and apoptosis after transient focal stroke. Stroke **32**, 2356-2361.

37. NOBLE L.J., and FERRIERO D.M. (2001). Delayed cell death in neonatal mouse hippocampus from hypoxia-ischemia is neither apoptotic nor necrotic. Neurosci. Lett. **304**, 165-168.

38. OMAR A.I., SENATOROV V.V., and HU B. (2001a). Sodium-potassium adenosine triphosphatase inhibition enhances membrane accumulation of DiI in rat hippocampus in vivo. Neuroscience **102**, 353-359.

39. OMAR A.I. and HU B. (2001b). Monitoring DNA condensation in vivo using the DNA fluorescent probe Hoechst 33342 following ouabain-induced injury. Soc. Neurosci. Abstr. **27**, 109.

40. OMAR A.I., SENATOROV V.V., and HU B. (2000). Ethidium bromide staining reveals rapid cell dispersion in the rat dentate gyrus following ouabain-induced injury. Neuroscience **95**, 73-80.

41. ORMEROD M.G., SUN X.M., BROWN D., SNOWDEN R.T., and COHEN G.M. (1993a). Quantification of apoptosis and necrosis by flow cytometry. Acta Oncol. **32**, 417-424.

42. ORMEROD M.G., SUN X.M., SNOWDEN R.T., DAVIES R., FEARNHEAD H., COHEN G.M. (1993b). Increased membrane permeability of apoptotic thymocytes: a flow cytometric study. Cytometry **14**, 595-602.

43. PAXINOS G. AND WATSON C. (1982) *The Rat Brain in Stereotaxic Coordinates*. 3rd edn. Academic Press: Sydney.

44. PORTERA-CAILLIAU C., PRICE D.L., and MARTIN L.J. (1997). Excitotoxic neuronal death in the immature brain is an apoptosis-necrosis morphological continuum. J. Comp. Neurol. **378**, 70-87.

45. PULERA M.R., ADAMS L.M., LIU H. (1998). Apoptosis in a neonatal rat model of cerebral hypoxia-ischemia. Stroke **29**, 2622-2630.

46. REGAN R.F., PANTER S.S., WITZ A., TILLY J.L., and GIFFARD R.G. (1995). Ultrastructure of excitotoxic neuronal death in murine cortical culture. Brain Res. **705**, 188-198.

47. ROY M., and SAPOLSKY R. (1999). Neuronal apoptosis in acute necrotic insults: why is this subject such a mess? Trends Neurosci. **22**, 419-422.

48. SENATOROV V.V., STYS P.K., and HU B. (2000). Regulation of Na+,K+-ATPase by persistent sodium accumulation in adult rat thalamic neurones. J. Physiol. **525**, 343-353.

49. SHELDON R.A., HALL J.J., NOBLE L.J., and FERRIERO D.M. (2001). Delayed cell death in neonatal mouse hippocampus from hypoxia-ischemia is neither apoptotic nor necrotic. Neurosci. Lett. **304**, 165-168.

50. SMITH D.H., CHEN X.H., PIERCE J.E., et al. (1997). Progressive atrophy and neuron death for one year following brain trauma in the rat. J. Neurotrauma **14**, 715-727.

51. TIROSH O., SEN C.K., ROY S., and PACKER L. (2000). Cellular and mitochondrial changes in glutamate-induced HT4 neuronal cell death. Neuroscience **97**, 531-541.

52. Tissue plasminogen activator for acute ischemic stroke. The National Institute of Neurological Disorders and Stroke rt-PA Stroke Study Group. (1995). N. Engl. J. Med. **333**, 1581-1587.

53. TOWFIGHI J., and MAUGER D. (1998). Temporal evolution of neuronal changes in cerebral hypoxia-ischemia in developing rats: a quantitative light microscopic study. Brain Res. Dev. Brain Res. **109**, 169-77.

54. WHITESIDE G., COUGNON N., HUNT S.P., and MUNGLANI R. (1998). An improved method for detection of apoptosis in tissue sections and cell culture, using the TUNEL technique combined with Hoechst stain. Brain Res. Brain Res. Protoc. **2**, 160-164.

55. YANG Y., LI Q. MIYASHITA H., YANG T. and SHUAIB A. (2001). Different dynamic patterns of extracellular glutamate release in rat hippocampus after permanent or 30-min transient cerebral ischemia and histological correlation. Neuropathology **21**, 181-187.

56. ZENG Y.S., and XU Z.C. (2000) Co-existence of necrosis and apoptosis in rat hippocampus following transient forebrain ischemia. Neurosci. Res. **37**, 113-125.

Figure 1. Na^+, K^+, ATPase pump inhibition increases membrane permeability of dentate granule cells in a time-dependent manner. Two hours following pump inhibition, granule cells exhibited an increase in EB fluorescence (B) when compared to the saline treated control (A). The increase in EB fluorescence further intensified, 4h following pump inhibition (D) when compared to the previous 2h time point. (C) shows EB fluorescence from dentate granule cells 4h following intra-hippocampal infusion of saline. At 12h following pump inhibition, EB fluorescence from granule cells continued to intensify (F) when compared to previous time points. At the 12h time point following saline infusion, dentate granule cells continued to show minimal EB fluorescence. Gcl: granule cell layer; h: hilus.

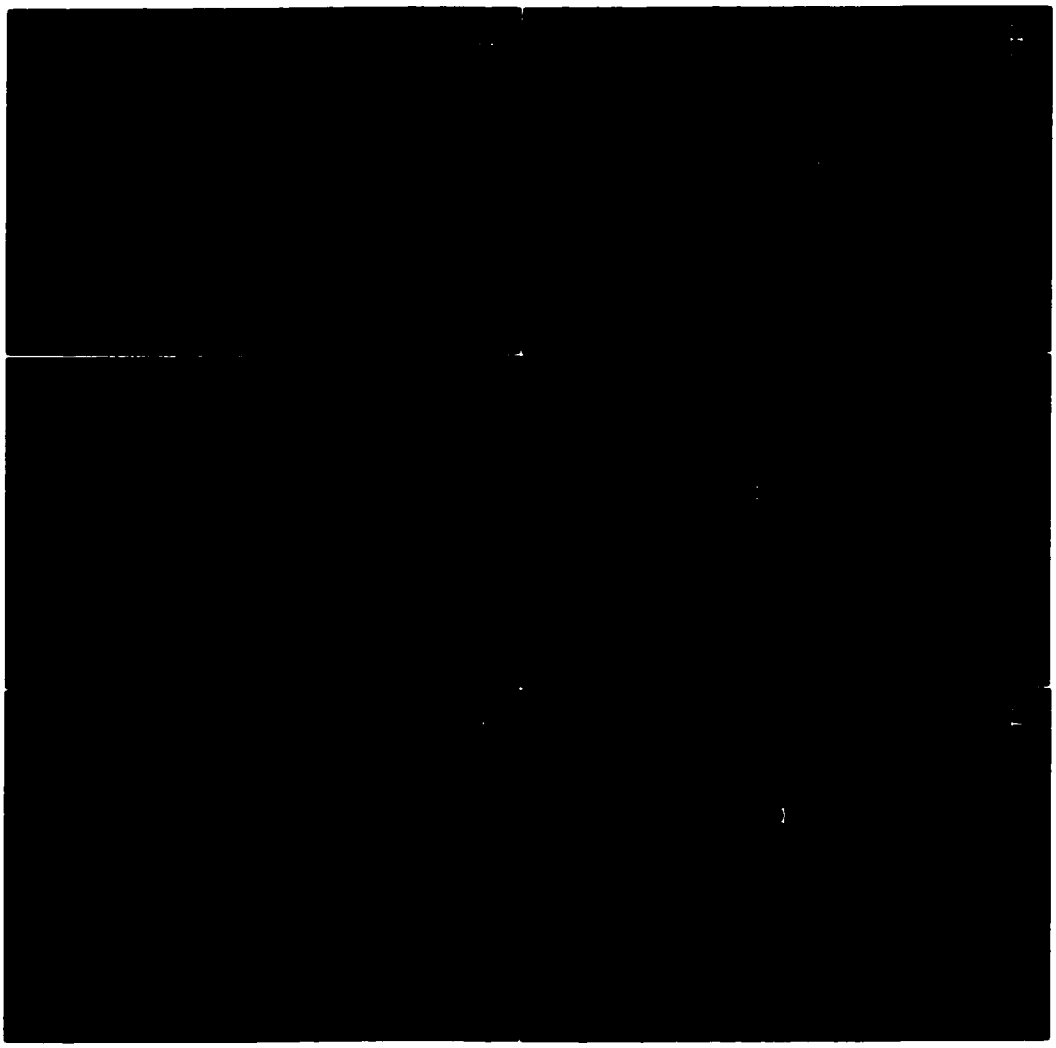

Figure 2. Na^+, K^+, ATPase pump inhibition results in nuclear condensation and enhanced Hoechst 33342 fluorescence. (A) Shows a nissl-stained section of the dentate gyrus 4h following intra-hippocampal saline infusion. Note the normal dentate granule cell morphology. (B) Shows a nissl-stained section of the dentate gyrus 4h following intra-hippocampal ouabain infusion. Dentate granule cells are noted to have undergone shrinkage, hyperchromatism and pyknosis. This is particularly prominent in the basal areas of the granule cell layer (arrowheads). (D) Shows an epifluorescence image of dentate granule cells showing Hoechst 33342 fluorescence signal 4h following intra-hippocampal coinfusion of Hoechst 33342 and ouabain. Note the particularly intense Hoechst 33342 labeling of a subpopulation of granule cells at the basal areas of the gcl. (Inset in D) shows a high magnification epifluorescence image of the Hoechst 33342 labeled granule cells 4h following pump inhibition. These cells colocalized spatio-temporally with shrunken and pyknotic cells as revealed through nissl staining. The fluorescence signal intensity was significantly higher when compared to the Hoechst 33342 / Saline infused side (C). (Inset in C) shows a high magnification epifluorescence image of the Hoechst 33342 labeled granule cells 4h following Hoechst 33342 / Saline infusion. Gcl: granule cell layer; h: hilus; Scale bars in A, B: 50μm; scale bars in insets: 25μm.

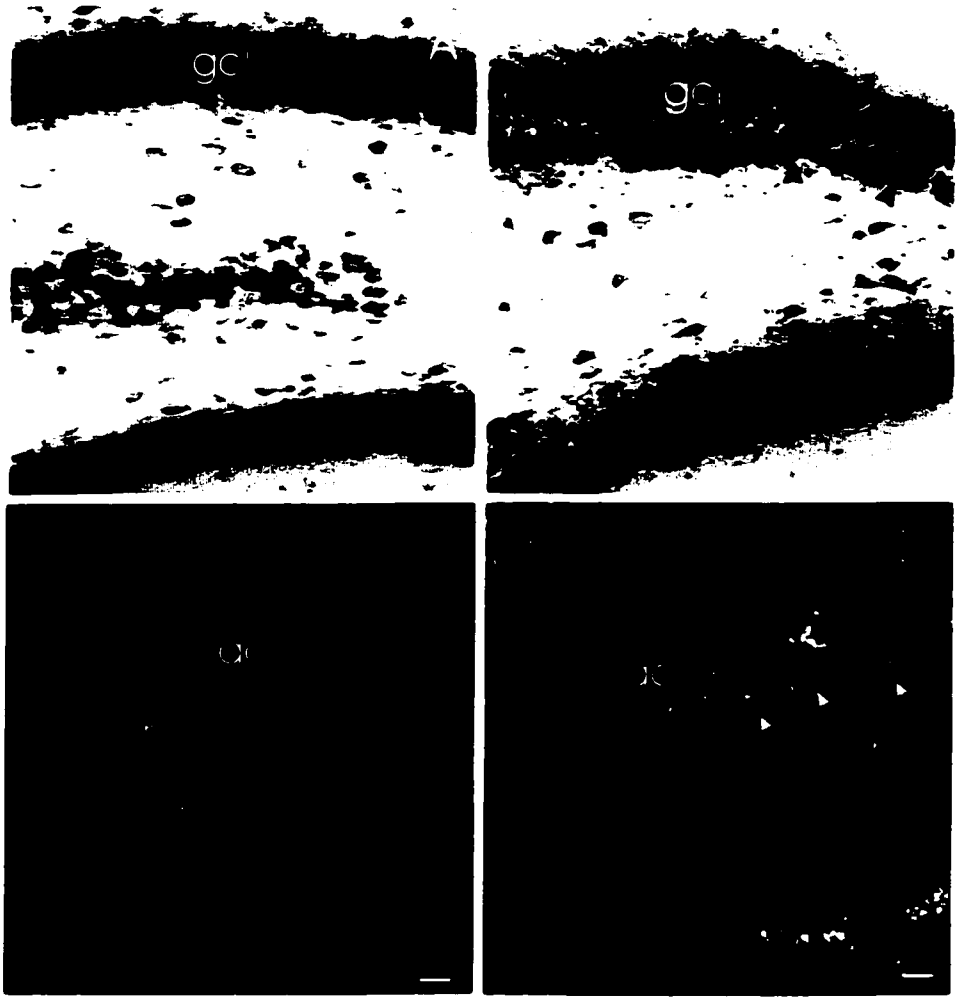

Figure 3. Time-dependent cellular morphological changes following Na^+, K^+, ATPase pump inhibition. (A) Shows an H/E stained section of dentate granule cells, 2h following pump inhibition. Cells have retained their normal morphological appearance at this time point. (B) Shows an H/E stained section of the dentate granule cells 2h following saline infusion. Note the normal granule cell morphology. (C) Shows an H/E stained section of the dentate granule cells, 4h following pump inhibition. Cells have undergone marked cell shrinkage, their nuclei exhibited condensation and hyperchromatism (arrows). The saline-treated control retained normal cell morphology at the 4h time point (D). At the 12h time point following pump inhibition, dentate granule cell loss was apparent (E, arrows) when compared to the saline treated control (F). Gcl: granule cell layer; h: hilus; mcl: molecular cell layer. Scale bars (A-D: 25μm; E,F: 50μm).

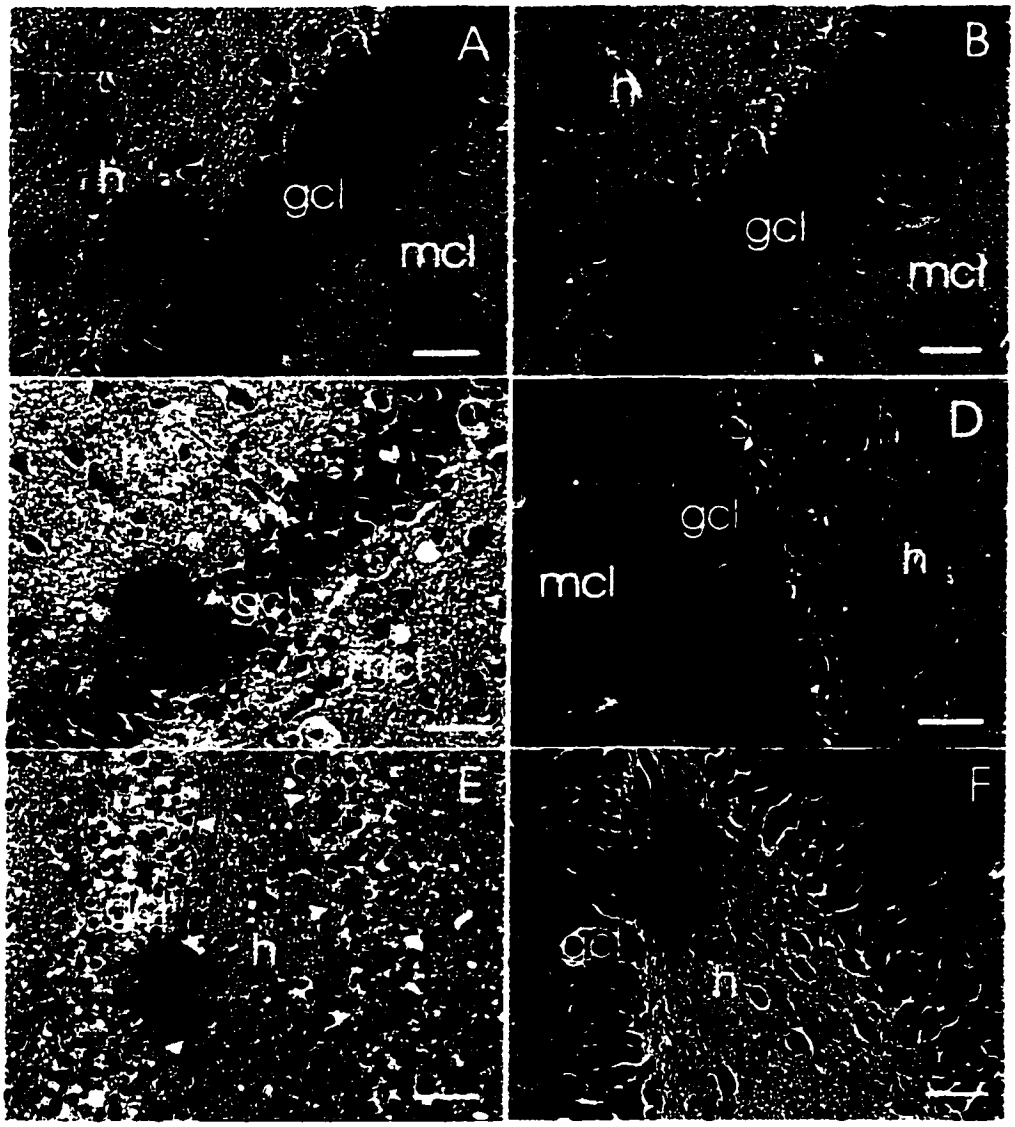
A
h
gcl
mcl
B
h
gcl
mcl
C
gcl
mcl
D
gcl
mcl
h
E
gcl
h
F
gcl
h

Figure 4. Quantitative digital image analysis showing granule cell responses to Na^+, K^+, ATPase pump inhibition. (A) EB fluorescence signal intensity from granule cells as a function of time. Pump inhibition resulted in an incremental rise in membrane permeability as measured by the mean EB fluorescence intensity. (B) Shows the mean percent object area of dentate granule cells as a function of time. Cells have undergone marked cell shrinkage in response to pump inhibition. (C) Shows Hoechst 33342 fluorescence signal intensity from granule cells as a function of time. The steepest rise in Hoechst 33342 uptake and fluorescence emission occurred between the 2h and 4h time points. Error bars denote SEM.

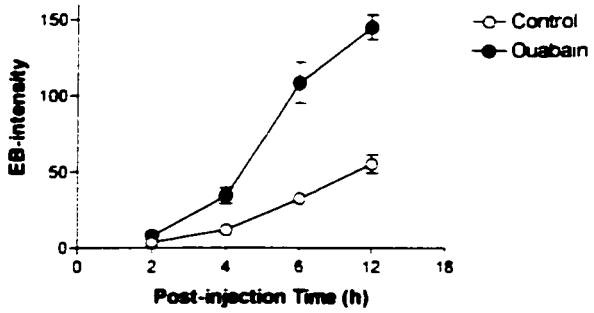
150
100
50
0
EB-intensity
0
2
4
6
12
18
Post-injection Time (h)
Control
Ouabain

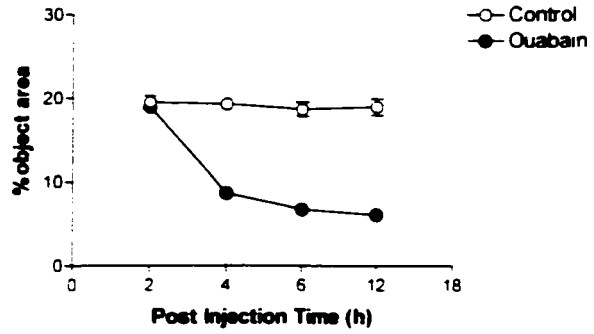
30
20
10
0
% object area
0
2
4
6
12
18
Post injection Time (h)
Control
Ouabain

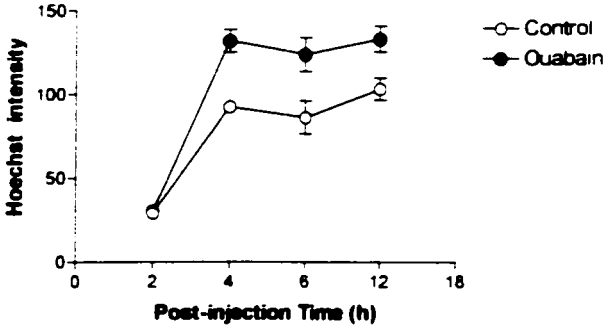
150
100
50
0
Hoechst intensity
0
2
4
6
12
18
Post-injection Time (h)
Control
Ouabain

Figure 5. Blocking K^+ efflux significantly attenuates hippocampal cell injury associated with pump inhibition. The micrographs of H/E-stained sections on the left panels were taken from the injury side, 8 hr following a single ouabain infusion into the dentate gyrus. The right panels were taken from contralateral side where ouabain and charybdotoxin were co-infused. (A) Ouabain resulted in extensive tissue damage in the dentate gyrus as illustrated by significant granule cell shrinkage, shape change of hilar cells (arrows) and vacuolization (arrowheads). A tissue seperation close to the area of vacuoles was routinely observed. (B) Charybdotoxin infusion provided dramatic tissue protection as shown by a significant reduction of granule cell shrinkage (arrowheads, compare with A), complete prevention of cell shape changes in hilus and lack of vacuolization. (C and D) High magnification images of the hilar region from ouabain-infused side showing hilar shape changes (arrows) and marked vacuolization and the absence of such tissue damage in the presence of charybdotoxin (D). (E) Tissue damage in CA1 region following ouabain infusion. Note the significant cell shrinkage, pyknosis and hyperchromatism (arrows). (F) Images from the contralateral CA1, illustrating that co-infusion of ouabain and charybdotoxin led to the appearance of healthy looking cells (arrows) alternating with shrunken, pyknotic and hyperchromatic neurons (arrowheads).

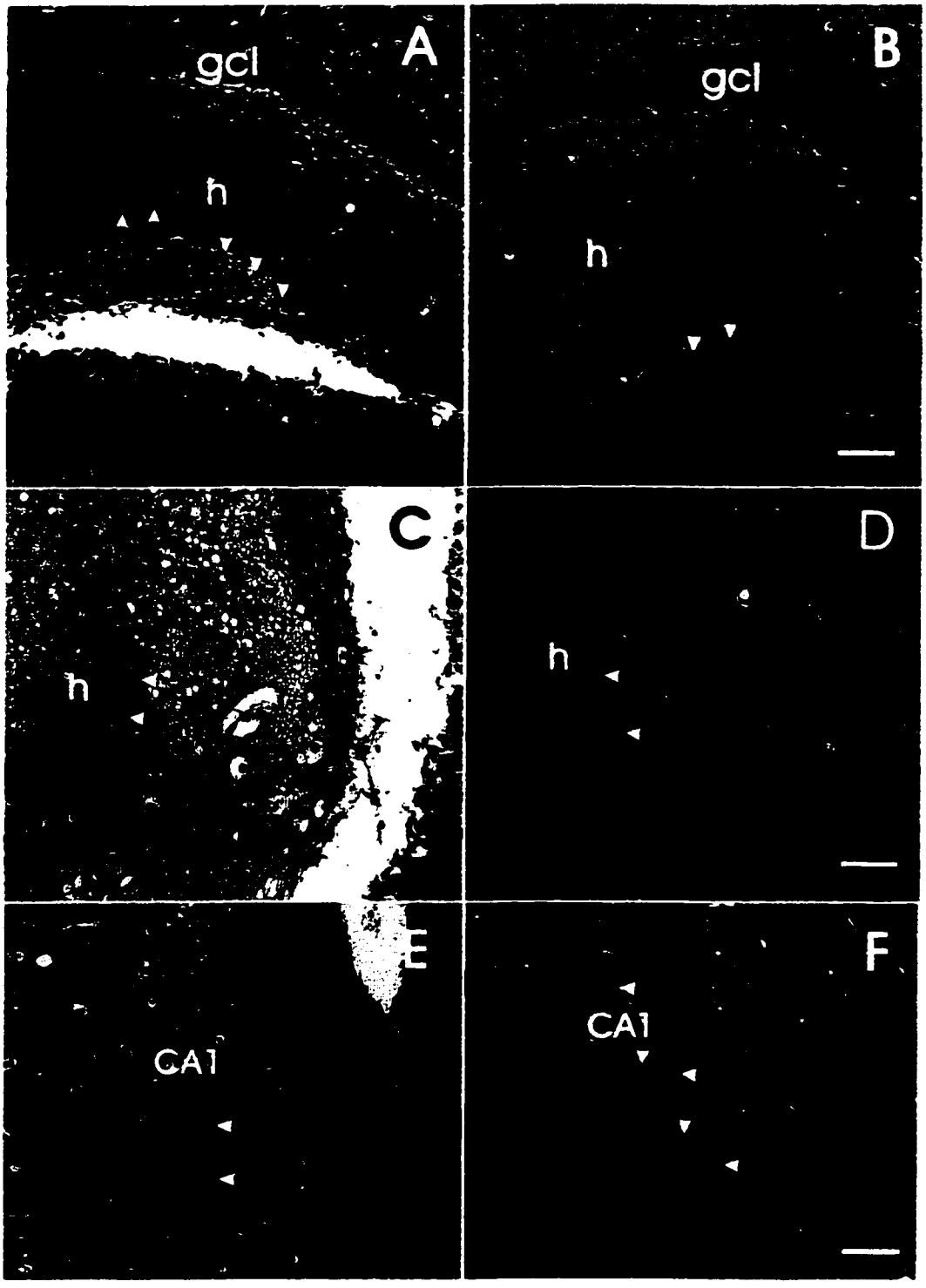
gcl
A
h
gcl
B
h
C
h
D
h
E
CA1
F
CA1

Table 1. Effects of charybdotoxin on the apoptotic (A.I.) and necrotic (N.I.) indices in the hippocampal dentate gyrus

Agent	N.I.	A.I.
Ouabain	6.70 ± 1.08	1.71 ± 0.21
Ouabain + Charybdotoxin	0.21 ± 0.06	0.13 ± 0.03
P	< 0.005	< 0.001

Chapter 4.

A.I. Omar, V.V. Senatorov, and B. Hu. 1999. Ethidium bromide staining reveals rapid cell dispersion in the rat dentate gyrus following ouabain-induced injury. Neuroscience. 95 (1): 73 – 80.

Title: **Ethidium Bromide Staining Reveals Rapid Cell Dispersion in the Rat Dentate Gyrus Following Ouabain-Induced Injury**

Author: A.I. Omar, V.V. Senatorov, and B. Hu

Origin of Work: Laboratory of Dr. Bin Hu
Loeb Health Research Institute
Ottawa Hospital - Civic Campus
University of Ottawa
Ottawa, Ontario
Canada, K1Y 4E9

Source: *Neuroscience*, Volume 95, Number 1, pages 73-80, November, 1999

Running Title: Rapid Cell Dispersion in Rat Hippocampus

Correspondence: Bin Hu, MD, Ph.D.

Loeb Health Research Institute

1053 Carling Ave

Ottawa Hospital - Civic Campus

Ottawa, Ontario

Canada K1Y 4E9

Tel: 613-761-5355

Fax: 613-761-5330

binh@civich.ottawa.on.ca

Statistics: Text, 27 pages; figures, 5; tables, 2

Abbreviations: CCD, Charge-coupled device; EB, ethidium bromide; EtHD-1, ethidium homodimer; GCL, Granule cell layer; H/E, Hematoxylin and eosin; ILC, intensely labelled cell; MCL, Molecular cell layer; PoDH, Polymorphic interneurons of dentate hilus; SLM, stratum lacunosum moleculare; TLE, temporal lobe epilepsy.

ABSTRACT

The dentate gyrus of the hippocampal formation undergoes extensive network remodelling including progenitor cell proliferation, migration as well as apoptotic cell death in response to prolonged excitotoxic insults. Previous studies have shown that such a proliferative cell population may undergo aberrant migration and later persist in ectopically located positions within the molecular cell layer. In this study we have developed an experimental model to characterize the spatiotemporal patterns of such an injury-induced network remodelling. Ouabain (1μl, 1mM), a Na^+, K^+-ATPase blocker, was stereotactically co-injected into the rat dentate gyrus with ethidium bromide (1μl, 40μM). The latter is a fluorescent nucleic acid intercalating dye, which was used for labeling cells undergoing early phases of apoptosis or proliferation. Our results revealed that within an hour after the injection, a subpopulation of cells characterized by spindle or ovoid shaped somata and bipolar morphology, were intensely labeled with ethidium bromide. These cells were found initially clustered both inside and outside the dentate granule cell layer and later on markedly increased in number as well as spread radially in the next few hours into the dentate molecular layer. The unusual pattern of cell dispersion encountered in our study may represent aberrantly migrating progenitor cells consistent with earlier observations of ectopically located granule cells in human temporal lobe epilepsy specimens and epilepsy animal models. Alternatively, the described phenomenon may represent dispersion of Cajal-Retzius cells that may be involved in post-lesion network remodelling.

Key Words: hippocampus, ethidium bromide, ouabain, Na^+, K^+- ATPase, neuronal dispersion and apoptosis

INTRODUCTION

Excitotoxicity is a major pathological mechanism underlying acute and delayed neuronal death induced by ischemia and prolonged seizure status.[26] Unlike in many other brain regions, the excitotoxic injury in the adult hippocampal dentate is associated with pronounced neurogenesis which is characterized by enhanced proliferative activity, production and relocation as well as migration of newly born cells.[17,18,280,35] For example, ectopically located granule cells have been consistently observed in patients with long standing temporal lobe epilepsy (TLE).[20,21,30,31] Recent studies using various animal models of TLE and global ischemia showed that neurogenic responses, such as the appearance of ectopically located cells in the dentate gyrus, may present an important mechanism underlying brain injury and repair.[17,28] Indeed, neurogenic activities in the dentate and cerebral cortex were also often accompanied by increased apoptotic cell death,[3,41] presumably reflecting part of the repair process of network remodelling.

Injury-induced neural network reorganization is an important yet poorly understood physiological phenomenon. For instance, it has not been determined how early and to what extent neurogenic responses can be initiated by severe excitotoxic insult. In this study we sought to examine this issue using a ouabain brain injury model by investigating the acute cellular responses to injury in the adult rat hippocampus. Ouabain has been previously used as an experimental drug for the induction of hippocampal epilepsy and for simulating ischemic tissue injury.[6,27] Pump inhibition results in membrane depolarization, excessive release of excitatory amino acids, and an increase in intracellular sodium and calcium, changes that closely mimic ischemic and epileptic conditions.[7,26]

In order to maximize the likelihood of early labeling of proliferative/apoptotic cells, which are also the most likely source of dispersing cells,[35] we used a fluorescent nucleic acid dye, ethidium bromide (EB). The approach was undertaken because previous studies show that proliferative/apoptotic activity is invariably associated with enhanced nucleic acid metabolism, topological changes in DNA structure, an enhanced membrane permeability and accessibility of DNA to nucleic acid intercalating dyes.[5,14,15] Preliminary results of this study have been reported elsewhere in an abstract form.[34]

EXPERIMENTAL PROCEDURES

Preparation

Male Long-Evans rats (300-350 g; Charles River, Canada) were anaesthetised with intramuscular injections of 0.2 ml /300 g body weight of a Ketamine (Ketalar®) and Xylazine (Rompun®) mixture according to the following regimen: 4 ml of Ketamine (50 mg/ml) + 1ml of Xylazine (20 mg/ml). After attaining a surgical plane of anaesthesia, rats were further anaesthetised with Halothane (2-3% in 100% oxygen), which was used for maintenance throughout the surgery. The anaesthesia, surgical and experimental protocol was approved by the Hospital Animal Care Council, which ensures conformity with the guidelines of the National Institutes of Health and the Canadian Council on Animal Care. After mounting onto a stereotactic frame, a midsagittal scalp incision was performed, the skull exposed and periosteum removed. A burr hole was drilled into the skull at stereotactic coordinates corresponding to the dentate gyrus granule cell layer (Bregma: -3.8; Lateral:2.2; and Ventral to dura:3.3).[36] A borosilicate micropipette filled from its rear with 1μl of a 40μM solution of ethidium bromide (Molecular Probes Inc., Eugene, OR) and 1μl of a 1mM solution of ouabain (Sigma Aldrich Corp., St. Louis, MO) was then lowered towards the target site and the solution was pressure-injected using a 1 ml syringe attached through plastic tubing to the back of the micropipette (Fig. 1). The solution was injected at a rate of 0.3 - 0.5 μl/min as monitored through the level of the meniscus observed under a stereomicroscope. The micropipette was then left in place for 10 - 15 min to minimize backdiffusion of the solution. The same procedure was then repeated in the contralateral hippocampus (control), where only 1μl of 40μM ethidium bromide together with 1μl of physiological saline were injected at identical stereotactic

coordinates. In some experiments, 1μl of 4μM ethidium homodimer (EthD-1; Molecular probes Inc., Eugene, OR) was substituted for ethidium bromide to test the specificity of the dye. The burr hole was finally filled with bone wax and the scalp sutured. No special handling above regular husbandry was required following successful recovery from anaesthesia.

(Fig. 1 near here)

Tissue processing

A series of 27 rats were used during this experiment. At varying time points following the injections (1, 2, 3, 4, 6, 8, and 72 hours), rats were deeply anaesthetised with sodium pentobarbital (Somnotol®, 0.22 ml/100 g body weight, i.p.) and were then transcardially perfused with 200 ml of 4% paraformaldehyde in 0.1 M phosphate buffer at pH 7.4. The rats were decapitated and their brains sectioned in the coronal plane on a cryostat, at 30 μm. Sections mounted on gelatin-coated slides, were first examined uncoverslipped. Finally, a number of sections were selected for staining with Thionine (0.25%) or Haematoxylin & Eosin (H&E) in order to assess cell density and/or morphological changes.

Data analysis

Thionine and H&E stained sections were examined with a light microscope, while ethidium bromide was visualized using an Olympus epifluorescence (IX50/IX70) and /or a BioRad MRC (1000/1024) confocal laser scanning microscope. The images of ethidium

bromide labeled cells were captured through a tetrarhodamine isothiocyanate (TRITC) filter (Chroma Technology Corporation, Vermont, Brattleboro, U.S.A.) using a Sony CCD colour video camera connected to a PC with a Windows 95 platform and image acquisition software (Northern Exposure, Empix Imaging Inc., Mississauga, Canada). In order to compare tissue responses, corresponding regions on both sides were selected for acquisition.

Quantitative analysis of CCD images was performed using the public domain NIH Image 1.62 software (U.S. National Institutes of Health; available from the Internet by anonymous ftp from zippy.nimh.nih.gov). Images of the dentate gyrus were divided into the following subregions for independent assessment: granule cell layer, an inner (ventral) ⅓, a middle ⅓ and an outer (dorsal) ⅓ of the molecular cell layer and finally, the stratum lacunosum moleculare. ILCs were counted through direct observation from 10 sections, 50μm apart. The number of cell somata in each section was corrected with the Abercrombie equation[1] and the results were averaged for each subregion and plotted against the different post-injection time points. ANOVA and Student's *t*-test were used for statistical analysis. Results are expressed as mean ± S.E.M.

RESULTS

Examination of brain sections one hour following ouabain administration revealed a macroscopic EB fluorescence in the GCL and the immediately adjacent hilar and molecular regions (Fig. 3a). At higher magnification it was found that the GCL neurons were faintly labeled with the exception of a subpopulation of cells that showed intense EB accumulation and an abundant EB signal from the cytoplasmic compartment as well as the proximal dendritic processes (Fig.2a,b). These intensely labeled cells have a characteristic morphological appearance, namely a small oval or rounded soma with a bipolar, long arborization (Fig. 2b).

(Fig. 2 near here)

Time course study suggests ouabain-induced cell dispersion

Examination of brain sections at varying survival periods following pump inhibition revealed a characteristic spatiotemporal distribution, in which ILCs were seen at increasingly farther distances from their initial site of appearance as a function of time. One hour following pump inhibition, ILCs were exclusively observed along the dentate GCL and the immediately adjacent hilar and molecular regions, while an hour later (2hr), ILCs were also observed in the middle ⅓ of the MCL, a subregion that was completely devoid of ILCs at the earlier 1 hour time point (Fig. 3b and Table 1). The number of ILCs at this same time point was significantly higher in the GCL compared to the other dentate subregions ($p < 0.001$) (Fig. 3a,b and Table 1). At the 3-hour time point, a further significant rise in the number of ILCs was seen in the middle ⅓ of the MCL when

compared to the previous 2 hr value ($p < 0.05$), while the number of ILCs in the GCL was still significantly higher than the other dentate subregions ($p < 0.01$). On the other hand, cell count at the 4 hr time point exhibited a sharp rise from all hippocampal subregions when compared to the previous 3 hr values ($p < 0.0001$). In addition, ILCs followed a strikingly organized spatiotemporal pattern and distributed along the entire volume of the MCL and furthermore, assumed a radial orientation relative to the long axis of the GCL (Fig.3c). This pattern was also observed at the 6 hr time point, where the maximal number of ILCs was seen (Fig. 4c, Table 2). At 6 hours, a significant proportion of those ILCs were located in the GCL relative to the other subregions ($p < 0.01$). In contrast, the control side was completely devoid of ILCs, (Fig. 3d) and remained so throughout the time points examined. At the 8 hour time point, ILCs were mainly seen clustered within the stratum lacunosum moleculare (SLM), adjacent to the hippocampal fissure, in significantly higher numbers when compared to the other dentate subregions ($p < 0.0001$) and also when compared to the previous 6 hr count obtained from the SLM ($p < 0.01$) (Fig.4c,d). A sharp drop in the number of ILCs was also observed in the granule cell as well as the molecular cell layers, compared to the previous 6 hr values ($p < 0.0001$). Three days following surgery, ILCs were virtually undetectable in any of the brain sections examined. The disappearance of ILCs was associated with massive cell loss in the GCL (data not shown).

(Fig. 3 and Table 1 near here)

(Fig. 4 and Table 2 near here)

On the other hand, EthD-1, a probe for overt membrane disintegration that characterizes necrosis and/or late stages of apoptosis,[10] when co-injected with ouabain into the dentate GCL, did not reveal any labeling of cells, both at 4 hours as well as 6 hours post-injection (data not shown).

Tissue "reactionary response" following ouabain administration

Nissl and H&E stained sections exhibited a reactionary response typically seen in ischemic tissue,[40] which was characterized by a dramatic cell shrinkage of the dentate GCL as well as the appearance of pyknotic and hyperchromatic nuclei, 4 hours post-injection (Fig. 5a). Many neurons in the CA3, polymorphic dentate hilus (PoDH) as well as the distant subiculum changed their shape from a regular rounded to a triangular and slightly irregular appearance (Fig.5c,d). In addition, a splitting of the GCL along its long axis, which often appeared in TLE specimens,[20] was also observed. Granule cells have been consistently observed to have apparently aligned themselves into radial columns relative to the long axis of the GCL, 4 hours following ouabain administration. This alignment was particularly prominent in the crest of the dentate GCL (Fig 5a). Interestingly, ILCs were found in higher numbers when counted from the molecular layer around the crest, than those counted from the molecular layer around the supra or infrapyramidal blades of the dentate GCL.

(Fig. 5 near here)

DISCUSSION

In this study we have demonstrated that Na^+, K^+-ATPase inhibition in the dentate of the adult rat hippocampus results in the appearance of a population of ectopically located cells, together with a typical host of morphological changes seen in epileptic and ischemic tissues. The selective labeling of these ectopically located cells by EB, their rapid appearance and their wide range of dispersion have not been described before.

Intrahippocampal ouabain administration replicates limbic epilepsy pathology

Grey matter heterotopic neuronal masses in white matter regions and misplaced granule cells in the dentate inner molecular layer have been observed in post mortem and lobectomy specimens from subjects with limbic seizures.[13] Epilepsy animal models employing administration of kainate as well as kindling, or repetitive electrical stimulation of the rat hippocampus replicate many of these pathological features, including hippocampal sclerosis, granule cell dispersion as well as appearance of ectopically located granule cells both in the dentate hilar and inner molecular regions.[32,35] Misplacement of granule cells and their persistence in ectopic locations are thought to contribute to epileptogenesis, presumably through the formation of abnormal afferent and efferent connections leading to alterations of hippocampal circuitry.[20] We have observed degeneration of cells in the hilar and CA3 regions similar to that seen in TLE hippocampal sclerosis, as well as separation of the GCL along its long axis into a bilaminar column of cells with a cell deficient region in between, as early as 4 hours following ouabain administration. This bilaminar appearance of the GCL was strikingly similar to that observed by Houser in post mortem specimens from TLE subjects,[20]

suggesting that pump inhibition induces many early pathological changes seen in TLE. Houser reported that in post mortem specimens of TLE subjects, ectopically located granule cells were arranged vertically within the molecular layer relative to the GCL, a strikingly similar arrangement to the spatial distribution of EB labeled cells seen in our study.[20] Furthermore, ectopically located granule cells seen in surgical and post-mortem specimens from TLE subjects as well as TLE animal models had a typical bipolar morphology and spindle shaped somata.[17,20] Such morphological features are also characteristic of EB labeled cells, although the exact phenotype of ILCs remains to be determined in future studies.

The anatomical origin of misplaced granule cells as well as the mechanism of aberrant neuronal migration has been a subject of intense research. Cells residing in the subgranular zone are known to continue proliferation throughout adulthood and migrate into the GCL where they differentiate into mature granule cells and extend processes to their post-synaptic targets.[37,38] A previous study showed that ibotenic acid, an excitatory amino acid, when injected directly into the GCL resulted in a dramatic rise in progenitor cell proliferation as well as appearance of granule cells in ectopic locations, whereas a similar injection in the subiculum or other hippocampal subregions failed to induce this same response.[17] In chemoconvulsant pilocarpine model of TLE, the newly generated progenitor cells of the subgranular zone appear to be the source of such ectopically located granule cells.[35] In compatibility with the above studies, we found ILCs were initially clustered within the granule cell layer and the immediately adjacent subgranular, hilar and molecular regions. However, it is unknown at this time whether EB labeled cells

solely originated from the potential "progenitor" cells in the subgranular zone or cells pre-existing within the granular cell layer.

Intense ethidium bromide staining reflects enhanced nucleic acid metabolism

Various animal models of epilepsy consistently demonstrate that excitotoxicity-mediated upregulation of proliferative activity also coincides with an increase in apoptotic cell death.[3] Such fine balanced activities between cell birth and programmed cell death may serve to fine tune the lesion-induced remodelling process thereby ensuring the timely elimination of defective and superfluous cells.

Three lines of evidence support the possibility that intense EB accumulation in ectopically located cells observed in our study may reflect an early proliferative/apoptotic activity and enhanced nucleic acid metabolism. First, an increase in DNA content is a feature of actively proliferating cells that would therefore exhibit higher fluorescence peaks when labeled by EB.[5] Second, previous studies reported the appearance of an increase in DNA stainability by EB during the early phases of apoptosis, known as the hyperdiploid peak,[15] that usually precedes another delayed hypodiploid peak occurring at the final stages of apoptosis, typically characterized by internucleosomal cleavage and the shedding of fragmented DNA.[8] Initial phases of apoptosis are often accompanied by a minimal increase in membrane permeability, thus specifically allowing admission of the low molecular weight, EB, while excluding the bulkier EthD-1. This is consistent with the negative labeling by EthD-1described in this study. On the other hand, intracellular EB fluorescence could also be enhanced by an increase in DNA base pair accessibility.[12] Breakdown of the closed DNA loops specifically at their site of attachment to the nuclear

matrix is one of the earliest signs of apoptosis at the chromatin level.[14] Third, a recent study indeed suggests that cell proliferation and apoptosis can co-exist in dentate gyrus cells obtained from epilepsy tissue.[33]

Alternative explanations for the data presented in our study however do exist. ILCs may represent Cajal-Retzius cells normally found in the developing hippocampus. Indeed, in addition to the enhanced proliferative activity observed in limbic epilepsy animal models, recent reports demonstrated the persistence as well as an increase in number of the normally transient Cajal-Retzius cell population in specimens obtained from TLE patients.[4] Such Cajal-Retzius cells are generally believed to be involved in regulation of neuronal migration during corticogenesis and rapidly disappear by the 2nd or 3rd postnatal weeks.[39] However, recent studies present evidence that such cells are capable of migrating away from the injury core following a freezing insult to the neonatal mouse cortex. These cells repopulated the lesioned zone presumably through migrating from peri-lesion areas and later on persisted into more advanced postnatal stages.[40] Consistent with this explanation is the morphological appearance of Cajal-Retzius cells that are typically characterized by ovoid or spindle shaped somata and a bipolar arborization,[11] an appearance similar to ILCs observed in our study. It is intriguing to think of ILCs as cells that are capable of migrating from the injury core early on following an excitotoxic insult and to possibly participate in the later injury-induced remodelling process including the regulation of progenitor cell migration. On the other hand, the possibility of ILCs representing a rapidly proliferating glial cell population, particularly radial glia, cannot be ruled out. A recent report showed that mature stellate astrocytes are capable of "dedifferentiating" into the developmentally transient radial

glia following transplantation of embryonic neurons into areas undergoing targeted neuronal apoptosis in the adult mouse neocortex.[25] This transient rejuvenation of radial glia provided a scaffold for directing migration of the transplanted embryonic neurons indicating that, in areas of neuronal damage, the adult cortex is capable of reverting to an embryonic microenvironment that may facilitate network remodelling. Our data showed that ILCs not only markedly increased in number but also spread over a 2-8 hour period into the outer molecular layer, approximately 1 mm away from the granule cell zone. Such a time-dependent cell dispersion cannot be however explained by a slow diffusion of ouabain and ethidium bromide within the dentate gyrus. This is because within 2 hr post-injection, a comparable number of ILCs within the GCL were found 2mm along the septo-temporal axis while the outer a of the molecular layer much closer to the injection core was completely devoid of labeled cells.

Long range cell migration has been well-documented in post-natal developing forebrain.[12,29] Stem cells located in the subventricular zone can move rapidly in mass towards frontal cortex and refill a lesion cavity within two days.[22] In adult brain, such large scale cell migration is uncommon. Rather, we suggest that ouabain-induced cell dispersion represents an "escaping" mechanism utilized by cells that are capable of migrating away from the injury core. There are a number of factors that may play an important role in triggering cell dispersion, including NMDA receptor activation,[23] Ca^{2+} current fluctuations,[24] certain nerve growth factors[2] and tissue plasminogen activator release,[16] particularly in response to sustained membrane depolarization.[19] Interestingly, all these factors can be activated directly or indirectly as a result of pump inhibition.[26]

CONCLUSION

The present study describes a novel cellular response to acute toxic injury in the adult rat dentate gyrus. We have shown that intrahippocampal co-administration of ouabain and ethidium bromide results in rapid staining of a distinct cell subpopulation that undergoes dispersion as a function of time. The described phenomenon may represent aberrantly migrating progenitor cells that have been implicated in the initiation and maintenance of temporal lobe epilepsy. Alternatively, the described cell subpopulation may represent Cajal-Retzius cells that may participate in the regulation and positional rearrangement of progenitor cells during the lesion-induced remodelling process.

ACKNOWLEDGEMENTS

This work was supported by the Medical Research Council (MRC) of Canada and partially by the Heart and Stroke Foundation of Canada.

REFERENCES

1. Abercrombie M. (1946) Estimation of nuclear population from microtome sections. *Anat. Rec.* **94**, 239-247.

2. Behar T. N., Dugich-Djordjevic M. M., Li Y. X., Ma W., Somogyi R., Wen X., Brown E., Scott C., McKay R. D. and Barker J. L. (1997) Neurotrophins stimulate chemotaxis of embryonic cortical neurons. *Eur. J. Neurosci.* **9**, 2561-2570.

3. Bengzon J., Kokaia Z., Elmer E., Nanobashvili A., Kokaia M. and Lindvall O. (1997) Apoptosis and proliferation of dentate gyrus neurons after single and intermittent limbic seizures. *Proc. Natl. Acad. Sci. U. S. A.* **94**, 10432-10437.

4. Blumcke I., Beck H., Suter B., Hoffmann D., Fodisch H. J., Wolf H. K., Schramm J., Elger C. E., Wiestler O. D. (1999) An increase of hippocampal calretinin-immunoreactive neurons correlates with early febrile seizures in temporal lobe epilepsy. *Acta Neuropathol (Berl.)* **97**, 31-39.

5. Bonaly J. and Mestre J. C. (1981) Flow fluorometric study of DNA content in nonproliferative Euglena gracilis cells and during proliferation. *Cytometry* **2**, 35-38.

6. Brines M. L., Dare A. O. and de Lanerolle N. C. (1995) The cardiac glycoside ouabain potentiates excitotoxic injury of adult neurons in rat hippocampus. *Neurosci. Lett.* **191**, 145-148.

7. Brines M. L., Tabuteau H., Sundaresan S., Kim J., Spencer D. D. and de Lanerolle N. (1995) Regional distributions of hippocampal Na+,K (+)-ATPase, cytochrome oxidase, and total protein in temporal lobe epilepsy. *Epilepsia* **36**, 371-383.

8. Darzynkiewicz Z., Bruno S., Del Bino G., Gorczyca W., Hotz M. A., Lassota P. and Traganos F. (1992) Features of apoptotic cells measured by flow cytometry. *Cytometry* **13**, 795-808.

9. Darzynkiewicz Z., Traganos F., Kapuscinski J., Staiano-Coico L. and Melamed M. R. (1984) Accessibility of DNA in situ to various fluorochromes: relationship to chromatin changes during erythroid differentiation of Friend leukemia cells. *Cytometry* **5**, 355-363.

10. Decherchi P., Cochard P. and Gauthier P. (1997) Dual staining assessment of Schwann cell viability within whole peripheral nerves using calcein-AM and ethidium homodimer. *J. Neurosci. Methods* **71**, 205-213.

11. Derer P., Derer M. (1990) Cajal-Retzius cell ontogenesis and death in mouse brain visualized with horseradish peroxidase and electron microscopy. *Neuroscience* **36**, 839-856.

12. Doetsch F. and Alvarez-Buylla A. (1996) Network of tangential pathways for neuronal migration in adult mammalian brain. *Proc. Natl. Acad. Sci. U. S. A.* **93**, 14895-14900.

13. Emery J. A., Roper S. N. and Rojiani A. M. (1997) White matter neuronal heterotopia in temporal lobe epilepsy: a morphometric and immunohistochemical study. *J. Neuropathol. Exp. Neurol.* **56**, 1276-1282.

14. Ferlini C., Biselli R., Scambia G. and Fattorossi A. (1996) Probing chromatin structure in the early phases of apoptosis. *Cell. Prolif.* **29**, 427-436.

15. Ferlini C., Di Cesare S., Rainaldi G., Malorni W., Samoggia P., Biselli R. and Fattorossi A. (1996) Flow cytometric analysis of the early phases of apoptosis by cellular and nuclear techniques. *Cytometry* **24**, 106-115.

16. Friedman G. C. and Seeds N. W. (1995) Tissue plasminogen activator mRNA expression in granule neurons coincides with their migration in the developing cerebellum. *J. Comp. Neurol.* **360**, 658-670.

17. Gould E. and Tanapat P. (1997) Lesion-induced proliferation of neuronal progenitors in the dentate gyrus of the adult rat. *Neuroscience* **80**, 427-436.

18. Gray W. P. and Sundstrom L. E. (1998) Kainic acid increases the proliferation of granule cell progenitors in the dentate gyrus of the adult rat. *Brain Res.* **790**, 52-59.

19. Gualandris A., Jones T. E., Strickland S. and Tsirka S. E. (1996) Membrane depolarization induces calcium-dependent secretion of tissue plasminogen activator *J. Neurosci.* **16**, 2220-2225.

20. Houser C. R. (1990) Granule cell dispersion in the dentate gyrus of humans with temporal lobe epilepsy. *Brain Res.* **535**, 195-204.

21. Houser C. R. (1992) Morphological changes in the dentate gyrus in human temporal lobe epilepsy. *Epilepsy Res. Suppl.* 7, 223-234.

22. Kolb B., Gibb R., Gorny G. and Whishaw I. Q. (1998) Possible regeneration of rat medial frontal cortex following neonatal frontal lesions. *Behav. Brain Res.* **91**, 127-141.

23. Komuro H. and Rakic P. (1993) Modulation of neuronal migration by NMDA receptors. *Science* **260**, 95-97.

24. Komuro H. and Rakic P. (1996) Intracellular Ca2+ fluctuations modulate the rate of neuronal migration. *Neuron* **17**, 275-285.

25. Leavitt B. R., Hernit-Grant C. S., Macklis J. D. (1999) Mature astrocytes transform into transitional radial glia within adult mouse neocortex that supports directed migration of transplanted immature neurons. *Exp. Neurol.* **157**, 43-57.

26. Lees G. J. (1991) Inhibition of sodium-potassium-ATPase: a potentially ubiquitous mechanism contributing to central nervous system neuropathology. *Brain Res. Brain Res. Rev.* **16**, 283-300.

27. Lees G. J., Lehmann A., Sandberg M. and Hamberger A. (1990) The neurotoxicity of ouabain, a sodium-potassium ATPase inhibitor, in the rat hippocampus. *Neurosci. Lett.* **120**, 159-162.

28. Liu J., Solway K., Messing R. O. and Sharp F .R. (1998) Increased neurogenesis in the dentate gyrus after transient global ischemia in gerbils. *J. Neurosci.* **18**, 7768-7778.

29. Lois C. and Alvarez-Buylla A. (1994) Long-distance neuronal migration in the adult mammalian brain. *Science* **264**, 1145-1148.

30. Lurton D., El Bahh B., Sundstrom L. and Rougier A. (1998) Granule cell dispersion is correlated with early epileptic events in human temporal lobe epilepsy. *J. Neurol. Sci.* **154**, 133-136.

31. Lurton D., Sundstrom L., Brana C., Bloch B. and Rougier A. (1997) Possible mechanisms inducing granule cell dispersion in humans with temporal lobe epilepsy. *Epilepsy Res.* **26**, 351-361.

32. Mello L. E., Cavalheiro E. A., Tan A. M., Kupfer W. R., Pretorius J. K., Babb T.L. and Finch D. M. (1993) Circuit mechanisms of seizures in the pilocarpine model of chronic epilepsy: cell loss and mossy fiber sprouting. *Epilepsia* **34**, 985-995.

33. Nagy Z. and Esiri M. M. (1998) Neuronal cyclin expression in the hippocampus in temporal lobe epilepsy. *Exp. Neurol.* **150**, 240-247.

34. Omar A. I., Senatorov V. V., Tiberi M. and Hu B. (1998) Rapid induction of granule cell dispersion in the dentate gyrus of the adult rat hippocampal formation by ouabain. *Soc. Neurosci. Abstr.* **24**, 718.

35. Parent J. M., Yu T. W., Leibowitz R. T., Geschwind D. H., Sloviter R. S. and Lowenstein D. H. (1997) Dentate granule cell neurogenesis is increased by

seizures and contributes to aberrant network reorganization in the adult rat hippocampus. *J. Neurosci.* **17**, 3727-3738.

36. Paxinos G. and Watson C. (1982) *The Rat Brain in Stereotaxic Coordinates*. 3rd edition, Sydney: Academic Press.

37. Seki T. and Arai Y. (1993) Highly polysialylated neural cell adhesion molecule (NCAM-H) is expressed by newly generated granule cells in the dentate gyrus of the adult rat. *J. Neurosci.* **13**, 2351-2358.

38. Stanfield B. B. and Trice J. E. (1988) Evidence that granule cells generated in the dentate gyrus of adult rats extend axonal projections. *Exp. Brain Res.***72**, 399-406.

39. Super H., Soriano E., Uylings H. B. (1998) The functions of the preplate in development and evolution of the neocortex and hippocampus. *Brain Res. Brain Res. Rev.* **27**, 40-64.

40. Super H., Perez Sust P., Soriano E. (1997) Survival of Cajal-Retzius cells after cortical lesions in newborn mice: a possible role for Cajal-Retzius cells in brain repair. *Brain Res. Dev. Brain Res.* **98**, 9-14.

41. Thomaidou D., Mione M. C., Cavanagh J. F. and Parnavelas J. G. (1997) Apoptosis and its relation to the cell cycle in the developing cerebral cortex. *J. Neurosci.* **17**, 1075-1085.

42. Towfighi J. and Mauger D. (1998) Temporal evolution of neuronal changes in cerebral hypoxia-ischemia in developing rats: a quantitative light microscopic study. *Brain Res. Dev. Brain Res.* **109**, 169-177.

Figure 1: Experimental configuration showing the dentate gyrus where the stereotaxic injection was directed. The arrow represents the micropipette introduced into the dentate granule cell layer. The image is of a H/E stained section taken at a coronal plane corresponding to that of the injection. GCL: granule cell layer; MCL: molecular cell layer; PoDH: polymorphic dentate hilus.

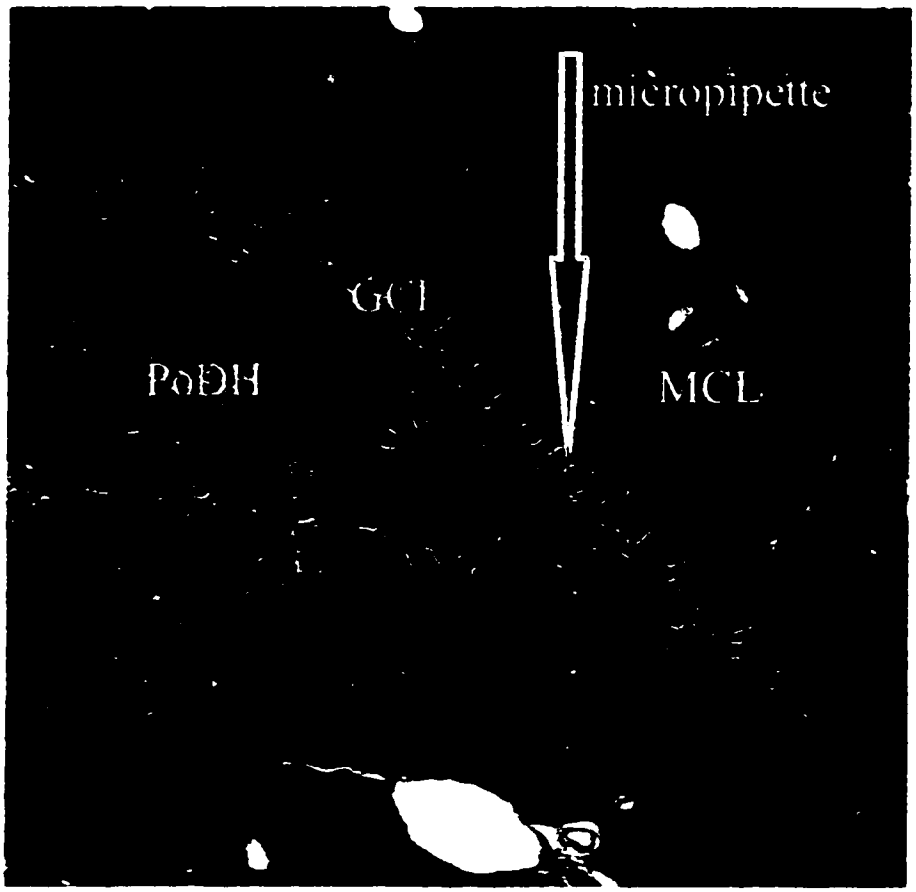
micropipette
GCL
PoDH
MCL

Figure 2: Morphology of ILCs. (a) The ILCs, as seen through epifluorescence microscopy, under low magnification, showing an ovoid or spindle shaped perikaryon and a bipolar structure. Note the processes extending from both poles (arrows). (b) Confocal image of ILCs, under high magnification. Processes are clearly observed extending from either poles. gcl: granule cell layer; mcl: molecular cell layer; h: hilus. Scale bars in (a): 50μm; (b): 10μm.

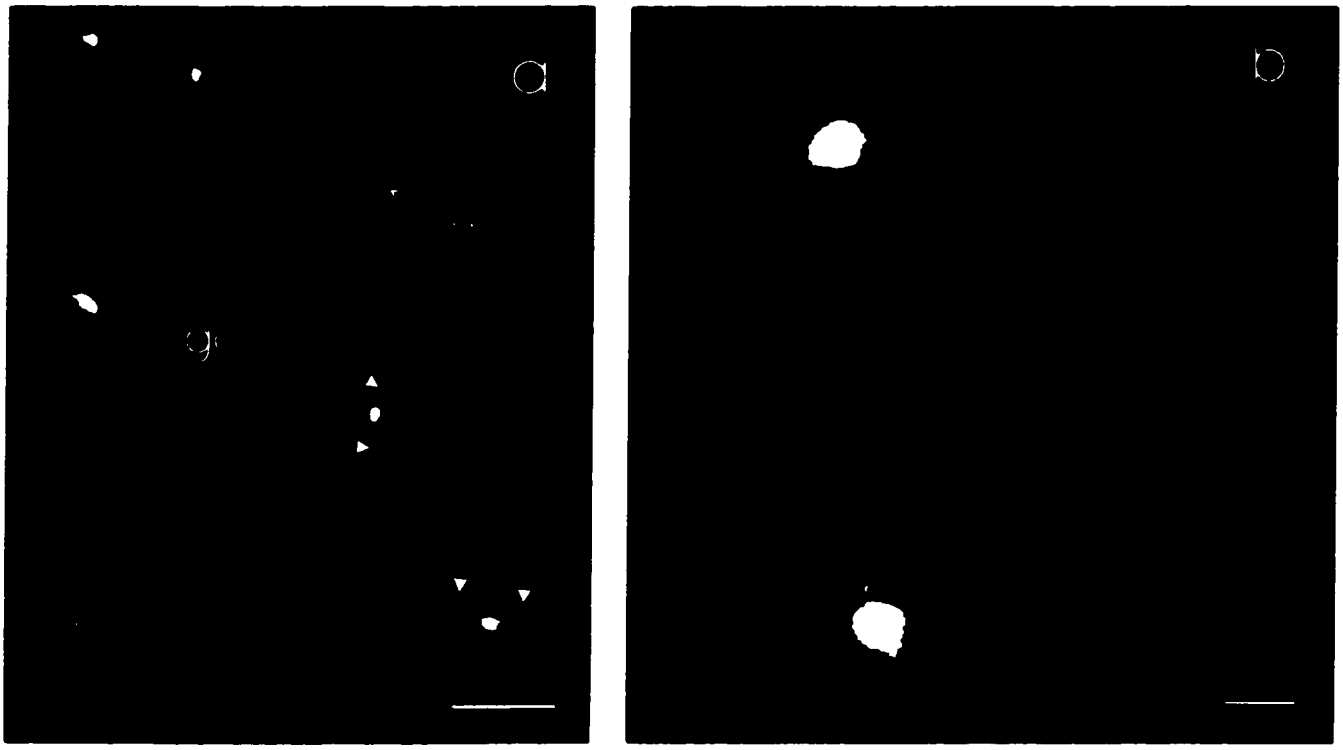
a
b

Figure 3: Time course study revealed the appearance of ILCs at progressively farther distances from the injection site as a function of time. (a) Fluorescent image showing ILCs mainly within the GCL (site of injection) at the 1-hour time point. (b) Two hours following surgery, ILCs appear within the inner ⅓ of the MCL. (c) At the 4-hour time point, ILCs have arranged themselves in a radial direction within the molecular cell layer relative to the long axis of the granule cell layer. They are now clearly seen along the entire volume of the MCL. The contralateral hippocampus receiving vehicle injection (control) did not contain any ILCs (d). GCL: granule cell layer; MCL: molecular cell layer; H: hilus.

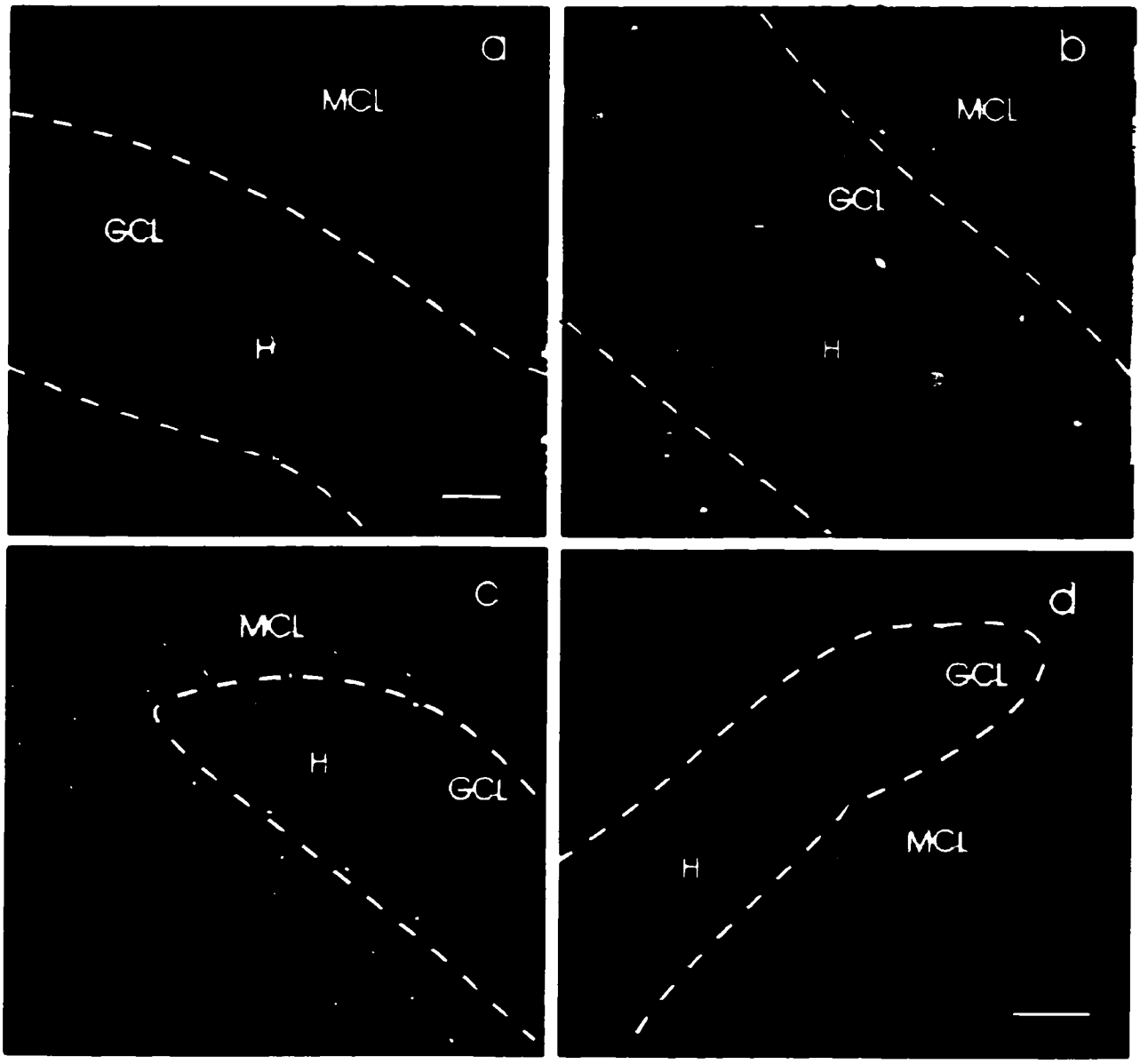

FIG. 1

Figure 4: Schematic representation (modified from ref. 33) depicting position of ILCs at increasing survival periods. Two hours post-injection (a), ILCs were seen scattered along the GCL, GCL/Hilar border and inner ⅓ of MCL. (b) Two hours later (4hr), ILCs sharply increased in number and were scattered along the entire volume of the MCL as well as the SLM. (c) ILCs increased in number at the 6 hr time point (mainly within inner ⅓ of MCL). (d) Shows the distribution of ILCs, 8 hr post-injection, where they were mainly clustered along the SLM with few remaining ILCs in the MCL. GCL: granule cell layer; MCL: molecular cell layer; PoDG: polymorphic dentate gyrus; SLM: stratum lacunosum moleculare.

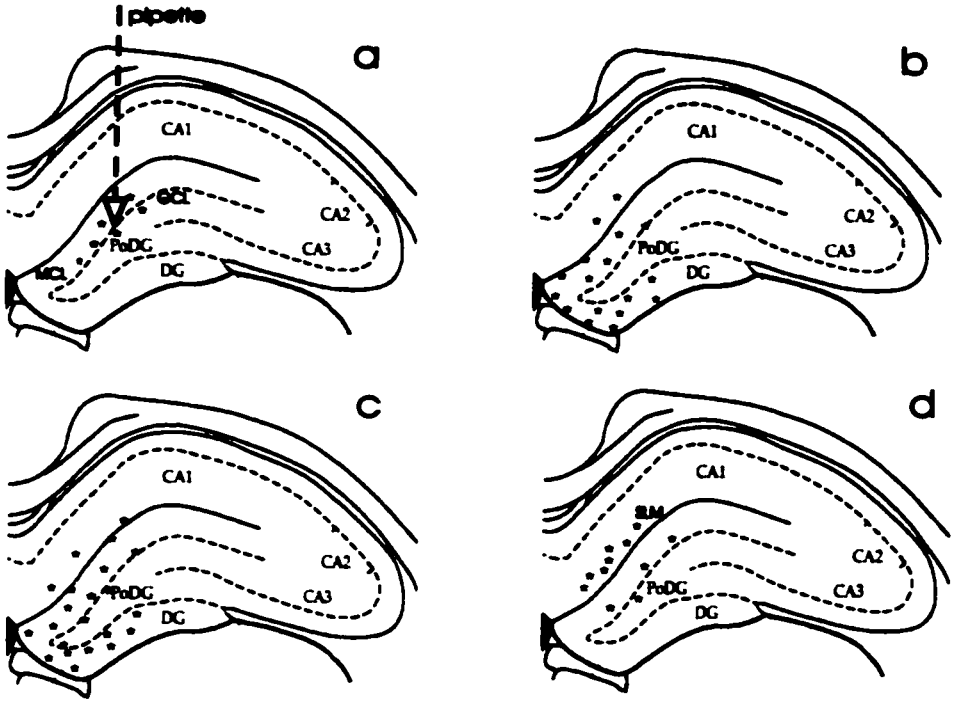
pipette
a
CA1
CA2
CA3
PoDG
DG
b
CA1
CA2
CA3
PoDG
DG
c
CA1
CA2
CA3
PoDG
DG
d
CA1
SLM
CA2
CA3
PoDG
DG

Figure 5: Reactionary changes in dentate gyrus 4 hours following ouabain and ethidium bromide administration. (a) Nissl stained section of ouabain treated granule cells showing splitting of the GCL along its long axis with a cell devoid region in between. Granule cells have also undergone a reactionary response characterized by cell shrinkage and hyperchromatism. (b) Nissl stained section from the contralateral hippocampus receiving saline injection; note the healthy morphological appearance. (c) Hilar neurons have changed shape from a rounded to a triangular and slightly irregular appearance 4 hours following ouabain administration. (d) Hilar neurons from the saline treated control showing a rounded appearance. GCL: granule cell layer; MCL: molecular cell layer; H: hilus. Scale bars: 50μm.

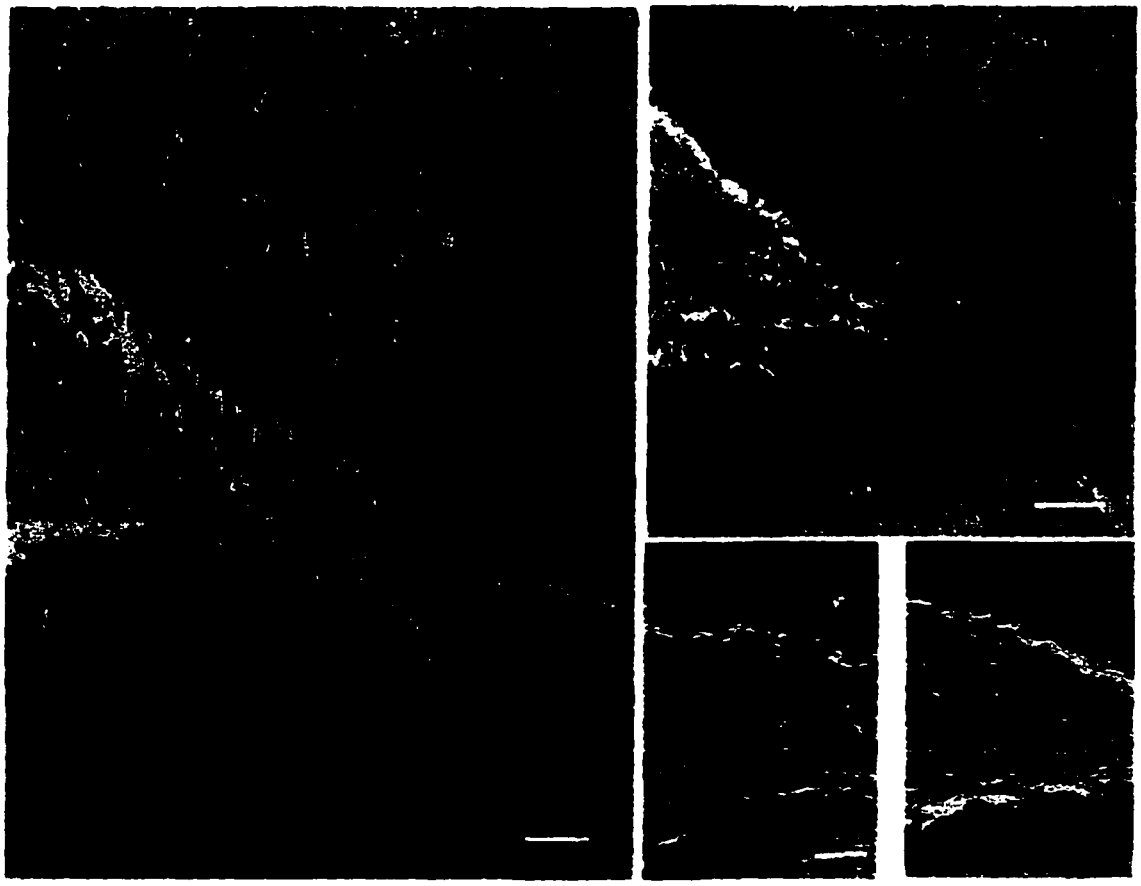

Table 1. Number of intensely-labeled cells within different hippocampal subregions at different time-points

	GCL + M1	M2	M3	S.L.M.
1 hr	**10 ± 2**	-	-	-
2 hr	**14 ± 2**	**3 ± 1**	-	-
3 hr	**12 ± 1**	**6 ± 2**	-	-
4 hr	**19 ±2**	**15 ± 1**	**16 ± 2**	**10 ± 3**
6 hr	**33 ± 4**	**13 ± 1**	**17 ± 2**	**11 ± 2**
8 hr	**2 ± 1**	**2 ± 1**	**3 ± 1**	**23 ± 3**
72 hr	-	-	-	-

Table 2. Average number of intensely labeled cells (per section) at increasing survival periods

1 h	2 h	3 h	4 h	6 h	8 h	72 h
10 ± 2	17 ± 2	18 ± 2	60 ± 1	74 ± 3	30 ± 3	-

Chapter 5.

A.I. Omar and B. Hu. Enhancement of progenitor cell proliferation and migration in rat hippocampal dentate gyrus following Na^+, K^+- pump inhibition. To be submitted to Experimental Neurology.

Title: **Enhancement of Progenitor Cell Proliferation and Migration in Rat Hippocampal Dentate Gyrus Following Na^+, K^+- Pump Inhibition**

Author: A.I. Omar and B. Hu

Origin of Work: Laboratory of Dr. Bin Hu

Loeb Health Research Institute

Ottawa Hospital - Civic Campus

University of Ottawa

Ottawa, Ontario

Canada, K1Y 4E9

Running Title: Enhancement of proliferation and migration

Correspondence: Bin Hu, MD, Ph.D.

Loeb Health Research Institute

1053 Carling Ave

Ottawa Hospital - Civic Campus

Ottawa, Ontario

Canada K1Y 4E9

Tel: 613-761-5355

Fax: 613-761-5330

binh@civich.ottawa.on.ca

Statistics: Text, 25 pages; figures, 2; table, 1

Abbreviations: SGZ, subgranular zone; GCL, granule cell layer; Na^+, K^+, ATPase, sodium-potassium adenosine triphosphatase; BrDU, 5'-bromo-2'-deoxyuridine; SSC, sodium chloride / sodium citrate; TBS: tris buffered saline; TBS-Tds: tris buffered saline / triton X / normal donkey serum; TRITC: tetrarhodamine isothiocyanate; H/E: hematoxylin/eosin; CCD: charge coupled device; NMDA: N-methyl, D-aspartate; ATP: adenosine triphosphate.

ABSTRACT

The adult rodent subgranular zone (SGZ) is known to harbour a multipotent stem cell population that undergoes proliferation throughout adulthood giving rise to newly born cells (1, 3, 4, 8, 9, 14). These precursor cells migrate into the granule cell layer (GCL) and differentiate into mature granule neurons (17, 39). To determine progenitor cell responses to acute neuronal injury, we stereotactically infused, a Na^+, K^+, ATPase pump blocker ouabain into the adult rat SGZ. The contralateral SGZ was infused with saline and used as a control. Rats were injected intraoperatively with the S-phase marker, 5'-bromo-2'-deoxyuridine (BrDU, 50 mg/Kg b.w., i.p.) and either at 1 and 2 h or 2 and 4h following surgery. Pump inhibition resulted in an increase in proliferative activity of subgranular zone progenitors at the 6 h time point. In addition, proliferating progenitors appeared to have migrated farther into the GCL in a radial orientation compared to the vehicle-treated control. At 2 h, there was no significant difference in the number, location and orientation of proliferating progenitors between ouabain and vehicle-treated SGZ. Nissl staining at 6 h but not at 2 h, following pump inhibition revealed granule cell injury characterized by marked cell shrinkage, chromophilia and pyknosis. The above results suggest that pump inhibition in the adult rat dentate gyrus is associated with enhanced precursor cell proliferation and migration. This may reflect an endogenous neural repair mechanism that accelerates replacement of ouabain-induced granule cell damage.

INTRODUCTION

The adult rat dentate gyrus is one of a few regions within the brain that retains multipotent stem cells well into adulthood (21, 44). These stem cells are self-renewing and are capable of giving rise to progenitor cells committed to a glial or neuronal cell lineage (13, 14). In the dentate gyrus of various species including humans, such stem cells are found in the subgranular zone, an area at the boundary between the granule cell layer and the hilus (1, 9, 12, 14, 17, 18, 23). Newly born cells are continuously generated during adulthood, where they migrate from the SGZ and into the distal areas of the granule cell layer. Nascent cells differentiate into mature granule neurons, extend projections to postsynaptic targets, generate functional synapses and fully integrate into the hippocampal circuitry (19, 30, 32, 43, 44).

The presence of self-renewing stem cells within the adult brain led to the optimistic assumption that the adult brain may be, under optimal conditions, capable of regenerating areas of damage and restoring functional integrity (11, 16, 22, 24, 38). Extensive research has been conducted in recent years with this objective in mind. To achieve this goal it would be imperative to elucidate the myriad of molecular signals that control stem cell proliferation, migration and differentiation into functionally mature post-mitotic cells.

Insults to the brain that are capable of inducing cell death have also been shown to simultaneously upregulate stem cell proliferative activity, in some cases several fold above the baseline (6, 7). Indeed, stem cells have been shown to exhibit a robust increase in proliferative activity in response to ischemic, epileptic as well as excitotoxic insults (10, 31, 41, 45). It appears that the adult brain possesses a latent self-repair program that is ultimately invoked under conditions of brain damage. For this self-repair program to be meaningful, the enhanced rate of cellular proliferation would have to be accompanied by

an enhanced rate of migration into areas where cell death occurs. To date, studies have mainly focused on the absolute numbers of proliferating cells that are present following such insults. In this study, we sought to examine the numbers and relative locations of progenitor cells following hippocampal damage induced by Na^+, K^+- pump inhibition.

EXPERIMENTAL PROCEDURES

Preparation

Male Long-Evans rats (300-350 g) rats were anesthetised with intramuscular injections of 0.2 ml /300 g body weight of a Ketamine (Ketalar®) and Xylazine (Rompun®) mixture according to the following regimen: 4 ml of Ketamine (50 mg/ml) + 1ml of Xylazine (20 mg/ml). After attaining a surgical plane of anesthesia, rats were further anaesthetised with Halothane (2-3% in 100% oxygen using a wall vaporizer unit), which was also used for maintenance throughout the surgery. The anesthesia protocol was approved by the Animal Care Council of the Ottawa Hospital.

After mounting onto a Kopf stereotactic frame, a midsagittal scalp incision was performed, the skull exposed and periosteum removed. A burr hole was drilled into the skull at stereotactic coordinates corresponding to the dentate subgranular zone (Bregma: -3.8; Lateral: 2.2; and Ventral to dura: 3.3) (46). A borosilicate micropipette filled from its rear with 1µl of a 1mM solution of ouabain (Sigma Aldrich Corp., St. Louis, MO) was then lowered towards the target site and the solution was pressure-injected using a 1 ml syringe attached through plastic tubing to the back of the micropipette. The solution was injected at a rate of 0.3 - 0.5 µl/min as monitored through the level of the meniscus observed under a stereomicroscope. The micropipette was then left in place for 10 - 15 min to minimize backdiffusion of the solution. The same procedure was then repeated in the contralateral hippocampus (control), where only 1µl of physiological saline were injected at identical stereotactic coordinates. The burr hole was finally filled with bone wax and the scalp sutured using 4-0 prolene. No special handling above regular husbandry was required following successful recovery from anesthesia.

BrDU injections

Male Long-Evans rats (300-350 g) were divided into 2 groups. Group 1 was intraperitonealy pulse injected with 5'-bromo-2'-deoxyuridine (BrDU, Sigma-Aldrich, Oakville, ON; 50 mg/Kg body weight) intra-operatively and 1h and 1.5h following the stereotactic procedure. Group 2 received 3 BrDU pulse injections. The 1st BrDU injection was administered during the stereotactic ouabain infusion, while the 2nd and 3rd BrDU injections were administered following surgery at 2h and 4h, respectively. Rats in group 1 were subsequently intracardially perfused at 2h postoperatively. Rats in group 2 were on the other hand perfused 6 h postoperatively.

Immunofluorescence

Rats in group 1 and group 2 were intracardially perfused at 2h and 6h, respectively. Rats were deeply anesthetised with sodium pentobarbital (Somnotol®, 0.22 ml/100g body weight, i.p.) and were then transcardially perfused with 200 ml of 4% paraformaldehyde in 0.1 M phosphate buffer at pH 7.4, following a brief flushing of the vasculature with 60cc of ice cold saline. The rats were decapitated and the brains were dissected from the skull and immersed in 30% sucrose dissolved in 4% paraformaldehyde and stored at 4^{0}C for 24 hr. Brains were later cryosectioned at 40μm and 10 sections from each brain were collected free floating in 50% formamide / 2x SSC (0.3M NaCl and 0.03M sodium citrate). Sections were then incubated in the latter solution at 65^{0}C for 2 hr, rinsed for 5 min in 2x SSC and incubated once again in 2N hydrochloric acid at 37^{0}C for 30 min. Sections were then rinsed for 10 min in 0.1 M boric acid, pH 8.5, rinsed 3x (5 min each) in 50mM Tris Buffered Saline (TBS), and later incubated in 50mM TBS /

0.2% Triton X-100 / 3% normal donkey serum (TBS-Tds) for 30 min at room temperature. Finally, half the sections were incubated in mouse anti-BrDU monoclonal antibody (Chemicon Inc, Temecula, CA) diluted 1:200 in TBS-Tds and the other half was incubated in a 1:400 dilution for 48 hr at 4^0C. Sections were then rinsed 3x in TBS (10 min each) and once again rinsed for 10 min in TBS-Tds. Sections were then incubated with serial dilutions of anti-mouse secondary antibody. In order to determine the optimal dilution, some sections were incubated in 1:100 dilution, while others were incubated in 1:200 dilution of Alexa-488 anti-mouse IgG (H+L) conjugate (Molecular Probes Inc., Eugene, OR) in TBS-Tds for 2 hr at room temperature and in the dark. Sections were finally mounted on chrome-alum gelatin-coated slides and coverslipped with glycerol/phosphate buffered saline (3:1 v/v) in 2% N-propylgalate. Finally, a number of sections were selected for staining with thionine (0.25%) or hematoxylin/eosin (H/E) in order to assess cell density and/or morphological changes.

Digital image analysis

Thionine and H/E-stained sections were examined with a light microscope, while BrDU was visualized using an Olympus epifluorescence (IX50/IX70) and/or a BioRad MRC (1000/1024) confocal laser scanning microscope. The images of BrDU labeled nuclei were excited by an Ar-Kr laser source (Excitation, 495 nm / Emission, 519 nm) and captured through a tetrarhodamine isothiocyanate (TRITC) filter (Chroma Technology Corporation, Vermont, Brattleboro, U.S.A.) using a Sony CCD colour video camera, connected to a PC with a Windows 95 platform and equipped with a frame grabber and image acquisition software (Northern Eclipse, Empix Imaging Inc., Mississauga, Canada).

In order to compare tissue responses, corresponding regions on both sides were selected for acquisition. Digitally captured images were recalled and the following parameters were quantified. First, The number of BrDU(+) nuclei were manually counted from the SGZ (defined as two cell widths below the GCL) (45) and the GCL (counts from the hilus and mcl are not included). Counts were later confirmed by quantitative digital densitometry and all nuclear counts were corrected using the Abercrombie equation. (47) The number of BrDU(+) nuclear clusters were similarly assessed. BrDU labeled nuclei were considered to have formed a cluster if 3 or more nuclei were overlapping or were less than 1 nuclear diameter (~5μm) apart. To estimate cell migration, we measured the distance between the hilus / granule cell layer transition and the distal edge of the BrDU(+) nuclei. The mean thickness of the granule cell layer in the dorso-ventral axis was also measured from 10 nissl stained sections and was used to estimate the progenitors migration against the thickness of GCL. The orientation of the progenitor cells was determined by measuring the angle between the long axis of the BrDU(+) nuclei and the long axis of the GCL. Finally, all data were averaged and subjected to Student t-test or two-way ANOVA as indicated in the text. The level of statistical significance was set at $P < 0.05$. Results are expressed as mean ± S.E.M.

RESULTS

Upregulation of progenitor cell proliferation by ouabain

Following ouabain infusion, a large number of BrDU(+) cells can be observed in the subgranular zone, granule cell layer and the hilus (Fig. 1). They appeared either in isolation or forming clusters consists of apparently dividing nuclei (Fig. 2). We first examined the total number of BrDU(+) nuclei in the SGZ at 2 h and 6 h following pump inhibition. At 2 h, the SGZ contained comparable number of BrDU(+) cells both in ouabain- and vehicle-treated sides (Table 1). However, at 6 h following pump inhibition, the mean number of BrDU(+) nuclei was more than doubled in the ouabain-treated side whereas BrDU(+) nuclei in the control side exhibited no significant increase (Table 1). This led to an approximately 50% more BrDU(+) cells in the lesioned dentate gyrus (Table 1). Interestingly, at 6 h, but not 2 h, the number of BrDU(+) nuclear clusters also showed a significant increase in the ouabain-treated side (Table 1).

(Table 1 near here)

Ouabain-induced migration and re-orientation of progenitor cells

At 2 h following ouabain infusion the BrDU(+) cells were mainly found in the subgranular zone at the junction between the granule cell layer and the hilus, both in the ouabain as well as the vehicle-treated sides. (Fig.1). A migration index (MI) was then calculated for individual BrDU(+) cell clusters based on the distance between their locations to the edge of the GCL (see Methods). At 2 h, the mean MIs were largely comparable between the ouabain- and vehicle-treated sides (16.8 ± 2.9 μm vs. 18.1 ± 5.0 μm; n = 3; P =

0.68). At 6 h following ouabain infusion, however, progenitor cells in the lesioned side appeared at more distal locations (MI = 51.5 ± 11.1 μm) within the granule cell layer than that found in the vehicle-treated side (MI = 20.4 ± 2.0; $P < 0.0001$) (Fig. 2).

Ouabain infusion also resulted in a change in the orientation of progenitor cells relative to the long axis of the GCL when compared to the vehicle-treated control at 6 h (Fig. 2 and 3). The orientation of the progenitor cells was assessed by measuring the angle between the long axis of the BrDU(+) cluster and the long axis of the GCL (see Methods). The mean angle from the ouabain-treated side was 75.8 ± 6.9° versus 18.7 ± 4.7° from the vehicle-treated control ($P < 0.0001$; Fig. 3), suggesting that progenitor cell migration is directed towards the molecular layer (Fig. 2). At the 2 h time point, where the migration of BrDU(+) cells were undetected, this difference in cell orientation was not observed between ouabain-treated (15.7 ± 7.1°) and vehicle-treated sides (7.7 ± 0.8°; $P = 0.29$).

(Figure 1 near here)

(Figure 2 near here)

Ouabain-induced granule cell injury and death

To determine the temporal relationship between progenitor cell proliferation / migration and dentate neuronal injury, we examined the tissue morphology in nissl and H/E-stained sections. At 2 h following ouabain infusion, no difference was observed in the morphological appearance of granule cells between ouabain- and vehicle-treated sides (Fig. 1). At 6 h following ouabain infusion, however, granule cells in the ouabain-

injected side became markedly shrunken, dark and showed condensed and pyknotic nuclei (Figure 2).

DISCUSSION

In this study we have made two original observations. First, Na^+, K^+- pump inhibition rapidly upregulates progenitor cell proliferation in the adult rat dentate gyrus. Second, many proliferating cells appear to rapidly migrate toward the granule cell layer in a manner that is temporally correlated with neuronal injury and death.

Previous studies have shown that dentate gyrus lesions are associated with enhanced proliferative activity of neural stem cells in the SGZ (6, 10, 31). For example, Scott and co-workers have shown that kindling in rats increase neurogenesis by 75-140% leading to the appearance of numerous newly-born granule neurons (40). In a global ischemia model, Liu et al found a 12-fold increase in cell birth in the dentate subgranular zone, 1-2 weeks after 10 min bilateral common carotid artery occlusion (29). In the present study we utilized ouabain to induce hippocampal damage since Na^+, K^+ - pump inhibition is a common denominator in various neuropathological conditions such as traumatic/ischemic damage as well as various neurodegenerative diseases [see Lees for review, (25)]. Inhibition of the Na^+, K^+, ATPase pump by ouabain induces a sequence of excitotoxic events, which has been widely adopted in simulating the molecular events underlying ischemic and traumatic cell injury (15, 27, 34, 35). In the central nervous system, the cytotoxic reactions induced by ouabain and that induced by trauma or ischemia bear a striking similarity as demonstrated by both early Na^+/Ca^{2+} accumulation, occurrence of spreading depression, necrotic membrane injury (e.g. discharge of intracellular content) and delayed neuronal death (5, 33). At nanomolar concentrations, ouabain is equally or more potent than NMDA in inducing neuron-specific cell death in hippocampus in a seizure-independent manner (26, 28).

Since both NMDA receptor activation and intracellular Ca^{2+} fluctuations have been shown to play an important role in triggering progenitor cell proliferation (2, 36, 48), we speculate that this combination may partially be responsible for the rapid and nearly doubling of BrDU+ cells following ouabain injury. It remains, however to be determined whether this stimulatory effect of ouabain is mediated via a direct action of ouabain on progenitor cells and/or is indirectly caused by molecular signals associated with granule cell injury, possibly as part of a strategy for tissue remodeling and self-repair. The correlated temporal evolution of cell birth and death in the dentate gyrus is compatible with this latter contention.

Most previous studies on injury-induced neurogenesis in the hippocampus have focused on the absolute numbers of proliferating cells in the dentate gyrus, often days or weeks following the insults. The early (within hours) proliferative response as well as the rate of cell migration of SGZ neural progenitor cells has not been specifically addressed. Under physiological conditions, neural stem cells continue to proliferate within a narrow strip at the transition between the granule cell layer and the hilus (14). This strip of neural tissue, known as the subgranular zone, provides a continuous source of newly born cells that migrate toward the distal regions of the granule cell layer, where they differentiate into mature granule neurons. The migration of these progenitor cells from the SGZ to the superficial GCL takes ~ 3 weeks to complete (17). In the present study we showed that pump inhibition greatly facilitates progenitor cell migration. In addition, we have also observed a higher incidence of BrDU labeled clusters from the ouabain infused dentate gyrus at the same point where cell migration became apparent. The appearance of these BrDU(+) cell clusters suggests that these cells are derived from a common progenitor. It is

possible that the progenitor cells continue to proliferate *en route* and thereby are capable of traveling farther distances along the GCL. Consistent with this possibility, migrating progenitors in the rostral migratory stream were found to continue proliferation while undergoing long range migration toward the olfactory bulb (37).

Our data showed that BrDU(+) cells not only undergo rapid migration but also assume a radial orientation relative to the GCL. The cellular basis of this radial orientation of progenitor cells is unknown. Previous studies have demonstrated the persistence of the developmentally transient radial glia in the subgranular zone of adult rat dentate gyrus, (17) where they can be in close contact with the dendritic growth of the newly born BrDU(+) neuroblasts. (42) These radial glia were shown to extend their processes from the SGZ into the GCL in a radial direction. (17). Radial glia play an important role in embryogenesis, during which migrating neuroblasts utilize their radial glial processes as a scaffold that guides them to their final destination (20). The radial orientation of progenitor cells seen in our study, 6h following ouabain infusion, raises the possibility that such progenitor cells are utilizing the radially oriented radial glial processes as a means for their accelerated migration.

ACKNOWLEDGEMENT

This work was supported by the Heart and Stroke Foundation of Canada (HSF) and the Canadian Institutes of Health Research (CIHR). A.O. is a recipient of a Post-Doctoral Fellowship Award from the Canadian Institutes of Health Research (CIHR) under the Canadian Neurotrauma Research Program (CNRP).

REFERENCES

1. Nature Editorial (No Authors Listed). Take comfort in human neurogenesis. 1998. *Nat Med* 4: 1207.

2. Arvidsson, A., Kokaia, Z., and Lindvall, O. 2001. N-methyl-D-aspartate receptor-mediated increase of neurogenesis in adult rat dentate gyrus following stroke. *Eur J Neurosci* 14: 10-18.

3. Barinaga, M. 1992. Challenging the "no new neurons" dogma. *Science* 255: 1646.

4. Barinaga, M. 1998. No-new-neurons dogma loses ground. *Science* 279: 2041-2042.

5. Basarsky, T. A., Duffy, S. N., Andrew, R. D., and MacVicar, B. A. 1998. Imaging spreading depression and associated intracellular calcium waves in brain slices. *J Neurosci* 18: 7189-7199.

6. Bengzon, J., Kokaia, Z., Elmer, E., Nanobashvili, A., Kokaia, M., and Lindvall, O. 1997. Apoptosis and proliferation of dentate gyrus neurons after single and intermittent limbic seizures. *Proc Natl Acad Sci U S A* 94: 10432-10437.

7. Biebl, M., Cooper, C. M., Winkler, J., and Kuhn, H. G. 2000. Analysis of neurogenesis and programmed cell death reveals a self-renewing capacity in the adult rat brain. *Neurosci Lett* 291: 17-20.

8. Cameron, H. A., and Gould, E. 1994. Adult neurogenesis is regulated by adrenal steroids in the dentate gyrus. *Neuroscience* 61: 203-209.

9. Cameron, H. A., and McKay, R. D. 2001. Adult neurogenesis produces a large pool of new granule cells in the dentate gyrus. *J Comp Neurol* 435: 406-417.

10. Dash, P. K., Mach, S. A., and Moore, A. N. 2001. Enhanced neurogenesis in the rodent hippocampus following traumatic brain injury. *J Neurosci Res* 63: 313-319.

11. Doetsch, F., and Scharff, C. 2001. Challenges for brain repair: insights from adult neurogenesis in birds and mammals. *Brain Behav Evol* 58: 306-322.

12. Eriksson, P. S., Perfilieva, E., Bjork-Eriksson, T., Alborn, A. M., Nordborg, C., Peterson, D. A., and Gage, F. H. 1998. Neurogenesis in the adult human hippocampus. *Nat Med* 4: 1313-1317.

13. Gage, F. H. 2000. Mammalian neural stem cells. *Science* 287: 1433-1438.

14. Gage, F. H., Kempermann, G., Palmer, T. D., Peterson, D. A., and Ray, J. 1998. Multipotent progenitor cells in the adult dentate gyrus. *J Neurobiol* 36: 249-266.

15. Garthwaite, J., Garthwaite, G., and Hajos, F. 1986. Amino acid neurotoxicity: relationship to neuronal depolarization in rat cerebellar slices. *Neuroscience* 18: 449-460.

16. Goldman, S. A. 1998. Adult neurogenesis: from canaries to the clinic. *J Neurobiol* 36: 267-286.

17. Gould, E., McEwen, B. S., Tanapat, P., Galea, L. A., and Fuchs, E. 1997. Neurogenesis in the dentate gyrus of the adult tree shrew is regulated by psychosocial stress and NMDA receptor activation. *J Neurosci* 17: 2492-2498.

18. Gould, E., Reeves, A. J., Fallah, M., Tanapat, P., Gross, C. G., and Fuchs, E. 1999. Hippocampal neurogenesis in adult Old World primates. *Proc Natl Acad Sci U S A* 96: 5263-5267.

19. Hastings, N. B., and Gould, E. 1999. Rapid extension of axons into the CA3 region by adult-generated granule cells. *J Comp Neurol* 413: 146-154.

20. Hatten, M. E. 1990. Riding the glial monorail: a common mechanism for glial-guided neuronal migration in different regions of the developing mammalian brain. *Trends Neurosci* 13: 179-184.

21. Kaplan, M. S., and Hinds, J. W. 1977. Neurogenesis in the adult rat: electron microscopic analysis of light radioautographs. *Science* 197: 1092-1094.

22. Kempermann, G., van Praag, H., and Gage, F. H. 2000. Activity-dependent regulation of neuronal plasticity and self repair. *Prog Brain Res* 127: 35-48.

23. Kornack, D. R., and Rakic, P. 1999. Continuation of neurogenesis in the hippocampus of the adult macaque monkey. *Proc Natl Acad Sci U S A* 96: 5768-5773.

24. Kuhn, H. G., Palmer, T. D., and Fuchs, E. 2001. Adult neurogenesis: a compensatory mechanism for neuronal damage. *Eur Arch Psychiatry Clin Neurosci* 251: 152-158.

25. Lees, G. J. 1991. Inhibition of sodium-potassium-ATPase: a potentially ubiquitous mechanism contributing to central nervous system neuropathology. *Brain Res Brain Res Rev* 16: 283-300.

26. Lees, G. J., and Leong, W. 1994. Brain lesions induced by specific and non-specific inhibitors of sodium-potassium ATPase. *Brain Res* 649: 225-233.

27. Lees, G. J., and Leong, W. 1995. The sodium-potassium ATPase inhibitor ouabain is neurotoxic in the rat substantia nigra and striatum. *Neurosci Lett* 188: 113-116.

28. Lees, G. J., and Leong, W. 1996. Interactions between excitotoxins and the Na+/K+-ATPase inhibitor ouabain in causing neuronal lesions in the rat hippocampus. *Brain Res* 714: 145-155.

29. Liu, J., Solway, K., Messing, R. O., and Sharp, F. R. 1998. Increased neurogenesis in the dentate gyrus after transient global ischemia in gerbils. *J Neurosci* 18: 7768-7778.

30. Liu, X., Tilwalli, S., Ye, G., Lio, P. A., Pasternak, J. F., and Trommer, B. L. 2000. Morphologic and electrophysiologic maturation in developing dentate gyrus granule cells. *Brain Res* 856: 202-212.

31. Madsen, T. M., Treschow, A., Bengzon, J., Bolwig, T. G., Lindvall, O., and Tingstrom, A. 2000. Increased neurogenesis in a model of electroconvulsive therapy. *Biol Psychiatry* 47: 1043-1049.

32. Markakis, E. A., and Gage, F. H. 1999. Adult-generated neurons in the dentate gyrus send axonal projections to field CA3 and are surrounded by synaptic vesicles. *J Comp Neurol* 406: 449-460.

33. Obeidat, A. S., and Andrew, R. D. 1998. Spreading depression determines acute cellular damage in the hippocampal slice during oxygen/glucose deprivation. *Eur J Neurosci* 10: 3451-3461.

34. Omar, A. I., Senatorov, V. V., and Hu, B. 2000. Ethidium bromide staining reveals rapid cell dispersion in the rat dentate gyrus following ouabain-induced injury. *Neuroscience* 95: 73-80.

35. Omar, A. I., Senatorov, V. V., and Hu, B. 2001. Sodium-potassium adenosine triphosphatase inhibition enhances membrane accumulation of DiI in rat hippocampus in vivo. *Neuroscience* 102: 353-359.

36. Owens, D. F., and Kriegstein, A. R. 1998. Patterns of intracellular calcium fluctuation in precursor cells of the neocortical ventricular zone. *J Neurosci* 18: 5374-5388.

37. Pencea, V., Bingaman, K. D., Freedman, L. J., and Luskin, M. B. 2001. Neurogenesis in the subventricular zone and rostral migratory stream of the neonatal and adult primate forebrain. *Exp Neurol* 172: 1-16.

38. Peterson, D. A. 2002. Stem cells in brain plasticity and repair. *Curr Opin Pharmacol* 2: 34-42.

39. Reynolds, B. A., and Weiss, S. 1992. Generation of neurons and astrocytes from isolated cells of the adult mammalian central nervous system. *Science* 255: 1707-1710.

40. Scott, B. W., Wang, S., Burnham, W. M., De Boni, U., and Wojtowicz, J. M. 1998. Kindling-induced neurogenesis in the dentate gyrus of the rat. *Neurosci Lett* 248: 73-76.

41. Scott, B. W., Wojtowicz, J. M., and Burnham, W. M. 2000. Neurogenesis in the dentate gyrus of the rat following electroconvulsive shock seizures. *Exp Neurol* 165: 231-236.

42. Seki, T., and Arai, Y. 1999. Temporal and spacial relationships between PSA-NCAM-expressing, newly generated granule cells, and radial glia-like cells in the adult dentate gyrus. *J Comp Neurol* 410: 503-513.

43. Song, H. J., Stevens, C. F., and Gage, F. H. 2002. Neural stem cells from adult hippocampus develop essential properties of functional CNS neurons. *Nat Neurosci* 5: 438-445.

44. van Praag, H., Schinder, A. F., Christie, B. R., Toni, N., Palmer, T. D., and Gage, F. H. 2002. Functional neurogenesis in the adult hippocampus. *Nature* 415: 1030-1034.

45. Yagita, Y., Kitagawa, K., Ohtsuki, T., Takasawa, K., Miyata, T., Okano, H., Hori, M., and Matsumoto, M. 2001. Neurogenesis by progenitor cells in the ischemic adult rat hippocampus. *Stroke* 32: 1890-1896.

46. Abercrombie M. (1946) Estimation of nuclear population from microtome sections. *Anat. Rec.* 94: 239-247.

47. Paxinos G. and Watson C. (1982) *The Rat Brain in Stereotaxic Coordinates*. 3rd edition, Sydney: Academic Press.

48. Sadikot AF, Burhan AM, Belanger MC, Sasseville R. (1998) NMDA receptor antagonists influence early development of GABAergic interneurons in the mammalian striatum. *Brain Res. Dev. Brain Res.* 105: 35-42.

Figure 1. Granule and progenitor cells of the dentate gyrus appear unaffected 2 h following pump inhibition. (A) BrDU immunofluorescence showing progenitor cells mainly located in the subgranular zone at the junction between the granule cell layer and the hilus, 2 h following saline infusion into the dentate gyrus. (B) BrDU immunofluorescence showing progenitor cells located in the subgranular zone, 2 h following ouabain infusion. (C) shows an H/E-stained section of the granule cells, 2 h following saline infusion. Note the normal cell morphology. (D) shows an H/E-stained section of the granule cell layer, 2 h following ouabain infusion. Note that cell morphology remains unaffected. gcl: granule cell layer; mcl: molecular cell layer; h: hilus. Error bars: 100μm

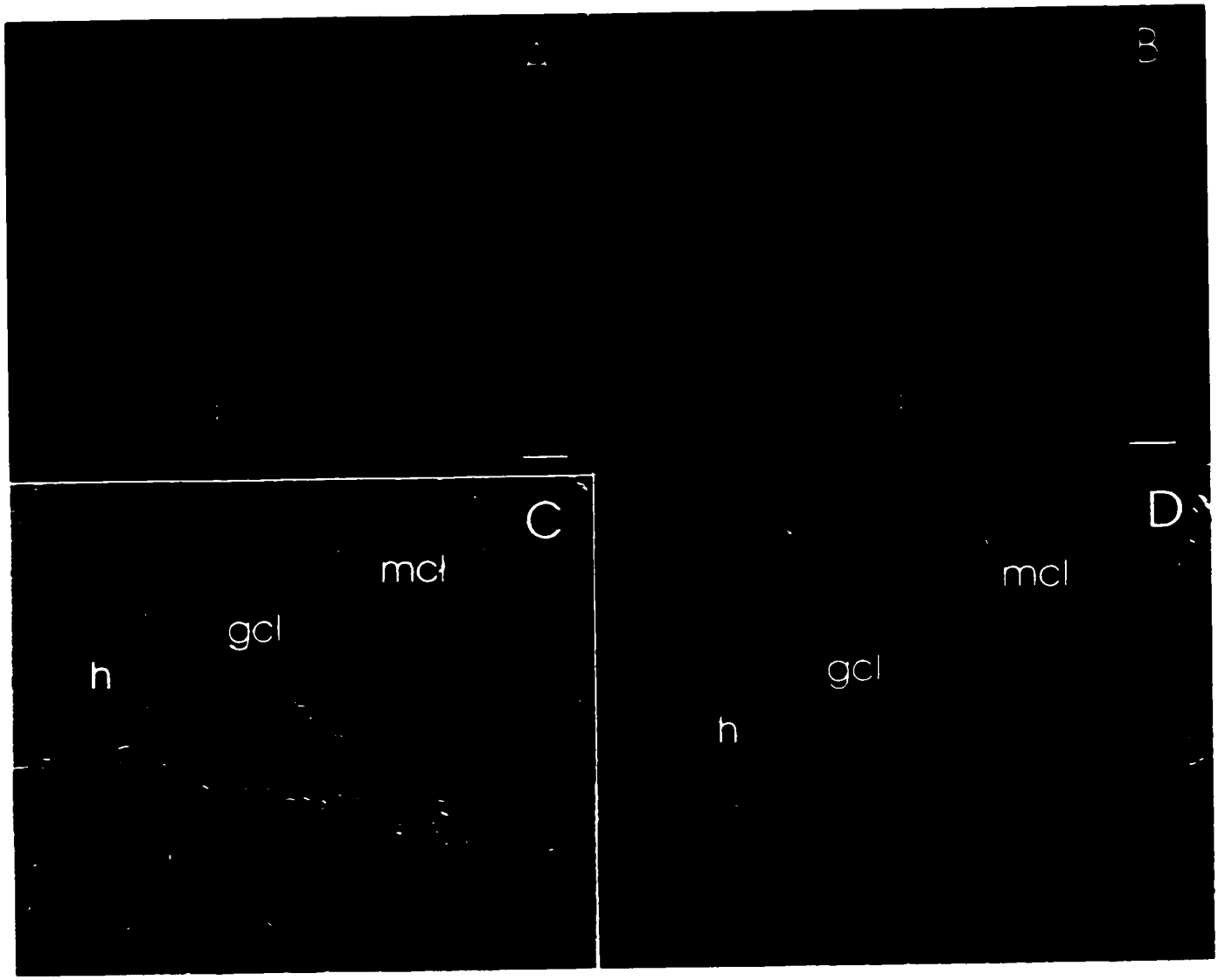
B
C
mcl
gcl
h
D
mcl
gcl
h

Figure 2. Na^+, K^+ pump inhibition simultaneously enhances granule cell injury and progenitor cell migration, 6 h following pump inhibition. (A) saline infused side showing BrDU(+) progenitor cells located at the subgranular zone. (B) ouabain-infused side showing enhancemet of progenitor cell migration into the the dentate granule cell layer. Arrowheads point to progenitor cells found at progressively superficial areas of the granule cell layer. (C) and (D) are higher magnifications of boxes in (A) and (b), respectively showing BrDU(+) progenitor cells. Note the formation of clusters in (D) and the altered orientation relative to the long axis of the gcl. The clustering of nuclei suggest that this grouping was a result of repeated cell divisions of a common progenitor cell. (E) shows a nissl-stained section of the dentate gyrus, 6 h following saline infusion. Note the healthy morphological appearance of granule cells. (F) shows a nissl-stained section of the dentate gyrus, 6 h following ouabain infusion. Note the tissue damage and the morphological appearance denotic granule cell injury. Arrows point to the micropipette track. gcl: granule cell layer; mcl: molecular cell layer; h: hilus. Error bars in (A) and (B): 100μm; (C) and (D):10μm; (E) and (F):50μm.

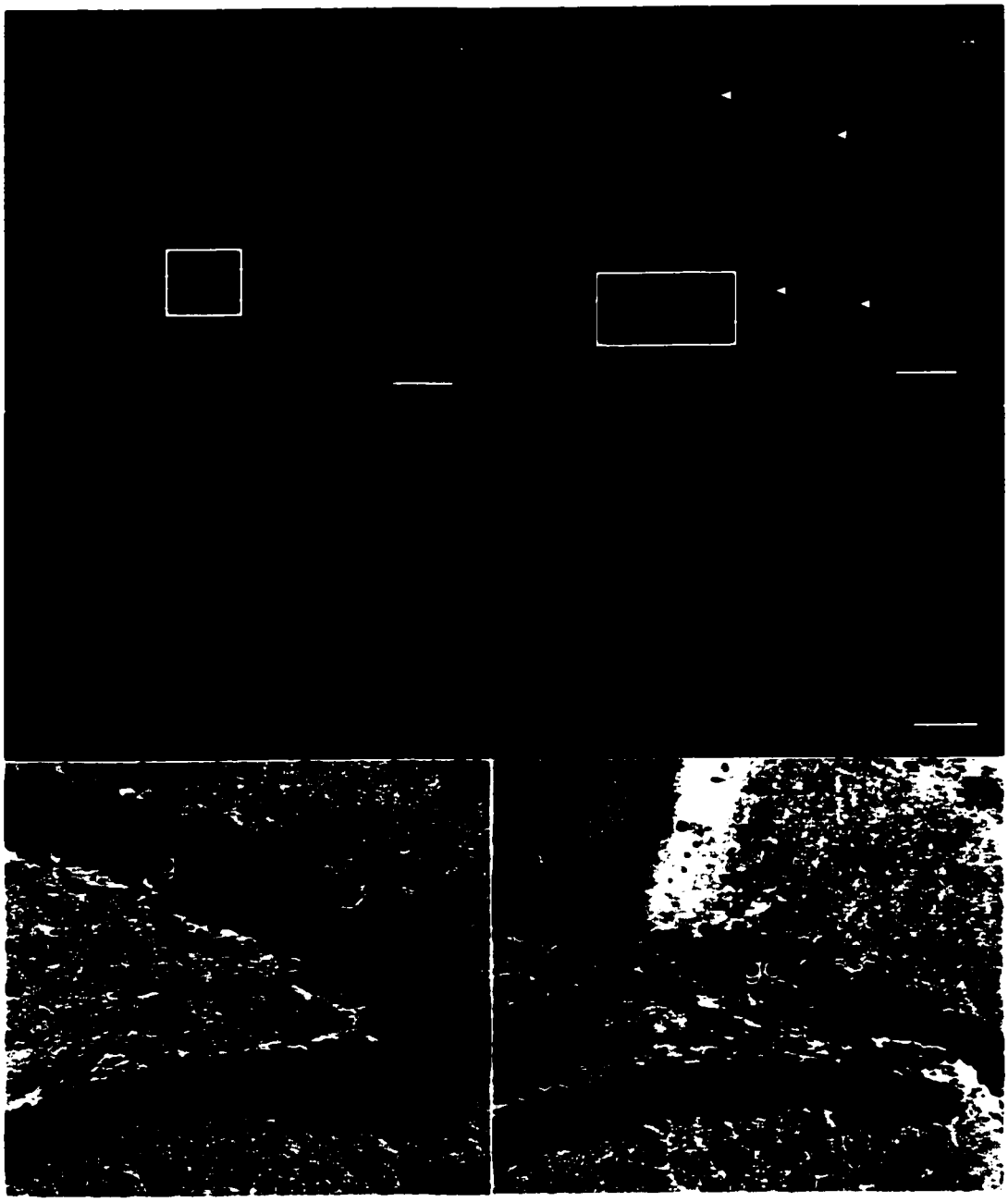

Table 1

	Total BrDU(+) cells			Clustered BrDU(+) cells		
	control	**ouabain**	***P***	**control**	**ouabain**	***P***
2h	9.3±2.7	7.9±1.2	=0.49	0.8±0.3	1.7±1.2	=0.57
6h	9.9±1.4	15±1.9	<0.05	0.6±0.4	2.7±0.7	<0.05

Chapter 6. General Discussion

The present thesis study examined the cellular and subcellular events that are associated with tissue injury and remodeling following inhibition of the Na^+, K^+- pump in rat dentate gyrus *in vivo*. Using stereotactic microinfusion of the Na^+, K^+- pump blocker together with a number of fluorescent probes that are exquisitely sensitive and specific in binding subcellular structures (Giuliano et al., 1998; Giuliano et al., 1995), we were able to characterize a series of injury-related events and their temporal profiles.

6.1 Methodological considerations

As outlined in the Introduction, Na^+,K^+-pump inhibition provides a valid and useful experimental model for delineating key and common cellular events underlying ischemic and traumatic tissue injury and repair, although the model itself hardly replicates the entire repertoire of ischemic pathophysiological reactions. We found ouabain-induced tissue injury to be highly reproducible in comparison with other insults such as MCA occlusion. The latter method often gives rise to variable results due in part to the variabilities in the collateral circulation (Small et al., 2000). In this regard, the dentate gyrus provides a highly useful model system because of its high sensitivity to pump inhibition and the preservation of neurogenesis capacity.

Up to this date, our studies are primarily conducted in an *in vivo* setting where the natural progression of cell death and tissue remodeling processes are largely preserved. It remains to be shown at this time that similar tissue reactive changes can also be faithfully reproduced in *in vitro* brain slices, a preparation that would greatly facilitate mechanistic studies with greater control of cellular milieu.

6.2 Principal findings of the present studies

6.2.1 Pump inhibition results in a transient surge of membrane accumulation of lipophilic dye

Changes in neuronal membrane structure and function play a key role in the pathophysiology of traumatic/ischemic cell injury and death. Despite its importance, directly examining lipid-related structural changes in plasma membranes remained a daunting task in *in vivo* animal models of neuronal injury.

Membrane phospholipids are essential constituents of neuronal membranes. They are also pivotal in receptor-mediated signal transduction cascades. For example, group I metabotropic glutamate receptor signaling is coupled to phospholipase C (PLC) activation (Conn et al., 1997). PLC mediates breakdown of the membrane phosphatidylinositol 4,5-bisphosphate (PIP2) into diacylglycerol (DAG) and inositol-1,4,5-triphosphate (IP3). DAG results in activation of protein kinase C (PKC) while IP3 results in Ca^{2+} release from the endoplasmic reticulum (Bockaert et al., 1993; Sladeczek et al., 1985). Under ischemic conditions and following administration of excitotoxins, glutamate receptor overstimulation results in widespread PLC activation, which in turn results in membrane phospholipid breakdown. In addition, PLC can be indirectly activated through NMDA receptor-mediated rise in $[Ca^{2+}]_i$. The resultant membrane phospholipid breakdown alters membrane characteristics and results in membrane permeability changes (Farooqui et al., 2001; Lu et al., 2001).

Because of its structural similarity to phospholipid molecules, 1,1'-dioctadecyl-3,3,3',3'-tetramethylindocarbocyanine perchlorate (DiI) has been widely used to probe membrane structure and dynamics. DiI molecules are amphiphilic, meaning they possess

both hydrophobic and hydrophilic regions within their structure. The hydrophilic portion consists of a fluorophore that localizes the probe to the membrane surface while the hydrophobic portion consists of aliphatic tails that serve to anchor the molecule into the plasma membranes (Axelrod, 1979).

Our goal was to probe neuronal plasma membrane dynamics *in vivo* during the first 12 hours following pump inhibition. We made two original observations. First, we showed that following a 4-hour delay, DiI fluorescence yield was markedly higher from pump-inhibited neurons compared to the vehicle-treated control. The DiI fluorescence yield thereafter increased in a time-dependent manner followed by a drop in fluorescence yield, 72 hours following pump inhibition. Secondly, we demonstrated that the initial rise in DiI fluorescence yield was spatio-temporally coincident with morphological features that characterize acute neuronal injury. These features included neuronal cell shrinkage and the appearance of hyperchromatic nuclei as detected through nissl staining. As cell loss became evident, 72 hours following pump inhibition, we observed a corresponding drop in DiI fluorescence.

To determine whether DiI accumulation was due to increased membrane porosity, we utilized two membrane-impermeable DNA intercalating dyes of different molecular weights, namely ethidium bromide (EB) and ethidium homodimer-1 (EthD-1). Both EB (MW: 394.31) and EthD-1 (MW: 856.77) undergo large fluorescence enhancement upon binding to DNA (Brawn et al., 1975). Our results showed that pump inhibition led to a time-dependent increase in ethidium bromide fluorescence that began as early as 1 hour following pump inhibition. On the other hand, there was no labeling when EthD-1 was used, up to 6 hours following pump inhibition. These results indicate that pump inhibition

resulted in an increase in membrane porosity as early as the 1-hour time point. This membrane porosity was sufficient to admit the low molecular weight EB but was not large enough to admit EthD-1. On the other hand, DiI fluorescence enhancement following pump inhibition occurred after a 4 hour delay. At the 1, 2 and 3-hour time points following pump inhibition, DiI fluorescence yield was comparable to the vehicle-treated control. This suggests that the DiI fluorescence enhancement is not due to an increase in membrane porosity but rather due to a specific DiI molecule / lipid bilayer interaction. The mild increase in membrane porosity detected at the earlier time points may be a separate phenomenon, possibly due to the formation of membrane pores.

A number of observations suggest the possible mechanism(s) underlying enhanced DiI accumulation following pump inhibition. For example, the exact molecular orientation of the DiI molecules with lipid bilayers was previously determined using fluorescence polarization microscopy (Axelrod, 1979). The long axis of the fluorophore component was shown to orient parallel to the surface of the plasma membrane while the two alkyl side chains were shown to insert with a perpendicular orientation relative to the membrane surface and between the phospholipid molecules. It is therefore conceivable that the enhanced DiI accumulation in pump-inhibited cells is a result of loosening of the normally tight membrane phospholipid packing resulting in higher number of DiI insertion per membrane unit area. In fact, a recent study employing a lipid-specific spin probe coupled with electron paramagnetic resonance imaging, demonstrated a decrease in lipid order and loosening of the tight packing of the phospholipid acyl chains within the interior of gerbil synaptosomal membrane, 3-12 hours following transient carotid artery occlusion (Hall et al., 1995).

The results of our study suggest that early membrane porosity and structural changes may contribute to ouabain-induced cell death. This raises the interesting possibility of membrane repair as a therapeutic strategy that may prevent or attenuate cell death. Indeed, in white matter injury, molecular repair of damaged membranes through administration of hydrophilic polymers such as polyethylene glycol has been recently shown to restore normal nerve conduction. Polyethylene glycol was shown to seal damaged nerve fibers through insertion of the polymers into the hydrophobic core of nerve membranes (Borgens et al., 2000). It would be interesting to test the ability of such polymers in sealing membrane damage in the gray matter and possibly preventing cell injury and death. Cytidine-5'-diphosphocholine (citicoline or CDP-choline), an intermediate in the biosynthesis of phosphatidylcholine (PtdCho), has been proven effective in ameliorating damage in a number of CNS injury models. Citicoline's neuroprotective action is thought to be mediated through its ability to enhance reconstruction (synthesis) of PtdCho and sphingomyelin as well as inhibition of membrane destructive processes such as activation of phospholipases (Adibhatla et al., 2001; Aronowski et al., 1996; Rao et al., 1999; Rao et al., 2000).

On the other hand, DiI fluorescence enhancement coincided spatio-temporally with morphological features that characterize neuronal injury namely, neuronal cell shrinkage and the appearance of hyperchromatic nuclei. These morphological features were previously seen early in the time course following middle cerebral artery occlusion in rats (Garcia et al., 1993; Li et al., 2002; Miyasaka et al., 2000; Petito et al., 1984). In addition, previous studies showed that ouabain exposure induced significant cell shrinkage of helix aspersa as well as cultured cortical neurons (Alvarez-Leefmans et al.,

1992; Xiao et al., 2002). The early onset of membrane porosity observed in our study may be linked to cell shrinkage, since membrane porosity can result in leakage of intracellular osmotically active solutes, which may in turn contribute to cell shrinkage. It is unknown at this point whether DiI fluorescence enhancement and neuronal shrinkage are mechanistically linked or whether they develop simultaneously through different pathways. We and others however, have shown that Na^+, K^+- pump inhibition can trigger cell death with both necrotic as well as apoptotic components (see chapter 3 and (Xiao et al., 2002)). It is therefore conceivable that membrane damage occurs as part of the necrotic component of cell death while cell shrinkage occurs as a result of the simultaneous induction of apoptosis.

6.2.2. Na^+, K^+- pump inhibition triggers "hybrid" cell death in dentate granule cells

In this phase of our thesis project we showed that Na^+, K^+- pump inhibition *in vivo*, can trigger a mode of cell death in dentate granule cells that has both a necrotic and an apoptotic component. This "hybrid" cell death had been previously detected in the brain following cerebral ischemic insults. However, its underlying mechanisms are yet to be identified (MacManus et al., 2000).

Cell death has traditionally been classified into two broad categories, apoptosis and necrosis. Apoptosis or "programmed cell death" is controlled by a genetically encoded self-destructive program that involves activation of a variety of pathways leading to caspase and endonuclease activation. Morphologically, apoptosis is characterized by cell shrinkage, intact plasma membranes, nuclear condensation and DNA internucleosomal cleavage. In contrast, necrosis is characterized by cell swelling,

membrane disintegration and irregular DNA cleavage ultimately leading to cell rupture (Martin, 2001; Wyllie, 1980). The mode of cell death following an ischemic insult to the brain has recently been the subject of intense debate. The most widely accepted theory is that of excitotoxic cell death following traumatic / ischemic insults. Excitotoxic cell death is mediated through excessive glutamate release resulting in glutamatergic receptor over-activation. This in turn triggers pathological Na^+ and Ca^{2+} accumulation leading to necrotic cell death (Choi, 1992; Choi, 1994; Choi et al., 1988). Recently however, several studies have argued for the occurrence of apoptosis following traumatic / ischemic injury, (Charriaut-Marlangue et al., 1996; Davis et al., 1997; Li et al., 1997; Yue et al., 1997) but the "classic" morphological features of apoptosis were often lacking (Colbourne et al., 1999; Sheldon et al., 2001). MacManus and coworkers suggest that ischemic cell death does not fit the classical definitions of necrosis or apoptosis, but rather falls along a "continuum", sharing features common to both forms of cell death (MacManus et al., 2000).

The diametrically opposing differences in cell volume changes associated with necrosis and apoptosis indicate that they each possess distinct ionic mechanisms. The pathological influx of Ca^{2+} and Na^+ and their intracellular accumulation results in cell swelling and necrotic cell death (Choi, 1988). On the other hand, K^+ efflux plays a key role in cell shrinkage and apoptotic cell death (Trimarchi et al., 2002; Xiao et al., 2002; Yu et al., 1999). As previously discussed, inhibition of the Na^+, K^+- pump results in collapse of the Na^+ gradient leading to Na^+ influx, Ca^{2+} influx through VSCCs and reverse operation of the Na^+/Ca^{2+} exchanger as well as K^+ efflux along its concentration gradient. We therefore hypothesized that Na^+ and Ca^{2+} influx can trigger necrotic cell

death, while K^+ efflux may trigger apoptosis in the setting of Na^+, K^+- pump inhibition. To assess the possible co-development of necrosis and apoptosis following pump inhibition we utilized several parameters indicative of either forms of cell death. For example, to examine necrosis with its associated loss of membrane integrity, we utilized two membrane impermeable DNA intercalating dyes, ethidium bromide (EB) and propidium iodide (PI). These dyes are normally excluded from intact plasma membranes but gain access to DNA upon membrane compromise (Brawn et al., 1975). Following DNA binding, they undergo several fold fluorescence enhancement and are therefore detectable using conventional fluorescence microscopy. Our results indicate that membrane compromise occurs as early as 1-hour following pump inhibition as detected by both EB and PI accumulation in dentate granule cells. Thereafter, there was a time-dependent increase in both EB and PI fluorescence (see Chapter 3, Figure 1 and 4a).

Since apoptosis is associated with nuclear condensation, we utilized a probe (Hoechst 33342) that preferentially binds to apoptotic cells undergoing DNA condensation. Our results indicate that DNA condensation begins at 4 hours following pump inhibition.

To detect volume changes associated with necrosis or apoptosis, we utilized nissl and hematoxylin and eosin (H/E) staining. At 2 hours following pump inhibition, we did not detect swelling or shrinkage but rather, cells looked morphologically "normal". At that same time point, dentate granule cells however were exhibiting EB and PI accumulation, indicating that membrane compromise was not associated with cell swelling. At 4 hours following pump inhibition, granule cells exhibited further EB and PI accumulation, DNA condensation as well as marked cell shrinkage suggesting that the

cell death detected in our preparation had both a necrotic as well as an apoptotic component. This suggests that failure of the Na^+, K^+ -pump may play a role in the development of the mixed cell death seen in cerebral ischemia.

Cell shrinkage has been detected before in cultured neurons following pump inhibition (Xiao et al., 2002) and in rats following common carotid artery occlusion (Garcia et al., 1993; Miyasaka et al., 2000; Petito et al., 1984). On the other hand, edema is a commonly associated finding following ischemic and hemorrhagic stroke in humans. The edema has commonly been attributed to leakage of the blood brain barrier leading to "vasogenic edema" or otherwise due to failure of the Na^+, K^+- pump leading to "cytotoxic edema" (Barzo et al., 1996; Barzo et al., 1997). Our findings of cell shrinkage rather than swelling following pump inhibition, therefore merits further discussion. First, cell swelling following stroke is largely detected in astrocytes and neuronal dendritic processes (Castejon et al., 2002; Di et al., 2000; Kimelberg, 1992; Maxwell et al., 1994). It may be that neuronal cell bodies have well-developed regulatory volume decrease (RVD) mechanisms compared to astrocytes or neuronal dendritic processes. The lack of initial cell swelling in the first 4 hours seen in our study may be due to activation of RVD as a result of Na^+ and water influx. Necrotic cell swelling or necrotic volume increase (NVI) is usually mediated by influx of Na^+ and Cl^- ions resulting in cell swelling (see Introduction). Cell swelling is known to trigger a volume regulatory mechanism known as regulatory volume decrease (RVD), mediated through KCl efflux as a result of activation of K^+ and Cl^- channels as well as the electroneutral operation of cotransporters such as the K^+-Cl^- symporter and the K^+-H^+ and Cl^--HCO_3^- antiporters. During a swelling emergency, cells rapidly extrude K^+ through the operation of the available K^+ channels. In

order to maintain electroneutrality, the simultaneous efflux of anions accompanies K^+ efflux. Anion efflux is achieved through the activation of a variety of swelling-activated anion channels, the most ubiquitous and specific of which is the volume-sensitive outwardly rectifying (VSOR) anion channel (Bond et al., 1998; Hazama et al., 2000). The VSOR anion channel has been shown to be largely dependent on the non-hydrolytic binding of ATP (Patel et al., 1998).

On the other hand, apoptotic cell shrinkage or apoptotic volume decrease (AVD) is commonly mediated through K^+ efflux, which has been shown to occur following Na^+, K^+- pump inhibition (Trimarchi et al., 2002; Xiao et al., 2001). In fact, intracellular K^+ ion concentration was shown to play a key role in the activation of death enzymes. It was shown that K^+ at normal intracellular levels exerts a "tonic suppressive force" on two key apoptotic enzymes, caspase-3-like protease and the internucleosomal DNA cleavage nuclease. Efflux of K^+ with the consequent decrease in intracellular K^+ concentration was shown to disinhibit these two key pro-apoptotic enzymes leading to apoptotic cell death (Hughes et al., 1997). It therefore appears that K^+ not only plays a key role in cell shrinkage, but is also directly involved in the induction of apoptosis. It should be noted that contraction of the cytosolic compartment as a result of water efflux and cell shrinkage leads to an increase in ionic concentration and potassium ions are no exception. However, since pump inhibition has been associated with apoptosis due to K^+ efflux *in vitro* (Xiao et al., 2002), it appears that the degree of K^+ efflux more than compensates for the intracellular volume contraction leading to a net decrease in $[K^+]_i$. In addition, a recent study demonstrated that cell shrinkage due to disordered volume regulation is an early prerequisite to apoptosis. Blocking K^+ channels was shown to prevent both cell

shrinkage as well as apoptotic cell death probably due to K^+ retention (Maeno et al., 2000).

It must be noted however that pharmacological inhibition of the Na^+, K^+- pump may not necessarily replicate the swelling seen after stroke. Ouabain-induced pump inhibition is not associated with a drop in ATP levels as can be expected following cerebral ischemia. In fact, inhibition of the Na^+, K^+- pump by ouabain may be associated with an increase in ATP levels as a result of sparing of the ATP otherwise required for the operation of the Na^+, K^+- pump (Robinson, 1982). Since VSOR anion channel was largely dependent on non-hydrolytic binding of ATP, it is therefore conceivable that the low ATP levels associated with stroke will result in failure of the VSOR channel and consequently failure of the regulatory volume decrease, which would in turn favor the development of cell swelling. Furthermore, the intracellular ATP concentration has been shown to act as a switch for the cell's decision to undergo necrotic or apoptotic cell death following exposure to pro-apoptotic signals. Human T cells were shown to change from apoptosis to necrosis, when cells were pre-emptied of ATP following exposure to common apoptotic triggers, namely staurosporin and CD95 stimulation (Leist et al., 1997).

In summary, we propose that inhibition of the Na^+, K^+ -ATPase with its resultant Na^+ and Ca^{2+} accumulation may trigger necrotic cell death. Efflux of K^+ on the other hand, may trigger cell shrinkage and the resultant low $[K^+]_i$ may in turn lead to disinhibition of pro-apoptotic enzymes. The converging effect is a cell morphology with mixed necrotic and apoptotic features.

6.2.3 Ethidium bromide staining reveals dispersion of a radial glia-like cell population following ouabain-induced injury

In this phase of our study, we describe the appearance of a cell subpopulation within the dentate gyrus with a radial glia-like cell morphology, which we termed intensely labelled cells (ILCs). These cells were selectively labeled by ethidium bromide and appeared as early as 1 hour following ouabain infusion. The ILCs were initially clustered both within the dentate granule cell layer as well as the adjacent hilar and molecular cell layer regions. These cells thereafter were found to undergo cell dispersion in a time-dependent manner. The appearance and cell dispersion of these ILCs were never described before.

Although the precise identity of the ILCs remains to be determined, several lines of argument suggest that ILCs represent radial glial cells. First, ILCs are bipolar cells with a characteristic spindle or oval cell body, a morphology that closely resembles radial glial cells. Second, the ILCs were shown to arrange themselves in a radial fashion throughout the dentate gyrus, a pattern strikingly similar to the arrangement of radial glial cells in the developing dentate gyrus (Rickmann et al., 1987).

It should be noted however that ILCs were selectively labeled by ethidium bromide, a normally membrane impermeable dye. This raises the possibility that such labeling is a result of membrane compromise. To test whether this pattern of labeling is a result of loss of membrane integrity, we used another membrane impermeable dye, propidium iodide, with comparable characteristics and molecular weight to ethidium bromide. Propidium iodide completely failed to label any cells with similar ILC characteristics, indicating that ILCs were not labeled by ethidium bromide simply due to

their membrane compromise. In addition, ILCs appeared morphologically healthy until they were no longer detectable past the 12-hour time point following ouabain infusion.

Following the publication of our manuscript in Chapter 4, we performed a series of experiments in order to further characterize the intensely labeled cells. First, we coinfused ouabain with DiI and ethidium bromide in order to delineate the extent of ILC processes. DiI is widely adopted as a lipophilic neuroanatomical tracer and is adopted in the selective labeling of neural fibers. We discovered that the ILC processes extended as an elaborate network of fibers that spanned across the dentate molecular cell layer. The vehicle-treated side however, was completely devoid of such a fiber network, indicating that the DiI-labeled processes were generated *de novo* following ouabain infusion. Furthermore, the DiI-labeled processes seen extending from the intensely labeled cell body disappeared completely when ILCs were no longer detectable, 12 hours following ouabain infusion. This pattern is highly reminiscent of the radial glial network seen during corticogenesis (Rickmann et al., 1987). The radial glia-like morphology of ILCs with its associated radially oriented processes suggests that the pattern seen in our study represents re-expression of the radial glial network. In fact, a recent study showed that mature stellate astrocytes were capable of "dedifferentiating" into the developmentally transient radial glia following transplantation of embryonic neurons into areas undergoing targeted neuronal apoptosis in the adult mouse neocortex (Leavitt et al., 1999). This transient rejuvenation of the radial glial network provided a scaffold for directing migration of the transplanted embryonic neurons indicating that, in areas of neuronal damage, the adult cortex is capable of reverting to an embryonic microenvironment that may facilitate network remodeling. This notion gains further support from studies

showing re-expression of nestin, a developmentally transient intermediate filament protein, in reactive astrocytes following transient middle cerebral artery occlusion in rats (Duggal et al., 1997; Li et al., 1999). Since nestin is expressed in radial glial cells and in CNS stem cells, the above mentioned studies raise the interesting possibility that re-expression of nestin may represent "dedifferentiation" of astrocytes into their radial glial precursor which may in turn serve a role in cell replacement and tissue remodeling. Since radial glia were shown to be the stem cells in the central nervous system, it may be that re-expression of the radial glial network serves the dual role of generating new neurons as well as guiding their migration. This raises the interesting notion of whether the brain possesses an endogenous repair program that is invoked following tissue damage.

6.2.4 Na^+, K^+- pump inhibition enhances proliferation and migration of neural progenitor cells

The principal findings of this part of our study were that Na^+, K^+- pump inhibition can simultaneously induce cell death as well as enhance progenitor cell proliferation and migration in the dentate GCL. To our knowledge, progenitor cell responses to pump inhibition have never been studied before.

6.2.4.1 Significance and possible mechanisms of progenitor cell proliferation and migration following pump inhibition

Ischemic and traumatic injuries have both been shown to upregulate progenitor cell proliferation, but the molecular mechanisms involved in such a response remains elusive (Bengzon et al., 1997; Dash et al., 2001; Madsen et al., 2000; Scott et al., 2000).

Since traumatic and ischemic injury is accompanied by a rapid decline in the energy-dependent sodium-potassium pump, our results indicate that pump inhibition and/or the molecular cascade of events that occur downstream to pump blockade may play a role in stimulating progenitor cell proliferation. Indeed, previous studies have shown that the increased proliferative activity of dentate neural progenitors was mediated through glutamatergic mechanisms acting on N-methyl-D-aspartate (NMDA) receptors. The elevated neurogenesis was completely abolished when the NMDA receptor blocker, dizocilpine (MK-801) was systemically or intrahippocampally administered (Arvidsson et al., 2001). Fluctuations of $[Ca^{2+}]_i$ were also implicated in the regulation of neurogenesis among the subventricular zone precursors (Owens et al., 1998). Furthermore, NMDA receptor activation through removal of magnesium or the addition of glycine was shown to enhance Ca^{2+}-dependent granule cell migration in the developing mouse cerebellum (Komuro et al., 1993). In addition, a recent study showed that progenitor cell migration was enhanced by the application of glutamate and NMDA in embryonic cortical slices. Progenitor cell migration was blocked by the addition of NMDA antagonists, MK801 or APV (Behar et al., 1999). Glutamate release via reverse Na^+-dependent transport (Li et al., 2001), NMDA receptor activation and increases in $[Ca^{2+}]_i$ (Choi, 1988) all occur downstream to membrane depolarization induced by pump inhibition.

6.2.4.2 Cell death and birth following various insults to the dentate gyrus

Extensive research has been conducted on dentate neural stem cell responses to ischemic, epileptic and excitotoxic insults. These studies however focused on the

absolute numbers of proliferating cells in the dentate gyrus, days or weeks following such insults. The early (within hours) proliferative response as well as the rate of cell migration of SGZ neural progenitor cells under pathological conditions however, has not been studied. Under physiological conditions, neural stem cells continue to proliferate within a narrow strip at the transition between the granule cell layer and the hilus. This strip of neural tissue known as the subgranular zone provides a continuous source of newly born cells that migrate towards the distal region of the granule cell layer, where they differentiate into mature granule neurons (Gage et al., 1998; Gould et al., 1997). The migration of these progenitor cells from the SGZ to the superficial GCL takes ~ 3 weeks to complete (Gould et al., 1997). Our data indicate that within 6h following pump inhibition, neural progenitor cells have been found at locations ranging from 19 μm to 66 μm and with a mean of 74% of the distance between the SGZ and the distal edge of the GCL.

On the other hand, previous studies have shown that various insults to the dentate gyrus are capable of increasing the proliferative activity of the neural stem cells in the SGZ. For example, Wojtowicz and co-workers have shown that kindling in rats enhanced neurogenesis by 75-140% leading to the appearance of numerous newly born granule neurons (Scott et al., 1998). In a global ischemia model, Liu et al found a 12-fold increase in cell birth in the dentate subgranular zone, 1-2 weeks after 10 min bilateral common carotid artery occlusion (Liu et al., 1998). In addition, traumatic brain injury and electroconvulsive shock seizures have been shown to enhance neurogenesis (Dash et al., 2001; Liu et al., 1998; Madsen et al., 2000). Interestingly, all of these insults are known to result in cell death, suggesting that dying cells may play a role in the enhanced

proliferative activity of neural stem cells, possibly as part of a self-repair strategy. Our data indicates that Na^+, K^+ -ATPase pump inhibition can simultaneously induce granule cell death as well enhance SGZ progenitor cell proliferation. The temporal evolution of cell birth and death in the dentate gyrus is compatible with the contention that cell death may directly or indirectly induce a compensatory increase in cell birth activity.

6.2.4.3 Possible role of radial glia in progenitor cell migration in the dentate gyrus

In this study, we showed that BrDU(+) cells are seen in clusters and assume a radial orientation relative to the GCL. The significance of this radial orientation of progenitor cells following ouabain-induced injury is not clear. On the other hand, previous studies have demonstrated the persistence of the developmentally transient radial glia in the subgranular zone of adult rat dentate gyrus (Gould et al., 1997). These radial glia play an important role during embryogenesis, where migrating neuroblasts utilize their radial glial processes as a scaffold that guides them to their final destinations. In the adult dentate gyrus, radial glia have been shown to extend their projections from the SGZ into the GCL in a radial direction. Given the role of radial glia during development as well as their strategic positioning in an area where continuous proliferation and migration of neural progenitors takes place, it is conceivable that they may play a similar role during adulthood. Indeed, a recent study using immunoelectron microscopy has demonstrated that vimentin(+) processes of the radial glia-like cells are in close contact with the dendritic growth of the newly born BrDU(+) neuroblasts in the adult dentate gyrus (Seki et al., 1999). The radial orientation of progenitor cells seen in our study 6h following ouabain infusion, raises the possibility that such progenitor cells

are utilizing the radially oriented radial glial processes as a means for their accelerated migration.

Additionally, we have observed a higher incidence of BrDU labeled clusters from the ouabain infused dentate gyrus than from the vehicle treated control. The appearance of these BrDU(+) cell clusters suggests that these cells are derived from a common progenitor. It may be possible that the progenitor cells continue to proliferate *en route* and thereby are capable of traveling farther distances along the GCL. This may be merely due to the plane of separation of daughter cell bodies occurring parallel to the long axis of the GCL during the process of cytokinesis. In fact, a previous study has shown that migrating progenitors in the rostral migratory stream continue to proliferate while undergoing long-range migration towards the olfactory bulb (Pencea et al., 2001).

In conclusion, we show that pump inhibition upregulates proliferative activity of SGZ progenitors and enhances their rate of migration into the granule cell layer. These changes appear at a time when cell death is apparent at 6h, but fail to appear before cell death is morphologically evident at 2h following pump inhibition.

6.3 Further work suggested by the present results

Our current thesis work raises several important questions that need to be addressed in future studies. 1) What is the mechanism of DiI accumulation in plasma membranes following Na^+, K^+ pump inhibition? This issue may be addressed through blocking of membrane destructive pathways and testing their ability to affect DiI accumulation. For example, the ability of phospholipase inhibitors to affect DiI uptake may be tested. 2) What is the identity of the ILCs seen in our studies? Despite repetitive

attempts, several technical factors have prevented us from obtaining double labeling of ILCs with immunohistochemical markers in fixed sections. For example, many ILCs seemed to be "washed" away during the procedures. To alleviate this problem, laser microdissection may be utilized to isolate ILCs from tissue slices, which would subsequently allow their molecular characterization. Alternatively, performing electrophysiological recordings and loading of ILCs with dyes such as lucifer yellow would help in identifying ILCs as neurons or glia. 3) What is the ultimate fate of neural progenitor cells that undergo proliferation and migration following pump inhibition? We may expand the time window of survival in order to allow for differentiation of such precursor cells and subsequently use immunophenotyping techniques (neuron-specific and glia-specific markers) to determine the ratio of newly born neurons to glial cells. Furthermore, the use of neurotrophic factors to enhance stem cell proliferation or to specifically enhance neuronal or glial differentiation may be attempted. These experiments may prove useful for developing cell replacement strategies following neural tissue damage.

6.4 Conclusions

In summary, we show that pump inhibition results in a rapid and drastic change in tissue structural properties represented by cell injury and death, together with the simultaneous enhancement of cell birth activity. We show that pump inhibition results in an increase in membrane porosity that occurs as early as the 1-hour time point. Furthermore, we report that pump inhibition triggers a form of cell death with "mixed" apoptotic and necrotic features. The K^+ channel blocker, charybdotoxin was capable of

significantly attenuating the neuronal damage associated with inhibition of the Na^+, K^+ pump, indicating that loss of intracellular K^+ plays an important role in cell death associated with pump inhibition. We also describe a novel tissue response whereby pump inhibition triggers the appearance of a radial glia-like cell population that undergoes time-dependent cell dispersion and rearrangement. Finally we found that pump inhibition can simultaneously trigger cell death as well as upregulate progenitor cell proliferation. Migration of such newly born progenitor cells was also enhanced towards areas of cell injury and tissue damage. We suggest that such a host of tissue responses may represent an early endogenous attempt at restoring tissue structural integrity through the enhancement of proliferation and migration of neural precursor cells as well as re-expression of the radial glial scaffold necessary for progenitor cell migration.

REFERENCES FOR GENERAL INTRODUCTION AND DISCUSSION

Ackermann, U., Geering, K. 1990. Mutual dependence of Na,K-ATPase alpha- and beta-subunits for correct posttranslational processing and intracellular transport. FEBS Lett 269, 105-8.

Adibhatla, R.M., Hatcher, J.F., Dempsey, R.J. 2001. Effects of citicoline on phospholipid and glutathione levels in transient cerebral ischemia. Stroke 32, 2376-81.

Alonso, G. 1999. Neuronal progenitor-like cells expressing polysialylated neural cell adhesion molecule are present on the ventricular surface of the adult rat brain and spinal cord. J Comp Neurol 414, 149-66.

Alvarez-Buylla, A., Nottebohm, F. 1988. Migration of young neurons in adult avian brain. Nature 335, 353-4.

Alvarez-Buylla, A., Garcia-Verdugo, J.M., Tramontin, A.D. 2001. A unified hypothesis on the lineage of neural stem cells. Nat Rev Neurosci 2, 287-93.

Alvarez-Leefmans, F.J., Gamino, S.M., Reuss, L. 1992. Cell volume changes upon sodium pump inhibition in Helix aspersa neurones. J Physiol 458, 603-19.

Andrew, R.D., Lobinowich, M.E., Osehobo, E.P. 1997. Evidence against volume regulation by cortical brain cells during acute osmotic stress. Exp Neurol 143, 300-12.

Aronowski, J., Strong, R., Grotta, J.C. 1996. Citicoline for treatment of experimental focal ischemia: histologic and behavioral outcome. Neurol Res 18, 570-4.

Arsenijevic, Y., Weiss, S. 1998. Insulin-like growth factor-I is a differentiation factor for postmitotic CNS stem cell-derived neuronal precursors: distinct actions from those of brain-derived neurotrophic factor. J Neurosci 18, 2118-28.

Arsenijevic, Y., Weiss, S., Schneider, B., Aebischer, P. 2001a. Insulin-like growth factor-I is necessary for neural stem cell proliferation and demonstrates distinct actions of epidermal growth factor and fibroblast growth factor-2. J Neurosci 21, 7194-202.

Arsenijevic, Y., Villemure, J.G., Brunet, J.F., Bloch, J.J., Deglon, N., Kostic, C., Zurn, A., Aebischer, P. 2001b. Isolation of multipotent neural precursors residing in the cortex of the adult human brain. Exp Neurol 170, 48-62.

Arvidsson, A., Kokaia, Z., Lindvall, O. 2001. N-methyl-D-aspartate receptor-mediated increase of neurogenesis in adult rat dentate gyrus following stroke. Eur J Neurosci 14, 10-8.

Astrup, J., Sorensen, P.M., Sorensen, H.R. 1981. Oxygen and glucose consumption related to Na+-K+ transport in canine brain. Stroke 12, 726-30.

Auer, R.N., Siesjo, B.K. 1988. Biological differences between ischemia, hypoglycemia, and epilepsy. Ann Neurol 24, 699-707.

Axelrod, D. 1979. Carbocyanine dye orientation in red cell membrane studied by microscopic fluorescence polarization. Biophys J 26, 557-73.

Ayata, C., Ropper, A.H. 2002. Ischaemic brain oedema. J Clin Neurosci 9, 113-24.

Balestrino, M. 1995. Pathophysiology of anoxic depolarization: new findings and a working hypothesis. J Neurosci Methods 59, 99-103.

Banasiak, K.J., Xia, Y., Haddad, G.G. 2000. Mechanisms underlying hypoxia-induced neuronal apoptosis. Prog Neurobiol 62, 215-49.

Barzo, P., Marmarou, A., Fatouros, P., Corwin, F., Dunbar, J. 1996. Magnetic resonance imaging-monitored acute blood-brain barrier changes in experimental traumatic brain injury. J Neurosurg 85, 1113-21.

Barzo, P., Marmarou, A., Fatouros, P., Hayasaki, K., Corwin, F. 1997. Contribution of vasogenic and cellular edema to traumatic brain swelling measured by diffusion-weighted imaging. J Neurosurg 87, 900-7.

Basarsky, T.A., Duffy, S.N., Andrew, R.D., MacVicar, B.A. 1998. Imaging spreading depression and associated intracellular calcium waves in brain slices. J Neurosci 18, 7189-99.

Behar, T.N., Scott, C.A., Greene, C.L., Wen, X., Smith, S.V., Maric, D., Liu, Q.Y., Colton, C.A., Barker, J.L. 1999. Glutamate acting at NMDA receptors stimulates embryonic cortical neuronal migration. J Neurosci 19, 4449-61.

Bengzon, J., Kokaia, Z., Elmer, E., Nanobashvili, A., Kokaia, M., Lindvall, O. 1997. Apoptosis and proliferation of dentate gyrus neurons after single and intermittent limbic seizures. Proc Natl Acad Sci U S A 94, 10432-7.

Benson, R.S., Heer, S., Dive, C., Watson, A.J. 1996. Characterization of cell volume loss in CEM-C7A cells during dexamethasone-induced apoptosis. Am J Physiol 270, C1190-203.

Bernardi, P., Petronilli, V., Di Lisa, F., Forte, M. 2001. A mitochondrial perspective on cell death. Trends Biochem Sci 26, 112-7.

Bernardini, G.L., DeShaies, E.M. 2001. Critical care of intracerebral and subarachnoid hemorrhage. Curr Neurol Neurosci Rep 1, 568-76.

Bernstein, R.A., Hemphill, J.C. 2001. Critical care of acute ischemic stroke. Curr Neurol Neurosci Rep 1, 587-92.

Bockaert, J., Pin, J., Fagni, L. 1993. Metabotropic glutamate receptors: an original family of G protein-coupled receptors. Fundam Clin Pharmacol 7, 473-85.

Bond, T.D., Ambikapathy, S., Mohammad, S., Valverde, M.A. 1998. Osmosensitive Cl- currents and their relevance to regulatory volume decrease in human intestinal T84 cells: outwardly vs. inwardly rectifying currents. J Physiol 511 (Pt 1), 45-54.

Bonfoco, E., Krainc, D., Ankarcrona, M., Nicotera, P., Lipton, S.A. 1995. Apoptosis and necrosis: two distinct events induced, respectively, by mild and intense insults with N-methyl-D-aspartate or nitric oxide/superoxide in cortical cell cultures. Proc Natl Acad Sci U S A 92, 7162-6.

Bonventre, J.V., Koroshetz, W.J. 1993. Phospholipase A2 (PLA2) activity in gerbil brain: characterization of cytosolic and membrane-associated forms and effects of ischemia and reperfusion on enzymatic activity. J Lipid Mediat 6, 457-71.

Borgens, R.B., Shi, R. 2000. Immediate recovery from spinal cord injury through molecular repair of nerve membranes with polyethylene glycol. Faseb J 14, 27-35.

Bortner, C.D., Cidlowski, J.A. 1996. Absence of volume regulatory mechanisms contributes to the rapid activation of apoptosis in thymocytes. Am J Physiol 271, C950-61.

Brawn, R.J., Barker, C.R., Oesterle, A.D., Kelly, R.J., Dandliker, W.B. 1975. An improved fluorescence probe cytotoxicity assay. J Immunol Methods 9, 7-26.

Bredt, D.S., Snyder, S.H. 1994. Nitric oxide: a physiologic messenger molecule. Annu Rev Biochem 63, 175-95.

Brodsky, J.L., Guidotti, G. 1990. Sodium affinity of brain Na(+)-K(+)-ATPase is dependent on isozyme and environment of the pump. Am J Physiol 258, C803-11.

Brott, T., Bogousslavsky, J. 2000. Treatment of acute ischemic stroke. N Engl J Med 343, 710-22.

Brustle, O., McKay, R.D. 1996. Neuronal progenitors as tools for cell replacement in the nervous system. Curr Opin Neurobiol 6, 688-95.

Brustle, O., Jones, K.N., Learish, R.D., Karram, K., Choudhary, K., Wiestler, O.D., Duncan, I.D., McKay, R.D. 1999. Embryonic stem cell-derived glial precursors: a source of myelinating transplants. Science 285, 754-6.

Bullock, R., Zauner, A., Woodward, J., Young, H.F. 1995a. Massive persistent release of excitatory amino acids following human occlusive stroke. Stroke 26, 2187-9.

Bullock, R., Zauner, A., Myseros, J.S., Marmarou, A., Woodward, J.J., Young, H.F. 1995b. Evidence for prolonged release of excitatory amino acids in severe human head trauma. Relationship to clinical events. Ann N Y Acad Sci 765, 290-7; discussion 298.

Cai, J., Yang, J., Jones, D.P. 1998. Mitochondrial control of apoptosis: the role of cytochrome c. Biochim Biophys Acta 1366, 139-49.

Caldwell, M., O'Neill, M., Earley, B., Kelly, J.P., Leonard, B.E. 1995. NG-nitro-L-arginine methyl ester protects against lipid peroxidation in the gerbil following cerebral ischaemia. Eur J Pharmacol 285, 203-6.

Castejon, O.J., Castejon, H.V., Zavala, M., Sanchez, M.E., Diaz, M. 2002. A light and electron microscopic study of oedematous human cerebral cortex in two patients with post-traumatic seizures. Brain Inj 16, 331-46.

Chalmers-Redman, R.M., Fraser, A.D., Ju, W.Y., Wadia, J., Tatton, N.A., Tatton, W.G. 1997. Mechanisms of nerve cell death: apoptosis or necrosis after cerebral ischaemia. Int Rev Neurobiol 40, 1-25.

Chan, P.H. 1994. Oxygen radicals in focal cerebral ischemia. Brain Pathol 4, 59-65.

Chan, P.H. 1996. Role of oxidants in ischemic brain damage. Stroke 27, 1124-9.

Charriaut-Marlangue, C., Pollard, H., Ben-Ari, Y. 1996. Is ischemic cell death of the apoptotic type? Adv Neurol 71, 425-30; discussion 430-1.

Chen, J., Nagayama, T., Jin, K., Stetler, R.A., Zhu, R.L., Graham, S.H., Simon, R.P. 1998. Induction of caspase-3-like protease may mediate delayed neuronal death in the hippocampus after transient cerebral ischemia. J Neurosci 18, 4914-28.

Choi, D.W. 1988. Calcium-mediated neurotoxicity: relationship to specific channel types and role in ischemic damage. Trends Neurosci 11, 465-9.

Choi, D.W. 1992. Excitotoxic cell death. J Neurobiol 23, 1261-76.

Choi, D.W. 1994. Glutamate receptors and the induction of excitotoxic neuronal death. Prog Brain Res 100, 47-51.

Choi, D.W., Koh, J.Y., Peters, S. 1988. Pharmacology of glutamate neurotoxicity in cortical cell culture: attenuation by NMDA antagonists. J Neurosci 8, 185-96.

Colbourne, F., Sutherland, G.R., Auer, R.N. 1999. Electron microscopic evidence against apoptosis as the mechanism of neuronal death in global ischemia. J Neurosci 19, 4200-10.

Cong, J., Goll, D.E., Peterson, A.M., Kapprell, H.P. 1989. The role of autolysis in activity of the Ca2+-dependent proteinases (mu-calpain and m-calpain). J Biol Chem 264, 10096-103.

Conn, P.J., Pin, J.P. 1997. Pharmacology and functions of metabotropic glutamate receptors. Annu Rev Pharmacol Toxicol 37, 205-37.

Cross, C.E., Halliwell, B., Borish, E.T., Pryor, W.A., Ames, B.N., Saul, R.L., McCord, J.M., Harman, D. 1987. Oxygen radicals and human disease. Ann Intern Med 107, 526-45.

Dash, P.K., Mach, S.A., Moore, A.N. 2001. Enhanced neurogenesis in the rodent hippocampus following traumatic brain injury. J Neurosci Res 63, 313-9.

Davis, J.N., Antonawich, F.J. 1997. Role of apoptotic proteins in ischemic hippocampal damage. Ann N Y Acad Sci 835, 309-20.

Dawson, V.L., Kizushi, V.M., Huang, P.L., Snyder, S.H., Dawson, T.M. 1996. Resistance to neurotoxicity in cortical cultures from neuronal nitric oxide synthase-deficient mice. J Neurosci 16, 2479-87.

del Zoppo, G.J., Hallenbeck, J.M. 2000. Advances in the vascular pathophysiology of ischemic stroke. Thromb Res 98, 73-81.

Demediuk, P., Faden, A.I., Romhanyi, R., Vink, R., McIntosh, T.K. 1989. Changes in lipid metabolism, tissue cations, and water content after fluid-percussion-induced traumatic brain injury in rats. J Neurotrauma 6, 229.

Denny, J.B., Polan-Curtain, J., Ghuman, A., Wayner, M.J., Armstrong, D.L. 1990. Calpain inhibitors block long-term potentiation. Brain Res 534, 317-20.

Di, X., Goforth, P.B., Bullock, R., Ellis, E., Satin, L. 2000. Mechanical injury alters volume activated ion channels in cortical astrocytes. Acta Neurochir Suppl 76, 379-83.

Doble, A. 1999. The role of excitotoxicity in neurodegenerative disease: implications for therapy. Pharmacol Ther 81, 163-221.

Dodd, P.R. 2002. Excited to death: different ways to lose your neurones. Biogerontology 3, 51-6.

Duan, D., Winter, C., Cowley, S., Hume, J.R., Horowitz, B. 1997. Molecular identification of a volume-regulated chloride channel. Nature 390, 417-21.

Dugan, L.L., Choi, D.W. 1994. Excitotoxicity, free radicals, and cell membrane changes. Ann Neurol 35 Suppl, S17-21.

Duggal, N., Schmidt-Kastner, R., Hakim, A.M. 1997. Nestin expression in reactive astrocytes following focal cerebral ischemia in rats. Brain Res 768, 1-9.

Edwards, M.A., Yamamoto, M., Caviness, V.S., Jr. 1990. Organization of radial glia and related cells in the developing murine CNS. An analysis based upon a new monoclonal antibody marker. Neuroscience 36, 121-44.

Ellis, R.E., Yuan, J.Y., Horvitz, H.R. 1991. Mechanisms and functions of cell death. Annu Rev Cell Biol 7, 663-98.

Enseleit, W.H., Domer, F.R., Jarrott, D.M., Baricos, W.H. 1984. Cerebral phospholipid content and Na+,K+-ATPase activity during ischemia and postischemic reperfusion in the mongolian gerbil. J Neurochem 43, 320-7.

Eriksson, P.S., Perfilieva, E., Bjork-Eriksson, T., Alborn, A.M., Nordborg, C., Peterson, D.A., Gage, F.H. 1998. Neurogenesis in the adult human hippocampus. Nat Med 4, 1313-7.

Faddis, B.T., Hasbani, M.J., Goldberg, M.P. 1997. Calpain activation contributes to dendritic remodeling after brief excitotoxic injury in vitro. J Neurosci 17, 951-9.

Faden, A.I., Simon, R.P. 1988. A potential role for excitotoxins in the pathophysiology of spinal cord injury. Ann Neurol 23, 623-6.

Faden, A.I., Demediuk, P., Panter, S.S., Vink, R. 1989. The role of excitatory amino acids and NMDA receptors in traumatic brain injury. Science 244, 798-800.

Farooqui, A.A., Yi Ong, W., Lu, X.R., Halliwell, B., Horrocks, L.A. 2001. Neurochemical consequences of kainate-induced toxicity in brain: involvement of arachidonic acid release and prevention of toxicity by phospholipase A(2) inhibitors. Brain Res Brain Res Rev 38, 61-78.

Felsenfeld, D.P., Sweadner, K.J. 1988. Fine specificity mapping and topography of an isozyme-specific epitope of the Na,K-ATPase catalytic subunit. J Biol Chem 263, 10932-42.

Ferrer, I., Lopez, E., Blanco, R., Rivera, R., Ballabriga, J., Pozas, E., Marti, E. 1998. Bcl-2, Bax, and Bcl-x expression in the CA1 area of the hippocampus following transient forebrain ischemia in the adult gerbil. Exp Brain Res 121, 167-73.

Floyd, R.A., Welch, K.M.A., Kaplan, L.R., Rice, J., et, a. 1997. Production of free radicals, Primer on Cerebrovascular disease. Academic Press, San Diego, CA. pp. 165-169.

Gage, F.H., Kempermann, G., Palmer, T.D., Peterson, D.A., Ray, J. 1998. Multipotent progenitor cells in the adult dentate gyrus. J Neurobiol 36, 249-66.

Garcia, J.H., Yoshida, Y., Chen, H., Li, Y., Zhang, Z.G., Lian, J., Chen, S., Chopp, M. 1993. Progression from ischemic injury to infarct following middle cerebral artery occlusion in the rat. Am J Pathol 142, 623-35.

Garthwaite, J., Garthwaite, G., Hajos, F. 1986. Amino acid neurotoxicity: relationship to neuronal depolarization in rat cerebellar slices. Neuroscience 18, 449-60.

Garthwaite, J., Charles, S.L., Chess-Williams, R. 1988. Endothelium-derived relaxing factor release on activation of NMDA receptors suggests role as intercellular messenger in the brain. Nature 336, 385-8.

Garthwaite, J., Garthwaite, G., Palmer, R.M., Moncada, S. 1989. NMDA receptor activation induces nitric oxide synthesis from arginine in rat brain slices. Eur J Pharmacol 172, 413-6.

Geering, K., Beggah, A., Good, P., Girardet, S., Roy, S., Schaer, D., Jaunin, P. 1996. Oligomerization and maturation of Na,K-ATPase: functional interaction of the cytoplasmic NH2 terminus of the beta subunit with the alpha subunit. J Cell Biol 133, 1193-204.

Giuliano, K.A., Taylor, D.L. 1998. Fluorescent-protein biosensors: new tools for drug discovery. Trends Biotechnol 16, 135-40.

Giuliano, K.A., Post, P.L., Hahn, K.M., Taylor, D.L. 1995. Fluorescent protein biosensors: measurement of molecular dynamics in living cells. Annu Rev Biophys Biomol Struct 24, 405-34.

Glading, A., Lauffenburger, D.A., Wells, A. 2002. Cutting to the chase: calpain proteases in cell motility. Trends Cell Biol 12, 46-54.

Glynn, I.M., Karlish, S.J. 1990. Occluded cations in active transport. Annu Rev Biochem 59, 171-205.

Goldberg, W.J., Dorman, R.V., Dabrowiecki, Z., Horrocks, L.A. 1985. The effects of ischemia and CDPamines on Na+, K+-ATPase and acetylcholinesterase activities in rat brain. Neurochem Pathol 3, 237-48.

Goldshleger, R., Patchornik, G., Shimon, M.B., Tal, D.M., Post, R.L., Karlish, S.J. 2001. Structural organization and energy transduction mechanism of Na+,K+-ATPase studied with transition metal-catalyzed oxidative cleavage. J Bioenerg Biomembr 33, 387-99.

Gould, E., Tanapat, P. 1997a. Lesion-induced proliferation of neuronal progenitors in the dentate gyrus of the adult rat. Neuroscience 80, 427-36.

Gould, E., Gross, C.G. 2002. Neurogenesis in adult mammals: some progress and problems. J Neurosci 22, 619-23.

Gould, E., McEwen, B.S., Tanapat, P., Galea, L.A., Fuchs, E. 1997b. Neurogenesis in the dentate gyrus of the adult tree shrew is regulated by psychosocial stress and NMDA receptor activation. J Neurosci 17, 2492-8.

Gould, E., Reeves, A.J., Fallah, M., Tanapat, P., Gross, C.G., Fuchs, E. 1999. Hippocampal neurogenesis in adult Old World primates. Proc Natl Acad Sci U S A 96, 5263-7.

Gray, W.P., Sundstrom, L.E. 1998. Kainic acid increases the proliferation of granule cell progenitors in the dentate gyrus of the adult rat. Brain Res 790, 52-9.

Green, D.R., Reed, J.C. 1998. Mitochondria and apoptosis. Science 281, 1309-12.

Grilli, M., Diodato, E., Lozza, G., Brusa, R., Casarini, M., Uberti, D., Rozmahel, R., Westaway, D., St George-Hyslop, P., Memo, M., Ongini, E. 2000. Presenilin-1 regulates the neuronal threshold to excitotoxicity both physiologically and pathologically. Proc Natl Acad Sci U S A 97, 12822-7.

Gross, C.G. 2000. Neurogenesis in the adult brain: death of a dogma. Nat Rev Neurosci 1, 67-73.

Guillaume, D., Grisar, T., Delgado-Escueta, A.V., Laschet, J., Bureau-Heeren, M. 1990. Two isoenzymes of Na+,K+-ATPase have different kinetics of K+ dephosphorylation in normal cat and human brain cortex. J Neurochem 54, 130-4.

Guo, Q., Fu, W., Sopher, B.L., Miller, M.W., Ware, C.B., Martin, G.M., Mattson, M.P. 1999. Increased vulnerability of hippocampal neurons to excitotoxic necrosis in presenilin-1 mutant knock-in mice. Nat Med 5, 101-6.

Gwag, B.J., Koh, J.Y., DeMaro, J.A., Ying, H.S., Jacquin, M., Choi, D.W. 1997. Slowly triggered excitotoxicity occurs by necrosis in cortical cultures. Neuroscience 77, 393-401.

Hall, N.C., Carney, J.M., Cheng, M.S., Butterfield, D.A. 1995. Ischemia/reperfusion-induced changes in membrane proteins and lipids of gerbil cortical synaptosomes. Neuroscience 64, 81-9.

Halliwell, B. 1987. Oxidants and human disease: some new concepts. Faseb J 1, 358-64.

Halliwell, J. 1994. Potassium channels in the central nervous system, Cjocjester.

Hansen, A.J. 1985. Effect of anoxia on ion distribution in the brain. Physiol Rev 65, 101-48.

Hara, E., Reinach, P.S., Wen, Q., Iserovich, P., Fischbarg, J. 1999. Fluoxetine inhibits K(+) transport pathways (K(+) efflux, Na(+)-K(+)-2Cl(-) cotransport, and Na(+) pump) underlying volume regulation in corneal endothelial cells. J Membr Biol 171, 75-85.

Hara, H., Friedlander, R.M., Gagliardini, V., Ayata, C., Fink, K., Huang, Z., Shimizu-Sasamata, M., Yuan, J., Moskowitz, M.A. 1997. Inhibition of interleukin 1beta

converting enzyme family proteases reduces ischemic and excitotoxic neuronal damage. Proc Natl Acad Sci U S A 94, 2007-12.

Hayes, R.L., Jenkins, L.W., Lyeth, B.G. 1992. Neurotransmitter-mediated mechanisms of traumatic brain injury: acetylcholine and excitatory amino acids. J Neurotrauma 9 Suppl 1, S173-87.

Hazama, A., Fan, H.T., Abdullaev, I., Maeno, E., Tanaka, S., Ando-Akatsuka, Y., Okada, Y. 2000. Swelling-activated, cystic fibrosis transmembrane conductance regulator-augmented ATP release and Cl- conductances in murine C127 cells. J Physiol 523 Pt 1, 1-11.

Hengartner, M.O. 1999. Programmed cell death in the nematode C. elegans. Recent Prog Horm Res 54, 213-22; discussion 222-4.

Herdegen, T., Claret, F.X., Kallunki, T., Martin-Villalba, A., Winter, C., Hunter, T., Karin, M. 1998. Lasting N-terminal phosphorylation of c-Jun and activation of c-Jun N-terminal kinases after neuronal injury. J Neurosci 18, 5124-35.

Hoffmann, E.K. 1986. Anion transport systems in the plasma membrane of vertebrate cells. Biochim Biophys Acta 864, 1-31.

Hoffmann, E.K., Simonsen, L.O. 1989. Membrane mechanisms in volume and pH regulation in vertebrate cells. Physiol Rev 69, 315-82.

Holcik, M., Gibson, H., Korneluk, R.G. 2001. XIAP: apoptotic brake and promising therapeutic target. Apoptosis 6, 253-61.

Hosler, B.A., Brown, R.H., Jr. 1996. Superoxide dismutase and oxygen radical neurotoxicity. Curr Opin Neurol 9, 486-91.

Huang, Z., Huang, P.L., Panahian, N., Dalkara, T., Fishman, M.C., Moskowitz, M.A. 1994. Effects of cerebral ischemia in mice deficient in neuronal nitric oxide synthase. Science 265, 1883-5.

Hughes, F.M., Jr., Bortner, C.D., Purdy, G.D., Cidlowski, J.A. 1997. Intracellular K+ suppresses the activation of apoptosis in lymphocytes. J Biol Chem 272, 30567-76.

Ignarro, L.J., Buga, G.M., Wood, K.S., Byrns, R.E., Chaudhuri, G. 1987. Endothelium-derived relaxing factor produced and released from artery and vein is nitric oxide. Proc Natl Acad Sci U S A 84, 9265-9.

Johnson, G.V., Guttmann, R.P. 1997. Calpains: intact and active? Bioessays 19, 1011-8.

Jones, D.G., Redpath, C.M. 1998. Regeneration in the central nervous system: pharmacological intervention, xenotransplantation, and stem cell transplantation. Clin Anat 11, 263-70.

Jorgensen, P.L., Nielsen, J.M., Rasmussen, J.H., Pedersen, P.A. 1998. Structure-function relationships of E1-E2 transitions and cation binding in Na,K-pump protein. Biochim Biophys Acta 1365, 65-70.

Kampfl, A., Posmantur, R., Nixon, R., Grynspan, F., Zhao, X., Liu, S.J., Newcomb, J.K., Clifton, G.L., Hayes, R.L. 1996. mu-calpain activation and calpain-mediated cytoskeletal proteolysis following traumatic brain injury. J Neurochem 67, 1575-83.

Kaplia, A.A. 1997. [Structural organization of Na+,K+-ATPase isoenzymes in the plasma membrane]. Ukr Biokhim Zh 69, 12-24.

Karlish, S.J., Yates, D.W., Glynn, I.M. 1976. Transient kinetics of (Na+ +K+)-ATPase studied with a fluorescent substrate. Nature 263, 251-3.

Katayama, Y., Becker, D.P., Tamura, T., Hovda, D.A. 1990. Massive increases in extracellular potassium and the indiscriminate release of glutamate following concussive brain injury. J Neurosurg 73, 889-900.

Kaufmann, S.H., Hengartner, M.O. 2001. Programmed cell death: alive and well in the new millennium. Trends Cell Biol 11, 526-34.

Kempermann, G. 2002. Why new neurons? Possible functions for adult hippocampal neurogenesis. J Neurosci 22, 635-8.

Kempermann, G., Gage, F.H. 1998. Closer to neurogenesis in adult humans. Nat Med 4, 555-7.

Kempermann, G., Gage, F.H. 2000. Neurogenesis in the adult hippocampus. Novartis Found Symp 231, 220-35; discussion 235-41, 302-6.

Kerr, J.F., Wyllie, A.H., Currie, A.R. 1972. Apoptosis: a basic biological phenomenon with wide-ranging implications in tissue kinetics. Br J Cancer 26, 239-57.

Kimelberg, H.K. 1992. Astrocytic edema in CNS trauma. J Neurotrauma 9 Suppl 1, S71-81.

Komuro, H., Rakic, P. 1993. Modulation of neuronal migration by NMDA receptors. Science 260, 95-7.

Kooy, N.W., Royall, J.A., Ischiropoulos, H., Beckman, J.S. 1994. Peroxynitrite-mediated oxidation of dihydrorhodamine 123. Free Radic Biol Med 16, 149-56.

Kornack, D.R., Rakic, P. 1999. Continuation of neurogenesis in the hippocampus of the adult macaque monkey. Proc Natl Acad Sci U S A 96, 5768-73.

Krajewski, S., Mai, J.K., Krajewska, M., Sikorska, M., Mossakowski, M.J., Reed, J.C. 1995. Upregulation of bax protein levels in neurons following cerebral ischemia. J Neurosci 15, 6364-76.

Kroemer, G., Dallaporta, B., Resche-Rigon, M. 1998. The mitochondrial death/life regulator in apoptosis and necrosis. Annu Rev Physiol 60, 619-42.

Kuida, K., Zheng, T.S., Na, S., Kuan, C., Yang, D., Karasuyama, H., Rakic, P., Flavell, R.A. 1996. Decreased apoptosis in the brain and premature lethality in CPP32-deficient mice. Nature 384, 368-72.

Kumar, S. 1997. The apoptotic cysteine protease CPP32. Int J Biochem Cell Biol 29, 393-6.

Lawrence, M.S., McLaughlin, J.R., Sun, G.H., Ho, D.Y., McIntosh, L., Kunis, D.M., Sapolsky, R.M., Steinberg, G.K. 1997. Herpes simplex viral vectors expressing Bcl-2 are neuroprotective when delivered after a stroke. J Cereb Blood Flow Metab 17, 740-4.

Leavitt, B.R., Hernit-Grant, C.S., Macklis, J.D. 1999. Mature astrocytes transform into transitional radial glia within adult mouse neocortex that supports directed migration of transplanted immature neurons. Exp Neurol 157, 43-57.

Lee, J.M., Zipfel, G.J., Choi, D.W. 1999a. The changing landscape of ischaemic brain injury mechanisms. Nature 399, A7-14.

Lee, S.M., Wong, M.D., Samii, A., Hovda, D.A. 1999b. Evidence for energy failure following irreversible traumatic brain injury. Ann N Y Acad Sci 893, 337-40.

Lees, G.J. 1991. Inhibition of sodium-potassium-ATPase: a potentially ubiquitous mechanism contributing to central nervous system neuropathology. Brain Res Brain Res Rev 16, 283-300.

Leist, M., Single, B., Castoldi, A.F., Kuhnle, S., Nicotera, P. 1997. Intracellular adenosine triphosphate (ATP) concentration: a switch in the decision between apoptosis and necrosis. J Exp Med 185, 1481-6.

Lemas, M.V., Hamrick, M., Takeyasu, K., Fambrough, D.M. 1994. 26 amino acids of an extracellular domain of the Na,K-ATPase alpha-subunit are sufficient for assembly with the Na,K-ATPase beta-subunit. J Biol Chem 269, 8255-9.

Li, F., Liu, K.F., Silva, M.D., Meng, X., Gerriets, T., Helmer, K.G., Fenstermacher, J.D., Sotak, C.H., Fisher, M. 2002. Acute postischemic renormalization of the apparent diffusion coefficient of water is not associated with reversal of astrocytic swelling and neuronal shrinkage in rats. AJNR Am J Neuroradiol 23, 180-8.

Li, S., Stys, P.K. 2001. Na(+)-K(+)-ATPase inhibition and depolarization induce glutamate release via reverse Na(+)-dependent transport in spinal cord white matter. Neuroscience 107, 675-83.

Li, S., Jiang, Q., Stys, P.K. 2000. Important role of reverse Na(+)-Ca(2+) exchange in spinal cord white matter injury at physiological temperature. J Neurophysiol 84, 1116-9.

Li, S., Mealing, G.A., Morley, P., Stys, P.K. 1999a. Novel injury mechanism in anoxia and trauma of spinal cord white matter: glutamate release via reverse Na+-dependent glutamate transport. J Neurosci 19, RC16.

Li, Y., Chopp, M. 1999b. Temporal profile of nestin expression after focal cerebral ischemia in adult rat. Brain Res 838, 1-10.

Li, Y., Chopp, M., Powers, C. 1997. Granule cell apoptosis and protein expression in hippocampal dentate gyrus after forebrain ischemia in the rat. J Neurol Sci 150, 93-102.

Lipton, P. 1999. Ischemic cell death in brain neurons. Physiol Rev 79, 1431-568.

Liu, J., Solway, K., Messing, R.O., Sharp, F.R. 1998. Increased neurogenesis in the dentate gyrus after transient global ischemia in gerbils. J Neurosci 18, 7768-78.

Liu, T.H., Beckman, J.S., Freeman, B.A., Hogan, E.L., Hsu, C.Y. 1989. Polyethylene glycol-conjugated superoxide dismutase and catalase reduce ischemic brain injury. Am J Physiol 256, H589-93.

Lo, C., Ferrier, J., Tenenbaum, H.C., McCulloch, C.A. 1995. Regulation of cell volume and intracellular pH in hyposmotically swollen rat osteosarcoma cells. Biochem Cell Biol 73, 535-44.

Lomneth, R., Medrano, S., Gruenstein, E.I. 1990. The role of transmembrane pH gradients in the lactic acid induced swelling of astrocytes. Brain Res 523, 69-77.

Lu, X., Ong, W., Halliwell, B., Horrocks, L.A., Farooqui, A.A. 2001. Differential effects of calcium-dependent and calcium-independent phospholipase A(2) inhibitors on kainate-induced neuronal injury in rat hippocampal slices. Free Radic Biol Med 30, 1263-73.

Lucas, D.R., Newhouse, J.P. 1957. The toxic effect of sodium L-glutamate on the inner layer of the retina. Arch Ophthalmol 58, 193-201.

Ludolph, A.C., Meyer, T., Riepe, M.W. 2000. The role of excitotoxicity in ALS--what is the evidence? J Neurol 247 Suppl 1, I7-16.

Luskin, M.B. 1998. Neuroblasts of the postnatal mammalian forebrain: their phenotype and fate. J Neurobiol 36, 221-33.

Macaya, A. 2000. [Cell death in neonatal hypoxia-ischemia]. Rev Neurol 31, 784-9.

Macknight, A.D. 1988. Principles of cell volume regulation. Ren Physiol Biochem 11, 114-41.

MacManus, J.P., Buchan, A.M. 2000. Apoptosis after experimental stroke: fact or fashion? J Neurotrauma 17, 899-914.

Macmillan-Crow, L.A., Cruthirds, D.L. 2001. Invited review: manganese superoxide dismutase in disease. Free Radic Res 34, 325-36.

Madden, D.R. 2002. The structure and function of glutamate receptor ion channels. Nat Rev Neurosci 3, 91-101.

Madsen, T.M., Treschow, A., Bengzon, J., Bolwig, T.G., Lindvall, O., Tingstrom, A. 2000. Increased neurogenesis in a model of electroconvulsive therapy. Biol Psychiatry 47, 1043-9.

Maeno, E., Ishizaki, Y., Kanaseki, T., Hazama, A., Okada, Y. 2000. Normotonic cell shrinkage because of disordered volume regulation is an early prerequisite to apoptosis. Proc Natl Acad Sci U S A 97, 9487-92.

Magavi, S.S., Leavitt, B.R., Macklis, J.D. 2000. Induction of neurogenesis in the neocortex of adult mice. Nature 405, 951-5.

Malatesta, P., Hartfuss, E., Gotz, M. 2000. Isolation of radial glial cells by fluorescent-activated cell sorting reveals a neuronal lineage. Development 127, 5253-63.

Malinski, T., Bailey, F., Zhang, Z.G., Chopp, M. 1993. Nitric oxide measured by a porphyrinic microsensor in rat brain after transient middle cerebral artery occlusion. J Cereb Blood Flow Metab 13, 355-8.

Mark, R.J., Hensley, K., Butterfield, D.A., Mattson, M.P. 1995. Amyloid beta-peptide impairs ion-motive ATPase activities: evidence for a role in loss of neuronal Ca2+ homeostasis and cell death. J Neurosci 15, 6239-49.

Marletta, M.A. 1994. Nitric oxide synthase: aspects concerning structure and catalysis. Cell 78, 927-30.

Martin, L.J. 2001. Neuronal cell death in nervous system development, disease, and injury (Review). Int J Mol Med 7, 455-78.

Martin-Villalba, A., Herr, I., Jeremias, I., Hahne, M., Brandt, R., Vogel, J., Schenkel, J., Herdegen, T., Debatin, K.M. 1999. CD95 ligand (Fas-L/APO-1L) and tumor necrosis factor-related apoptosis-inducing ligand mediate ischemia-induced apoptosis in neurons. J Neurosci 19, 3809-17.

Maxwell, W.L., Bullock, R., Landholt, H., Fujisawa, H. 1994. Massive astrocytic swelling in response to extracellular glutamate--a possible mechanism for post-traumatic brain swelling? Acta Neurochir Suppl (Wien) 60, 465-7.

McGrail, K.M., Phillips, J.M., Sweadner, K.J. 1991. Immunofluorescent localization of three Na,K-ATPase isozymes in the rat central nervous system: both neurons and glia can express more than one Na,K-ATPase. J Neurosci 11, 381-91.

Melloni, E., Pontremoli, S. 1989. The calpains. Trends Neurosci 12, 438-44.

Miller, C., Moczydlowski, E., Latorre, R., Phillips, M. 1985. Charybdotoxin, a protein inhibitor of single Ca2+-activated K+ channels from mammalian skeletal muscle. Nature 313, 316-318.

Miyasaka, N., Kuroiwa, T., Zhao, F.Y., Nagaoka, T., Akimoto, H., Yamada, I., Kubota, T., Aso, T. 2000. Cerebral ischemic hypoxia: discrepancy between apparent diffusion coefficients and histologic changes in rats. Radiology 215, 199-204.

Miyata, T., Kawaguchi, A., Okano, H., Ogawa, M. 2001. Asymmetric inheritance of radial glial fibers by cortical neurons. Neuron 31, 727-41.

Munir, M., Lu, L., McGonigle, P. 1995. Excitotoxic cell death and delayed rescue in human neurons derived from NT2 cells. J Neurosci 15, 7847-60.

Murachi, T. 1990. [Calpain and calpastatin]. Rinsho Byori 38, 337-46.

Murin, R., Drgova, A., Kaplan, P., Dobrota, D., Lehotsky, J. 2001. Ischemia/Reperfusion-induced oxidative stress causes structural changes of brain membrane proteins and lipids. Gen Physiol Biophys 20, 431-8.

Nait-Oumesmar, B., Decker, L., Lachapelle, F., Avellana-Adalid, V., Bachelin, C., Van Evercooren, A.B. 1999. Progenitor cells of the adult mouse subventricular zone

proliferate, migrate and differentiate into oligodendrocytes after demyelination. Eur J Neurosci 11, 4357-66.

Namura, S., Zhu, J., Fink, K., Endres, M., Srinivasan, A., Tomaselli, K.J., Yuan, J., Moskowitz, M.A. 1998. Activation and cleavage of caspase-3 in apoptosis induced by experimental cerebral ischemia. J Neurosci 18, 3659-68.

Nicholson, D.W., Thornberry, N.A. 1997. Caspases: killer proteases. Trends Biochem Sci 22, 299-306.

Nijhawan, D., Honarpour, N., Wang, X. 2000. Apoptosis in neural development and disease. Annu Rev Neurosci 23, 73-87.

Noctor, S.C., Flint, A.C., Weissman, T.A., Wong, W.S., Clinton, B.K., Kriegstein, A.R. 2002. Dividing precursor cells of the embryonic cortical ventricular zone have morphological and molecular characteristics of radial glia. J Neurosci 22, 3161-73.

Obeidat, A.S., Andrew, R.D. 1998. Spreading depression determines acute cellular damage in the hippocampal slice during oxygen/glucose deprivation. Eur J Neurosci 10, 3451-61.

O'Brien, W.J., Lingrel, J.B., Wallick, E.T. 1994. Ouabain binding kinetics of the rat alpha two and alpha three isoforms of the sodium-potassium adenosine triphosphate. Arch Biochem Biophys 310, 32-9.

Oiki, S., Kubo, M., Okada, Y. 1994. Mg2+ and ATP-dependence of volume-sensitive Cl-channels in human epithelial cells. Jpn J Physiol 44 Suppl 2, S77-9.

Okada, Y., Maeno, E., Shimizu, T., Dezaki, K., Wang, J., Morishima, S. 2001. Receptor-mediated control of regulatory volume decrease (RVD) and apoptotic volume decrease (AVD). J Physiol 532, 3-16.

Olney, J.W. 1969. Brain lesions, obesity, and other disturbances in mice treated with monosodium glutamate. Science 164, 719-21.

Olney, J.W. 1990. Excitotoxin-mediated neuron death in youth and old age. Prog Brain Res 86, 37-51.

Olney, J.W., Sharpe, L.G. 1969. Brain lesions in an infant rhesus monkey treated with monsodium glutamate. Science 166, 386-8.

Ovchinnikov Yu, A., Monastyrskaya, G.S., Broude, N.E., Ushkaryov Yu, A., Melkov, A.M., Smirnov Yu, V., Malyshev, I.V., Allikmets, R.L., Kostina, M.B., Dulubova, I.E., et al. 1988. Family of human Na+, K+-ATPase genes. Structure

of the gene for the catalytic subunit (alpha III-form) and its relationship with structural features of the protein. FEBS Lett 233, 87-94.

Owens, D.F., Kriegstein, A.R. 1998. Patterns of intracellular calcium fluctuation in precursor cells of the neocortical ventricular zone. J Neurosci 18, 5374-88.

Palmer, T.D., Takahashi, J., Gage, F.H. 1997. The adult rat hippocampus contains primordial neural stem cells. Mol Cell Neurosci 8, 389-404.

Palmer, T.D., Markakis, E.A., Willhoite, A.R., Safar, F., Gage, F.H. 1999. Fibroblast growth factor-2 activates a latent neurogenic program in neural stem cells from diverse regions of the adult CNS. J Neurosci 19, 8487-97.

Parent, J.M., Yu, T.W., Leibowitz, R.T., Geschwind, D.H., Sloviter, R.S., Lowenstein, D.H. 1997. Dentate granule cell neurogenesis is increased by seizures and contributes to aberrant network reorganization in the adult rat hippocampus. J Neurosci 17, 3727-38.

Patel, A.J., Lauritzen, I., Lazdunski, M., Honore, E. 1998. Disruption of mitochondrial respiration inhibits volume-regulated anion channels and provokes neuronal cell swelling. J Neurosci 18, 3117-23.

Pencea, V., Bingaman, K.D., Freedman, L.J., Luskin, M.B. 2001. Neurogenesis in the subventricular zone and rostral migratory stream of the neonatal and adult primate forebrain. Exp Neurol 172, 1-16.

Perrelet, D., Ferri, A., Liston, P., Muzzin, P., Korneluk, R.G., Kato, A.C. 2002. IAPs are essential for GDNF-mediated neuroprotective effects in injured motor neurons in vivo. Nat Cell Biol 4, 175-9.

Petito, C.K., Pulsinelli, W.A. 1984. Sequential development of reversible and irreversible neuronal damage following cerebral ischemia. J Neuropathol Exp Neurol 43, 141-53.

Pin, J.P., Duvoisin, R. 1995. The metabotropic glutamate receptors: structure and functions. Neuropharmacology 34, 1-26.

Puka-Sundvall, M., Gilland, E., Hagberg, H. 2001. Cerebral hypoxia-ischemia in immature rats: involvement of mitochondrial permeability transition? Dev Neurosci 23, 192-7.

Qian, X., Davis, A.A., Goderie, S.K., Temple, S. 1997. FGF2 concentration regulates the generation of neurons and glia from multipotent cortical stem cells. Neuron 18, 81-93.

Rao, A.M., Hatcher, J.F., Dempsey, R.J. 1999. CDP-choline: neuroprotection in transient forebrain ischemia of gerbils. J Neurosci Res 58, 697-705.

Rao, A.M., Hatcher, J.F., Dempsey, R.J. 2000. Lipid alterations in transient forebrain ischemia: possible new mechanisms of CDP-choline neuroprotection. J Neurochem 75, 2528-35.

Reichert, S.A., Kim-Han, J.S., Dugan, L.L. 2001. The mitochondrial permeability transition pore and nitric oxide synthase mediate early mitochondrial depolarization in astrocytes during oxygen-glucose deprivation. J Neurosci 21, 6608-16.

Rice, W.J., Young, H.S., Martin, D.W., Sachs, J.R., Stokes, D.L. 2001. Structure of Na+,K+-ATPase at 11-A resolution: comparison with Ca2+-ATPase in E1 and E2 states. Biophys J 80, 2187-97.

Rickmann, M., Amaral, D.G., Cowan, W.M. 1987. Organization of radial glial cells during the development of the rat dentate gyrus. J Comp Neurol 264, 449-79.

Robinson, J.D. 1982. Transport ATPase, In A. Laitha (Ed.) Handbook of Neurochemistry, Pergamon, New York, 173-193.

Ross, S.T., Soltesz, I. 2000. Selective depolarization of interneurons in the early posttraumatic dentate gyrus: involvement of the Na(+)/K(+)-ATPase. J Neurophysiol 83, 2916-30.

Rossi, D.J., Oshima, T., Attwell, D. 2000. Glutamate release in severe brain ischaemia is mainly by reversed uptake. Nature 403, 316-21.

Roy, M., Sapolsky, R. 1999. Neuronal apoptosis in acute necrotic insults: why is this subject such a mess? Trends Neurosci 22, 419-22.

Rubin, L.L. 1997. Neuronal cell death: when, why and how. Br Med Bull 53, 617-31.

Sapirstein, A., Bonventre, J.V. 2000. Phospholipases A2 in ischemic and toxic brain injury. Neurochem Res 25, 745-53.

Sattler, R., Tymianski, M. 2001. Molecular mechanisms of glutamate receptor-mediated excitotoxic neuronal cell death. Mol Neurobiol 24, 107-29.

Scheiner-Bobis, G. 2002. The sodium pump. Eur J Biochem 269, 2424-33.

Schoepp, D.D. 1994. Novel functions for subtypes of metabotropic glutamate receptors. Neurochem Int 24, 439-49.

Scott, B.W., Wojtowicz, J.M., Burnham, W.M. 2000. Neurogenesis in the dentate gyrus of the rat following electroconvulsive shock seizures. Exp Neurol 165, 231-6.

Scott, B.W., Wang, S., Burnham, W.M., De Boni, U., Wojtowicz, J.M. 1998. Kindling-induced neurogenesis in the dentate gyrus of the rat. Neurosci Lett 248, 73-6.

Seki, T., Arai, Y. 1999. Temporal and spacial relationships between PSA-NCAM-expressing, newly generated granule cells, and radial glia-like cells in the adult dentate gyrus. J Comp Neurol 410, 503-13.

Senatorov, V.V., Mooney, D., Hu, B. 1997. The electrogenic effects of Na(+)-K(+)-ATPase in rat auditory thalamus. J Physiol 502 (Pt 2), 375-85.

Senatorov, V.V., Stys, P.K., Hu, B. 2000. Regulation of Na+,K+-ATPase by persistent sodium accumulation in adult rat thalamic neurones. J Physiol 525 Pt 2, 343-53.

Sheldon, R.A., Hall, J.J., Noble, L.J., Ferriero, D.M. 2001. Delayed cell death in neonatal mouse hippocampus from hypoxia-ischemia is neither apoptotic nor necrotic. Neurosci Lett 304, 165-8.

Shi, R., Asano, T., Vining, N.C., Blight, A.R. 2000. Control of membrane sealing in injured mammalian spinal cord axons. J Neurophysiol 84, 1763-9.

Shi, Y. 2001. A structural view of mitochondria-mediated apoptosis. Nat Struct Biol 8, 394-401.

Sims, N.R., Anderson, M.F. 2002. Mitochondrial contributions to tissue damage in stroke. Neurochem Int 40, 511-26.

Skaper, S.D., Facci, L., Strijbos, P.J. 2001. Neuronal protein kinase signaling cascades and excitotoxic cell death. Ann N Y Acad Sci 939, 11-22.

Sladeczek, F., Pin, J.P., Recasens, M., Bockaert, J., Weiss, S. 1985. Glutamate stimulates inositol phosphate formation in striatal neurones. Nature 317, 717-9.

Small, D.L., Buchan, A.M. 2000. Animal models. Br Med Bull 56, 307-17.

Solenski, N.J., diPierro, C.G., Trimmer, P.A., Kwan, A.L., Helms, G.A. 2002. Ultrastructural changes of neuronal mitochondria after transient and permanent cerebral ischemia. Stroke 33, 816-24.

Song, D.K., Malmstrom, T., Kater, S.B., Mykles, D.L. 1994. Calpain inhibitors block Ca(2+)-induced suppression of neurite outgrowth in isolated hippocampal pyramidal neurons. J Neurosci Res 39, 474-81.

Song, H.J., Stevens, C.F., Gage, F.H. 2002. Neural stem cells from adult hippocampus develop essential properties of functional CNS neurons. Nat Neurosci 5, 438-45.

Spector, M.S., Desnoyers, S., Hoeppner, D.J., Hengartner, M.O. 1997. Interaction between the C. elegans cell-death regulators CED-9 and CED-4. Nature 385, 653-6.

Stanfield, B.B., Trice, J.E. 1988. Evidence that granule cells generated in the dentate gyrus of adult rats extend axonal projections. Exp Brain Res 72, 399-406.

Staub, F., Baethmann, A., Peters, J., Weigt, H., Kempski, O. 1990. Effects of lactacidosis on glial cell volume and viability. J Cereb Blood Flow Metab 10, 866-76.

Staub, F., Winkler, A., Haberstok, J., Plesnila, N., Peters, J., Chang, R.C., Kempski, O., Baethmann, A. 1996. Swelling, intracellular acidosis, and damage of glial cells. Acta Neurochir Suppl (Wien) 66, 56-62.

Stys, P.K. 1998. Anoxic and ischemic injury of myelinated axons in CNS white matter: from mechanistic concepts to therapeutics. J Cereb Blood Flow Metab 18, 2-25.

Su, G., Kintner, D.B., Sun, D. 2002a. Contribution of Na(+)-K(+)-Cl(-) cotransporter to high-[K(+)](o)- induced swelling and EAA release in astrocytes. Am J Physiol Cell Physiol 282, C1136-46.

Su, G., Kintner, D.B., Flagella, M., Shull, G.E., Sun, D. 2002b. Astrocytes from Na(+)-K(+)-Cl(-) cotransporter-null mice exhibit absence of swelling and decrease in EAA release. Am J Physiol Cell Physiol 282, C1147-60.

Sugawara, T., Noshita, N., Lewen, A., Gasche, Y., Ferrand-Drake, M., Fujimura, M., Morita-Fujimura, Y., Chan, P.H. 2002. Overexpression of copper/zinc superoxide dismutase in transgenic rats protects vulnerable neurons against ischemic damage by blocking the mitochondrial pathway of caspase activation. J Neurosci 22, 209-17.

Szatkowski, M., Attwell, D. 1994. Triggering and execution of neuronal death in brain ischaemia: two phases of glutamate release by different mechanisms. Trends Neurosci 17, 359-65.

Tamamaki, N., Nakamura, K., Okamoto, K., Kaneko, T. 2001. Radial glia is a progenitor of neocortical neurons in the developing cerebral cortex. Neurosci Res 41, 51-60.

Tanaka, E., Yamamoto, S., Inokuchi, H., Isagai, T., Higashi, H. 1999. Membrane dysfunction induced by in vitro ischemia in rat hippocampal CA1 pyramidal neurons. J Neurophysiol 81, 1872-80.

Tobin, T., Akera, T., Baskin, S.I., Brody, T.M. 1973. Calcium ion and sodium- and potassium-dependent adenosine triphosphatase: its mechanism of inhibition and identification of the E 1 -P intermediate. Mol Pharmacol 9, 336-49.

Trimarchi, J.R., Liu, L., Smith, P.J., Keefe, D.L. 2002. Apoptosis recruits two-pore domain potassium channels used for homeostatic volume regulation. Am J Physiol Cell Physiol 282, C588-94.

van Praag, H., Schinder, A.F., Christie, B.R., Toni, N., Palmer, T.D., Gage, F.H. 2002. Functional neurogenesis in the adult hippocampus. Nature 415, 1030-4.

Voigt, T. 1989. Development of glial cells in the cerebral wall of ferrets: direct tracing of their transformation from radial glia into astrocytes. J Comp Neurol 289, 74-88.

Weiss, S., Dunne, C., Hewson, J., Wohl, C., Wheatley, M., Peterson, A.C., Reynolds, B.A. 1996. Multipotent CNS stem cells are present in the adult mammalian spinal cord and ventricular neuroaxis. J Neurosci 16, 7599-609.

White, B.C., Sullivan, J.M., DeGracia, D.J., O'Neil, B.J., Neumar, R.W., Grossman, L.I., Rafols, J.A., Krause, G.S. 2000. Brain ischemia and reperfusion: molecular mechanisms of neuronal injury. J Neurol Sci 179, 1-33.

Wiesinger, H. 2001. Arginine metabolism and the synthesis of nitric oxide in the nervous system. Prog Neurobiol 64, 365-91.

Wyllie, A.H. 1980. Glucocorticoid-induced thymocyte apoptosis is associated with endogenous endonuclease activation. Nature 284, 555-6.

Xiao, A.Y., Homma, M., Wang, X.Q., Wang, X., Yu, S.P. 2001. Role of K(+) efflux in apoptosis induced by AMPA and kainate in mouse cortical neurons. Neuroscience 108, 61-7.

Xiao, A.Y., Wei, L., Xia, S., Rothman, S., Yu, S.P. 2002. Ionic mechanism of ouabain-induced concurrent apoptosis and necrosis in individual cultured cortical neurons. J Neurosci 22, 1350-62.

Yoshida, T., Limmroth, V., Irikura, K., Moskowitz, M.A. 1994. The NOS inhibitor, 7-nitroindazole, decreases focal infarct volume but not the response to topical acetylcholine in pial vessels. J Cereb Blood Flow Metab 14, 924-9.

Yoshino, A., Hovda, D.A., Kawamata, T., Katayama, Y., Becker, D.P. 1991. Dynamic changes in local cerebral glucose utilization following cerebral conclusion in rats: evidence of a hyper- and subsequent hypometabolic state. Brain Res 561, 106-19.

Yu, S.P., Yeh, C., Strasser, U., Tian, M., Choi, D.W. 1999. NMDA receptor-mediated K+ efflux and neuronal apoptosis. Science 284, 336-9.

Yue, X., Mehmet, H., Penrice, J., Cooper, C., Cady, E., Wyatt, J.S., Reynolds, E.O., Edwards, A.D., Squier, M.V. 1997. Apoptosis and necrosis in the newborn piglet brain following transient cerebral hypoxia-ischaemia. Neuropathol Appl Neurobiol 23, 16-25.

Zamzami, N., Kroemer, G. 2001. The mitochondrion in apoptosis: how Pandora's box opens. Nat Rev Mol Cell Biol 2, 67-71.

Zauner, A., Bullock, R. 1995a. The role of excitatory amino acids in severe brain trauma: opportunities for therapy: a review. J Neurotrauma 12, 547-54.

Zauner, A., Bullock, R., Di, X., Young, H.F. 1995b. Brain oxygen, CO2, pH, and temperature monitoring: evaluation in the feline brain. Neurosurgery 37, 1168-76; discussion 1176-7.

Zetterstrom, T.S., Vaughan-Jones, R.D., Grahame-Smith, D.G. 1995. A short period of hypoxia produces a rapid and transient rise in [K+]e in rat hippocampus in vivo which is inhibited by certain K(+)-channel blocking agents. Neuroscience 67, 815-21.

Zou, H., Henzel, W.J., Liu, X., Lutschg, A., Wang, X. 1997. Apaf-1, a human protein homologous to C. elegans CED-4, participates in cytochrome c-dependent activation of caspase-3. Cell 90, 405-13.